1-1-2012

Mechanistic Studies Of A Novel Ppar-Gamma Mutant That Causes Lipodystrophy And Diabetes

Olga Astapova
Wayne State University,

MECHANISTIC STUDIES OF A NOVEL PPARγ MUTANT THAT CAUSES LIPODYSTROPHY AND DIABETES

by

OLGA ASTAPOVA

DISSERTATION

Submitted to the Graduate School

of Wayne State University,

Detroit, Michigan

in partial fulfillment of the requirements

for the degree of

DOCTOR OF PHILOSOPHY

2014

MAJOR: PATHOLOGY

Approved by:

_____

Advisor Date

_____

_____

_____

ACKNOWLEDGEMENTS

I have been extremely fortunate to complete this part of my training in an environment that was both nurturing and scientifically challenging, and I have many people to thank for helping me through this process. First and foremost, my mentor, Dr. Todd Leff, who is not only a brilliant scientist but also a patient, dedicated and encouraging teacher. Dr. Leff has played a tremendous role in shaping my scientific thought process, while setting an example of effective communication, positive attitude and success in all aspects of a scientist's life. I am grateful as well to my dissertation committee members Dr. Hyeong-Reh Kim, Dr. Shijie Sheng and Dr. James Granneman for spending many hours of their time to think about this project and give me valuable advice and thoughtful critique. My co-mentor, Dr. Ramsi Haddad, has been enthusiastic and encouraging and was tremendously helpful in guiding me through the process of microarray analysis of gene expression.

A special thank you to Dr. Ambika Mathur and all the members of the MD/PhD Program at Wayne State University. Dr. Mathur has been extremely caring and supportive of my progress through this rigorous curriculum, welcoming me into her home, sharing career experiences as an MD/PhD and acting as an advocate for the students. Ms. Deanna Dona has provided administrative help beyond her professional responsibilities, allowing me to focus on my work. I am also extremely grateful to my classmates, some of whom have become dear friends, who have challenged me intellectually and created an informal, science-oriented social circle.

Many faculty members at this University and other institutions have contributed to this work. Our collaborators Dr. Claude Gagné at Laval University,

Dr. Philippe Campeau at Baylor College of Medicine, and Dr. Robert Hegele at Robarts Research Institute identified the E157D PPARγ mutant and described the clinical presentation of its carriers. Dr. Ladislau Kovari and Dr. Jianjun Wang at the Department of Biochemistry graciously allowed me to use machinery in their laboratories in order to complete my experiments and also spent time advising me on the technical and theoretical aspects of my project. Dr. Abdul Abou-Samra and Dr. Fateh Elkhatib shared their clinical expertise in the field of endocrinology, helping me better understand the clinical implications of my project. Dr. Ronald Cohen at the University of Chicago generously provided an expression plasmid for one of the experiments. Dr. Keith Yamamoto and Ms. Lisa Watson at the University of California have advised me on an exciting future direction for this project.

Last but not least, I greatly appreciate the kindness, smiles and support of past and present members of the Leff lab: Raj Amin, Yilan Li, Yun-Hee Lee, Jannifer Tyrrell, Lin Zhang, Xiangqun Ye, Mikhail Shteynvil, Angie Adhami and Mohamad Halabi, as well as all the other members of the CIMER research group at the University. Their input at journal clubs and research presentations was invaluable, and their personalities created a great working atmosphere.

TABLE OF CONTENTS

LIST OF TABLES

LIST OF FIGURES

1 INTRODUCTION

1.1 Obesity Epidemic and the Rise of Metabolic Disease.

The prevalence of obesity in the United States has risen dramatically in the last several decades. The Centers for Disease Control and Prevention (CDC) reported in 2011 that over a third of the adult population was obese, a sharp rise since 1985, when obesity rates in most US states were below 10% [1]. Moreover, recent analyses suggest that the body mass index (BMI) measure used to diagnose obesity in these reports may underestimate the prevalence of obesity. BMI, calculated as body mass in kilograms divided by height in meters squared, does not take into account body composition. As a result, individuals with diminished muscle weight, in particular elderly women, are commonly misclassified as not obese [2]. The reverse misclassification of individuals with high muscle mass, such as athletes, as overweight (25<BMI<30) or obese (BMI>30) also occurs, but the overall effect of the use of the BMI system in the general population is an underestimation of obesity prevalence. Based on these findings, alternative age-specific BMI cutoffs have been proposed, and by these new criteria the prevalence of obesity is even higher, about two-thirds [3]. Regardless of the metric used, the rising rates of obesity have led to its recognition in the US as an epidemic.

Obesity is a significant risk factor for a host of metabolic and cardiovascular disorders, and in particular it is highly associated with type II diabetes. The CDC reports a steep rise in the prevalence of diagnosed diabetes in the US that is concomitant with the obesity epidemic, up from 3.5% in 1980 to 9.1% in 2010, and predicting a continued increase [4]. This statistic holds true in the age-adjusted model as well, indicating that the increase in diabetes prevalence is independent of

the aging of the population. The inability to clear glucose from the bloodstream in diabetic individuals leads to microvascular and macrovascular complications, multiple end-organ damage and increased morbidity and mortality. Furthermore, insulin resistance is often associated with hypertension and dyslipidemia as part of the metabolic syndrome, leading to additional health risks. As a result, the toll from the obesity and diabetes epidemic on public health and healthcare spending is vast, and research to understand the mechanisms behind metabolic syndrome-related diseases is an important ongoing effort.

1.2 Nuclear Receptors in Metabolic Regulation.

Energy metabolism at the cellular levels is regulated in large part by the gene transcription activity of nuclear receptors. The nuclear receptor superfamily includes steroid hormone receptors, peroxisome proliferator-activated receptors (PPARs), thyroid hormone receptor, retinoic acid receptor and a number of others, as well as some orphan nuclear receptors with unidentified ligands. The characteristic feature of hormone receptors is their capacity to bind specific ligands, recognize and bind specific regulatory DNA sequences, and interact with gene transcription coregulators. Through these mechanisms nuclear receptors respond to changes in the extracellular environment, which are signaled by specific ligands, often hormones, and regulate the gene transcription program of the cell to adjust to these changes. Different types of nuclear receptors act by slightly different mechanisms. Type I, including the sex hormone receptors and the glucocorticoid receptor, dissociate from cytoplasmic heat shock proteins upon ligand binding, translocate into the nucleus and bind to hormone response elements as

homodimers [5]. PPARs are type II nuclear receptors, which are bound to DNA as heterodimers with the 9-*cis*-retinoic acid receptor (RXR), and recruit transcription corepressors to the local chromatin [6] (Figure 1). In the presence of ligands, the receptor undergoes a conformational change which alters its interaction with ATP-dependent chromatin remodeling and histone modifying enzymes, such as nuclear receptor corepressors NCoR and SMRT, BRG-1 associated factor (BAF) family, nuclear receptor coactivators SRC-1, the p300-CBP coactivator family and the mediator complex [7-9]. This transcriptionally active conformation favors the release of corepressors and recruitment of transcription coactivator complexes including histone acetyltransferases, altering the histone acetylation pattern and increasing transcription of nearby genes. The nuclear receptor and its associated protein complex cycle on and off the DNA molecule and are degraded by the proteasome as part of a carefully controlled transcriptional regulation equilibrium [10].

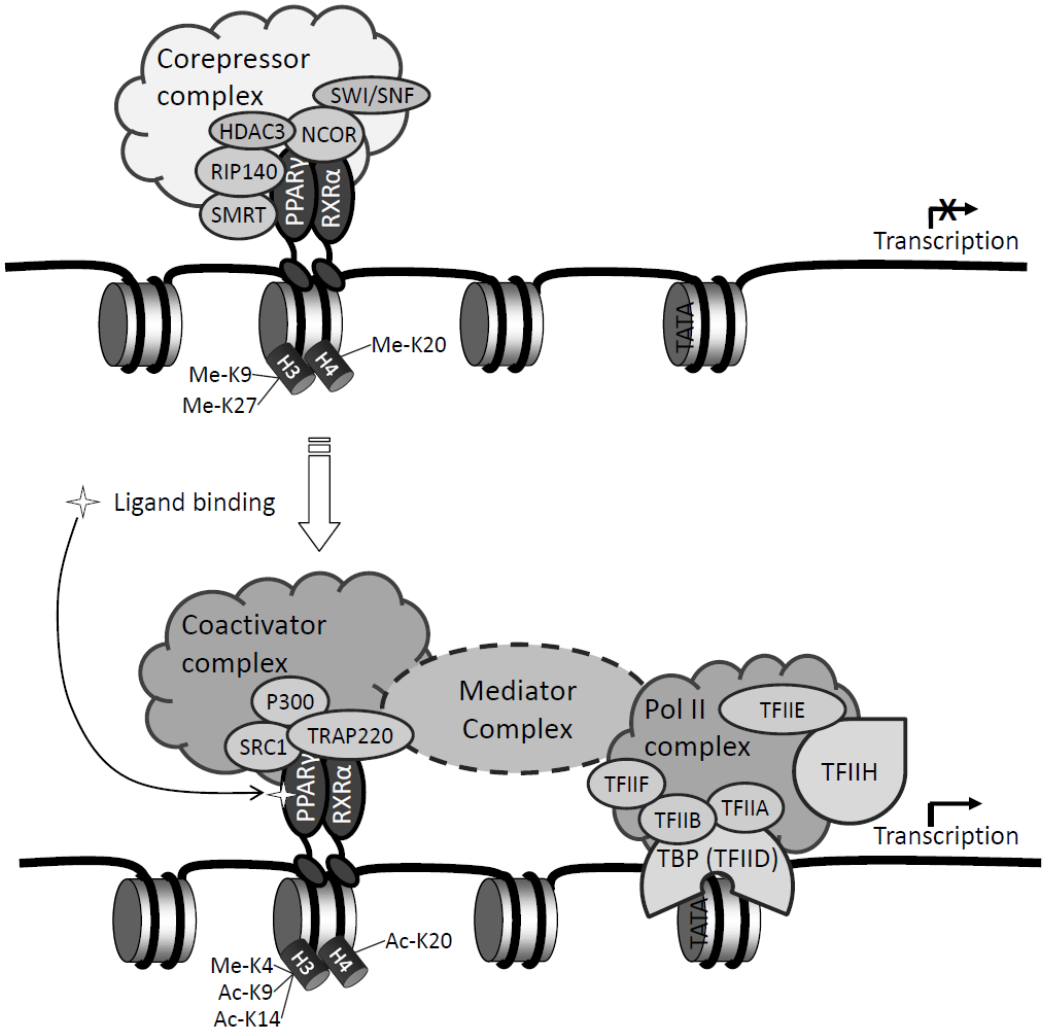

Figure 1. Schematic Representation of Transcription Regulation by Type II Nuclear Receptors.

Ligand binding induces a switch from gene repression (top panel) to activation (bottom panel). Some representative members of the coactivator and corepressor complexes are shown. Chromatin marks associated with repressed and activated states are indicated. Adopted from Rosenfeld *et al.* [11].

All nuclear receptors have homologous domains for DNA binding and ligand binding, separated by a hinge [12]; PPARs also share an N-terminal domain that is adjacent to the DNA binding domain [13]. The ligand binding domain is comprised

of several α-helices that create a ligand pocket and contain transcription coregulator interaction surfaces. Structurally, the DNA-binding domain is comprised of two zinc finger motifs. The "knuckle region" at the base of zinc finger one contains the six-amino-acid "P-box" (Figure 2). This is the region of the receptor that fits into the major groove of the DNA molecule and is important for the recognition of DNA binding sites [14-17]. The binding sites, or response elements, are *cis*-acting regulatory DNA sequences that are located within the promoters, gene coding sequences, or up to 100,000 base pairs away from the transcription start sites of the receptor target genes [18-20]. The response elements are receptor-specific; they are often direct or inverted repeats of a short base pair sequence with a variable number of spacing nucleotides. However, each receptor can recognize many deviations of its response element from the consensus sequence - a versatility that enables one receptor to regulate hundreds of genes. Moreover, it has been observed that there is a high degree of evolutionary conservation between the same response element in different species [21], indicating that the DNA sequence from which a nuclear receptor regulates the expression of a particular gene is of non-trivial importance. However, exactly how the interaction between a receptor and its DNA binding site directs subtle changes in gene transcription is not presently clear.

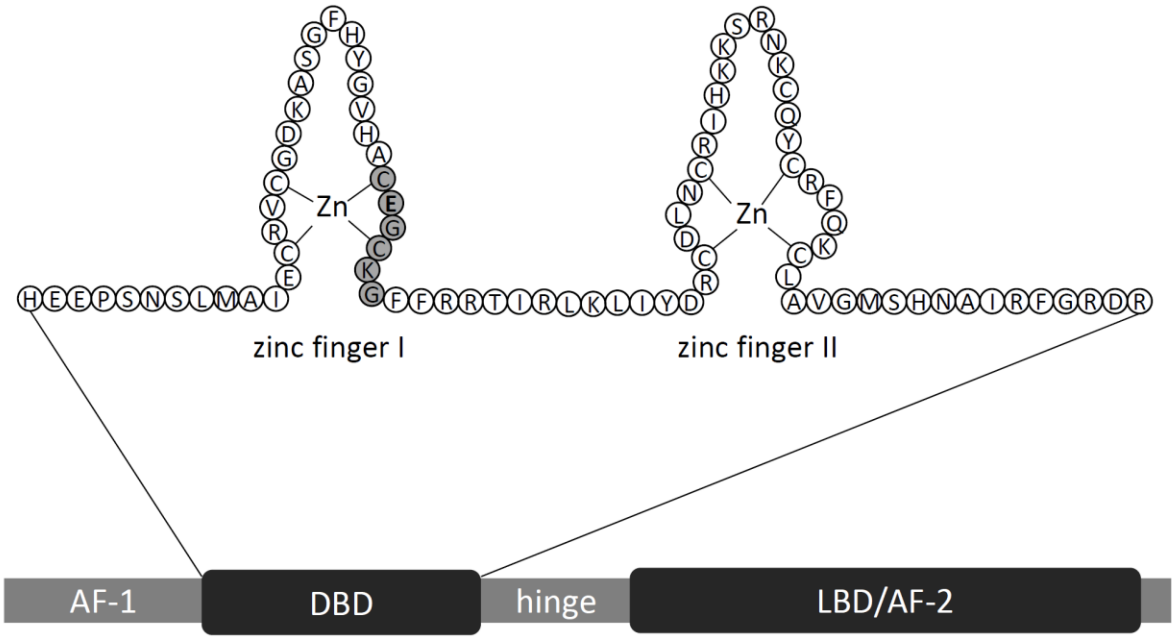

Figure 2. Schematic Representation of the Domain Structure of PPARγ.

Bottom panel shows conserved nuclear receptor domains: AF, activation function; DBD, DNA-binding domain; LBD, ligand-binding domain. Top panel represents the zinc finger structures in the DNA binding domain, with the p-box amino acids shaded and glutamate 157 shown in boldface. Adopted from Temple *et al.* [22].

PPARs are nuclear receptors that have evolved to regulate energy homeostasis by recognizing various fuel molecules as signals of metabolic changes in the body. PPARα, β/δ, and γ are isotypes of the PPAR family with unique tissue expression profiles and roles in metabolic regulation. PPARα is expressed most abundantly in the skeletal muscle and the liver, and functions to promote fatty acid oxidation. PPARβ/δ is expressed ubiquitously and is involved in the regulation of circulating lipoprotein particles [23]. PPARγ is expressed in multiple tissues, but

most abundantly in adipose, and is a potent promoter of insulin signaling, adipogenesis and lipid storage.

1.3 PPARγ is a Central Player in Energy Metabolism.

PPARγ entered the spotlight as a major player in metabolic regulation in the early 1990s [24] through the discovery of thiazolidinediones (TZDs) as potent synthetic insulin-sensitizing drugs. TZDs quickly passed clinical trials and became front-line agents in the treatment of type II diabetes for their robust glucose-lowering action, although their popularity has recently decreased due to safety concerns. The TZD prototype troglitazone, which has since been withdrawn for idiopathic hepatotoxicity, was shown to be a ligand activator of PPARγ, spurring an in-depth investigation of this receptor, which revealed its activity as a potent inducer of adipocyte differentiation [25]. Many synthetic PPARγ ligands, both TZDs and other classes, are thoroughly characterized and widely used both in the clinic and in basic science. Endogenous PPARγ ligands are less well known, but thought to be certain fatty acid metabolites, such as 15-deoxy-12,14-prostaglandin J2 [26-28], an intermediate in the arachidonic acid metabolism pathway.

Activation of PPARγ results in systemic insulin sensitization through complex mechanisms involving multiple organs. In the adipose tissue, PPARγ promotes lipid uptake and storage, increases the number of smaller adipocytes and recruits alternatively activated macrophages, resulting in a more plastic, less inflammatory adipose phenotype which acts as a better buffer of circulating lipids and reduces ectopic lipid accumulation. In the skeletal muscle, PPARγ potentiates insulin action, and in the liver it acts to suppress gluconeogenesis, altogether leading to lower

blood glucose levels. In addition to its central role in energy homeostasis, PPARγ has been recognized for its anti-inflammatory [25, 29-33] and anti-tumorigenic [34] activities. The former has been attributed in part to PPARγ-mediated downregulation of macrophage inflammatory cytokines and induction of the alternative macrophage phenotype. The latter is most likely due to a general pro-differentiation and anti-proliferation effect of PPARγ. Other areas of demonstrated PPARγ involvement include bone metabolism [35-37], nerve myelination [38], reproduction [39, 40], atherosclerosis and cardiovascular disease [25].

The PPARγ gene is expressed via alternative mRNA splicing into four transcript variants, each controlled by a separate promoter, which are translated into two distinct protein isoforms [41]. PPARγ1 (477 amino acids in the human) is expressed in a variety of tissues but most abundantly in the liver, muscle, intestine, and kidney [42]; PPARγ2 (505 amino acids in the human), which includes an additional 30-amino acid sequence at the N terminus, is expressed almost exclusively in adipocytes [43]. The two isoforms behave similarly in gene transcription and DNA binding assay, with minor differences in adipogenic potential and ligand responsiveness [44, 45].

Genome-wide DNA binding site analyses have confirmed the consensus PPAR response element (PPRE) as a direct repeat sequence with a single spacing nucleotide (DR1): AGGTCA A AGGTCA [19, 20]. As other type II nuclear receptors, PPARγ binds DNA as a heterodimer with RXR [46, 47]; however, the orientation of the heterodimer on the PPRE is reversed compared to other RXR-binding nuclear receptors: PPARγ makes contact with the 5’ half of the PPRE, while RXR binds to the 3’ half [48, 49].

Comprehensive sets of PPARγ target genes in adipocytes have been generated using mRNA profiling and ChIP-seq approaches [50-52]. During adipogenesis, PPARγ induces a gene transcription program consisting of several thousand genes that are involved in adipocyte differentiation, intracellular lipid metabolism, insulin signaling and other pathways. The PPREs from which PPARγ regulates the expression of many of its genes have been identified and confirmed in *in vitro* studies, and present a useful tool for studying the interaction of PPARγ with its DNA binding sites. The DNA binding affinity of PPARγ varies between different PPREs, however it is not clear what the determinants of this target DNA selectivity are; it appears that deviation of the PPRE from consensus is not the only factor, and may not play a role at all [53]. Furthermore, there has been some debate on the validity of the current PPRE consensus, and proposals of expanding it to include the 5' flanking nucleotides due to some evidence that PPARγ binding to its half-site is flexible, while the five nucleotides directly adjacent to the half site may be important for this binding, as may also be the spacing nucleotide [22, 49, 53]. Lack of recent studies involving the broad spectrum of PPREs further contributes to the present gaps in understanding of the selectivity of PPARγ/PPRE interaction.

While the molecular biology of PPARγ has been studied in detail, there are still large gaps in our understanding of how PPARγ transcriptional activity results in the wide-spectrum physiological changes *in vivo*. Genetic mutations in the PPARγ gene that cause clear diabetes-related phenotypes, such as the E157D mutation that is the subject of this dissertation, present a unique opportunity to develop a better understanding of the molecular mechanisms mediating the role of PPARγ in maintaining energy homeostasis and the development of metabolic disease.

1.4 Human PPARγ Mutations and Familial Partial Lipodystrophy.

1.4.1 General Characteristics of Familial Partial Lipodystrophy.

Human mutations in the PPARγ gene occur with a low frequency (estimated 1:100,000 in populations of North-European descent [54], but cause a severe metabolic phenotype called familial partial lipodystrophy (FPLD) type III [55]. These mutants act by a variety of mechanisms biochemically (discussed below), but all are inherited in a dominant pattern. Individuals with FPLD are phenotypically normal until puberty, when subcutaneous adipose tissue in the extremities is depleted, leading to a characteristic sharply-defined appearance of the limb musculature. At the same time, visceral central fat depots in the regions of the abdomen, shoulders, upper back, neck and occasionally the face become enlarged, and fatty infiltration of the liver and skeletal muscle is apparent on MRI [54]. It is not clear what induces this change, but there is likely to be increased adipose tissue remodeling during puberty, a process that apparently goes awry in the absence of two healthy copies of the PPARγ gene. Visceral adipose tissue is more lipolytic and inflammatory than subcutaneous fat, and is associated with metabolic syndrome, and this association is especially pronounced in FPLD patients, who develop insulin-resistant diabetes as early as in their 20s. Consistent with insulin resistance and adipose tissue dysfunction, biochemical evaluations show elevated plasma levels of glucose, insulin, C-peptide, triglycerides and glycosylated hemoglobin, as well as decreased HDL and adipose-derived insulin-sensitizing hormones leptin and

adiponectin [56-62]. In one case report, a lamin A mutation lead to the development of severe insulin resistance without the other abnormalities typically observed in FPLD [63], suggesting that insulin resistance may be an initial step in the development of FPLD, as it is in diabetes. In addition to lipodystrophy and diabetes, FPLD often includes hypertension, dyslipidemia, acanthosis nigricans and polycystic ovary syndrome with hirsutism in the females - all components of the metabolic syndrome [64]. Hypertriglyceridemia leads to the development of hepatic steatosis, pancreatitis and eruptive xanthomas; vascular complications of diabetes are observed, including neuropathy, retinopathy, nephropathy, and secondary atherosclerosis. Notably, the management of lipodystrophies is similar to diabetes, focusing on control of hyperglycemia, lipid lowering, and a low-fat diet; moreover, thiazolidinediones have been shown to improve metabolic function in lipodystrophy patients and preferentially increase subcutaneous fat stores [65, 66].

Although FPLD is a rare disease, it presents a useful model to improve the understanding of adipose tissue and the metabolic syndrome - an association that, as discussed above, is plainly evident from public health data, but poorly understood on a mechanistic level. In this model, a disruption of a single transcription factor - PPARγ - results in a severe and well-defined metabolic phenotype that closely resembles the common form of multi-factorial type II diabetes, but presents in a more exaggerated way. For this reason, FPLD III has been accepted as a monogenetic model of diabetes [67], and has been studied extensively, lending a large contribution to our current knowledge of the role of PPARγ in energy homeostasis and metabolic disease.

1.4.2 Known FPLD mutations.

More than a dozen naturally-occurring mutations in the human PPARγ coding region have been identified and reported as case studies [56-59, 61, 62, 68-73]; many of these have been examined on a molecular level by our group and others. These include single amino-acid substitutions and non-sense mutations in the ligand binding domain and the DNA binding domain, as well as frameshift mutation that results in a deletion of the DNA binding domain. In addition, two common polymorphisms have been identified within the PPARγ gene which confer modest protection from insulin resistance [74-78]. The molecular mechanisms by which these mutants disrupt PPARγ transcriptional activity are diverse: some of the ligand-binding domain mutants are dominant negative by way of binding the DNA and failing to induce transcription (V290M, Y355X, P467L); some have impaired transactivation without dominant negative activity (F388L, R425C). Among the DNA binding domain mutants, the loss of function can be accompanied by dominant negative activity in a non-DNA-binding mechanism (C114R, C131Y, C152W), or not (C190S, R194W). Considering the complex structure-function relationship of the PPARγ protein, including the zinc fingers in the DNA binding domain and the intricate spatial organization of helices in the ligand binding domain, it is not surprising that mutations in different regions of the molecule affect PPARγ activity by such a variety of mechanisms. However, any disruption in the receptor function reported to date, regardless of the molecular mechanism, has resulted in the typical FPLD presentation.

1.5 E157D PPARγ Cohort.

1.5.1 Unique Clinical Presentation of the E157D PPARγ Cohort.

The E157D mutation was discovered in a large French-Canadian kindred by clinical collaborators of our research group, Drs. Gagne, Campeau and Hegele. FPLD features were identified in the proband on a clinic visit for severe dyslipidemia; family history revealed similar appearance in many relatives. After a thorough clinical investigation of multiple family members and DNA sequencing, a diagnosis of FPLD caused by a novel PPARγ mutation, E157D, was made. Heterozygous family members are affected with the characteristic partial lipodystrophic fat distribution, have early-onset insulin-resistant diabetes, hypertriglyceridemia often complicated by pancreatitis, hypertension, and PCOS in several women. In addition, this FPLD cohort is unique for presenting with several abnormalities not previously associated with FPLD type III cases: there is an increased prevalence of neuromuscular and hematological abnormalities such as tinnitus, carpal tunnel syndrome, pancytopenia, bone fractures and myalgias. It has been noted that the small sizes of mutant PPARγ cohorts reported to date have limited our ability to draw meaningful conclusions about the relative severity of dominant versus haploinsufficient genotypes, as well as the relative environmental contribution to the disease presentation [69]. The E157D PPARγ cohort spans three generations and includes fifteen affected individuals (Figure 3) - by far the largest FPLD cohort known to date, affording an unprecedented opportunity to examine the effects of a single PPARγ mutation with some statistical power.

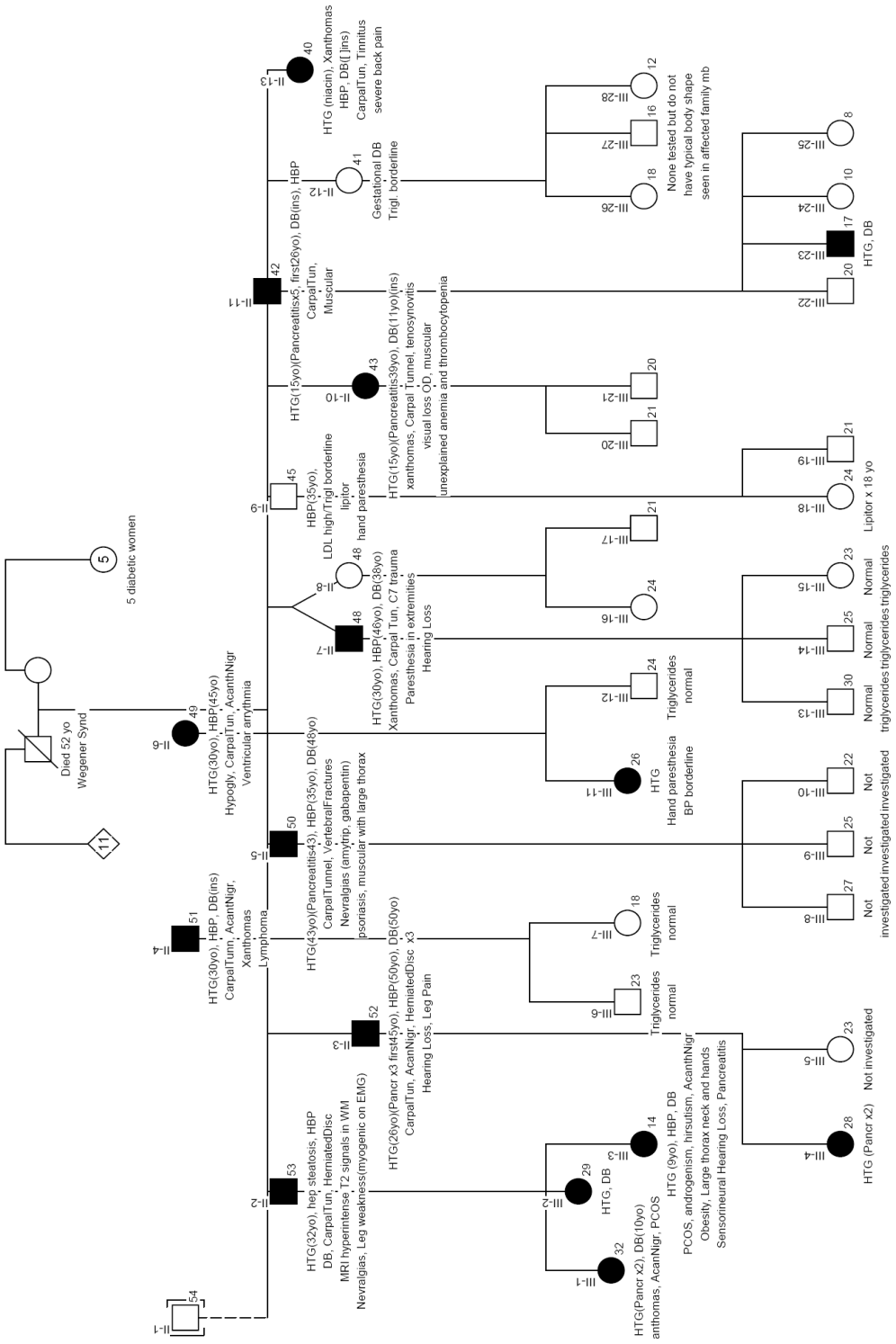

Figure 3. Family Tree of the E157D PPARγ Cohort.

Filled-in shapes represent individuals heterozygous for the mutation. Clinical presentations of study participants are summarized.

1.5.2 Potential implications of the p-box mutation.

The E157D PPARγ mutation is not only unique in its clinical phenotype but also on a molecular level. The amino acid substitution is localized to the p-box of the receptor (indicated in boldface in Figure 2) - a region comprised of only six amino acids that is notable for its importance in the interaction of the receptor with DNA and binding site selectivity, as described above. The p-boxes of various nuclear receptors have been studied in detail. The sequence of the PPARγ p-box is identical to those of its close evolutionary relatives, the thyroid hormone and retinoic acid receptors, while other receptors have evolved to have slightly or significantly different p-box sequences [79, 80]. This diversity is believed to be important for the ability of different nuclear receptors to recognize their cognate DNA binding sites. The E157D PPARγ mutation is the first reported case of a naturally-occurring p-box mutation in PPARγ. However, synthetic p-box mutations in PPARγ have been made by site-directed mutagenesis with the goal of investigating the role of these amino acids in DNA binding site recognition [22]. In this in-vitro study, alanine substitutions at positions 157 and 158 of the receptor did not abolish its ability to bind PPREs and activate gene transcription. However, the mutation changed the relative affinity of PPARγ for various PPREs, and this change was mirrored by transcriptional activity levels on the different PPREs. The E157D mutation is a more conservative substitution that the alanine mutations studied in vitro by Temple et al: the negative charge of the side chain is preserved, and the only difference is one unit of the carbon chain. We therefore reasoned that it is unlikely to dramatically affect the ability of the receptor to bind DNA, but more likely acts via a subtle mechanism such as observed by Temple et al, altering the

DNA binding site selectivity of PPARγ. We postulated a hypothesis that the E157D mutation causes lipodystrophy and diabetes by altering the target gene selectivity of the receptor. We expected to find a small set of genes that was misregulated by E157D PPARγ, revealing novel genes of interest for diabetes pathophysiology. Hence, this subtle, naturally-occurring PPARγ p-box mutation that causes a severe metabolic phenotype was promising to be a valuable tool for gaining insight into how PPARγ interacts with the DNA what molecular pathways are involved in its regulatory role in energy homeostasis.

2 MATERIALS AND METHODS

2.1 In-Silico Structure Prediction.

2.1.1 SIFT.

Sorting Intolerant from Tolerant (SIFT) is a method for predicting the effect of a mutation on protein function by assessing its degree of conservation in homologous proteins, and has been shown to be fairly accurate in identifying mutations which have a strong phenotype [81]. The identity of the residue and its chemical properties (eg, if it's always hydrophobic) are factored into the score. Therefore, a change in a highly conserved region is predicted to affect protein function. The protein sequence of E129D PPARγ1 was analyzed by SIFT Human Protein [82] in order to predict whether the substitution would have a major effect on the protein function.

2.1.2 Swiss-Model.

The structure of E157D mutant PPARγ was modeled using Swiss-Model [83]. The crystal structure of rosiglitazone-bound PPARγ1-RXRα-PPRE complex (PDB ID 3dzy, [84] was loaded into Swiss-Pdb viewer [85] as template, and glutamate 129 was changed to aspartate to represent the E157D mutant. Both the wild-type and mutant complexes were subjected to energy minimization using the GROMOS algorithm [86]. Hydrogen bond contacts were defined as 1.2 - 2.76 Å with a hydrogen atom present and 2.195 - 3.3 Å with no hydrogen present.

2.1.3 MolSoft ICM.

E157D PPARγ segment H122-I144 was used in homology modeling with 3dzy as template. Global energy minimization and Monte Carlo side chain optimization [87]; [88] were implemented to predict the folding of the E157D PPARγ segment. Local energy minimization was used to calculate hydrogen bond distances for E129 (or D129) and C4012 (which corresponds to the third position of the 5' half site of the PPRE) with default parameters defining the hydrogen bond.

2.2 Cell Lines and Culture.

NIH3T3 fibroblasts were maintained in Dulbecco's Modified Eagle's Medium (DMEM) supplemented with 10% fetal bovine serum, 100 units/mL penicillin and 100 µg/mL streptomycin, and passaged at sub-confluency.

3T3-L1 fibroblasts were grown to confluence in DMEM with 10% calf serum, then switched to 10% fetal bovine serum for two days, at which time adipogenic differentiation was induced as described previously [89].

293FT cells were maintained in DMEM with 10% fetal bovine serum, 0.1 mM non-essential amino acids, 100 units/mL penicillin, 100 µg/mL streptomycin and 500 µg/mL geneticin.

NLacZ, NPγ1 and NPγ2 cells were maintained as NIH3T3 cells with the addition of 2µg/mL blasticidin.

10% DMSO was added to freezing medium for all cell lines. Geneticin and blasticidin were omitted from the medium for the first day after thawing the corresponding cell lines.

2.3 Cloning of Plasmids.

Single-stranded oligonucleotides containing PPREs listed in Table 1 with NheI restriction site overhangs at the 5' end and XhoI overhangs at the 3' end were synthesized by IDT and annealed by slow cooling down from 100ºC in annealing buffer (10mM Tris pH 8.0, 1mM EDTA, 50mM NaCl). Double-stranded PPREs were then either biotinylated for the EMSA or inserted into the multiple cloning site of the pGL3-TK luciferase reporter plasmid (Promega).

Mammalian PPARγ1 expression plasmid (pTR151) was constructed by our lab previously using the tet-regulated pTRE vector system and contains an N-terminal double flag tag. The E157D mutation was introduced using site-directed mutagenesis (Stratagene) according to the manufacturer's directions using the following mutated primer: 5'-CACTATGGAGTTCATGCTTGTGA**C**GGATGCAAGGGT-3' (mutated nucleotide is indicated in boldface and underlined). Wild-type and E157D PPARγ2 expression plasmids were constructed by inserting the N-terminal unique segment of PPARγ2, amplified from human adipose cDNA by PCR, into the NcoI site of pTR151, and the correct orientation of the insert was verified by sequencing. Lentiviral vectors for stable PPARγ expression were constructed using the Gateway cloning system (Invitrogen). The Gateway entry clone was generated by inserting 2Xflag-tagged PPARγ1 or PPARγ2 cDNA into the pENTR4 vector, which was then recombined with the destination vector pLenti6.3/V5-DEST using LR Clonase II to generate the lentiviral PPARγ expression vectors.

The NCoR1 expression plasmid was generously provided by Dr. Ronald N. Cohen.

2.4 Transient Transfection.

NIH3T3 cells were plated to be ~90% confluent the next day in antibiotics-free medium. On the day after plating, the medium was replaced with a reduced volume of fresh antibiotics-free medium, and the lipofectamine 2000 transfection mix was added dropwise. After 12 hours of incubation, lipofectamine complexes were removed and replaced with fresh antibiotics-free medium. Cells were harvested 24 hours after the start of transfection.

2.5 Luciferase Transcription Reporter Assays.

For luciferase reporter assays, cells were grown in 12-well plates and each well was transfected in a total volume of 0.5 mL with the following plasmids: 200 ng of luciferase reporter, 100 ng of pTREshuttle2 vector or PPARγ (γ1 or 2, wild-type or E157D), 50 ng of tet-off, 100 ng of RXRα, 50 ng of β-galactosidase and 200 ng of blue script (pBS) as carrier. The plasmids were mixed in 50 µL of Opti-MEM and incubated with lipofectamine 2000 (2 µL per well) as instructed by Invitrogen before the start of transfection. Rosiglitazone (20 µM) or DMSO vehicle control was added to the media for the duration of transfection. Each transfection condition was replicated by two wells, and each experiment was repeated three times. At the end of transfection, the cells were washed with phosphate-buffered saline (PBS) and lysed with 150 µL of passive lysis buffer (Promega). For the luciferase assay, 20 µL of the cell lysate were diluted into 100 µL of luciferase assay buffer (15mM KH_2PO_4 pH 7.8, 15mM $MgSO_4$, 4mM EGTA, 2mM ATP, 1mM DTT) in a white 96-well plate, then 30 µL of D-luciferin was added for a final concentration of 60 µg/mL. The light output was quantified immediately using a luminometer, integrated over 10

seconds. The β-galactosidase assay was used to account for transfection efficiency. 20 µL of the cell lysate were mixed with 30µL of lysis buffer and then with 2X β-galactosidase assay buffer (200mM sodium phosphate pH 7.3, 2 mM $MgCl_2$, 100 mM β-mercaptoethanol, 1.33 mg/mL o-nitrophenyl-β-galactoside). Absorbance at 420 nm was read after 30 minutes at 37°C by the VersaMax microplate reader.

For transcription coregulator interaction assays, NIH3T3 cells were grown and transfected as above, with the addition of 200 ng of the indicated coregulator plasmid instead of pBS.

2.6 Electrophoretic Mobility Shift Assays.

The consensus PPRE and ADN PPRE oligonucleotides were biotinylated on the 5' end by IDT. All other double-stranded PPRE oligonucleotides were labeled with biotin-dUTP using Klenow DNA Polymerase (Fisher) according to the instructions. NIH3T3 cells were grown in 100mm plates and transfected with the following plasmids: 5 µg of pTREshuttle2 or PPARγ1 (wild-type or E157D), 5 µg of RXRα, and 2 µg of tet-off. Nuclear extracts were prepared using the NE-PER kit (Pierce) after 24 hours of transfection. The 20 µL EMSA binding reaction was optimized to contain 1.25 fmol/µL probe, 1 µL nuclear extract, 67 ng/µL poly dI:dC, 1% glycerol, 0.05% NP-40 and 1 mM $MgCl_2$ in the EMSA binding buffer (Pierce). A 200-fold molar excess of unlabeled probe was used as competitor. 1 µg of M2-Flag mouse monoclonal antibody (Sigma) or non-immune mouse IgG (Millipore) was used in supershift binding reaction. The binding reactions were incubated, separated on a 5% native polyacrylamide gel, transferred onto Biodyne-B membranes and detected using the Light-Shift EMSA kit (Pierce) as directed by the protocol.

2.7 Western Blotting.

Whole cell lysates for protein analysis by western blotting were prepared by washing the cells with PBS, incubating on ice in RIPA buffer for 10 minutes, then sonicating for a total of 30 seconds in 5-second bursts alternating with cooling the tube on ice. The lysates were cleared by centrifugation and stored at -80°C. Bio-Rad mini-protean system was used for SDS-PAGE with 20-80 µg of cell lysate per lane, normalized by measuring the protein concentration using the Bradford assay. Separated samples were transferred onto a PVDF membrane for blocking and detection. Primary antibodies used were PPARγ (E-8, Santa Cruz 7273), M2-Flag-HRP (Sigma), His-probe (G-18, Santa Cruz 804), TFIID (TBP) (SI-1, Santa Cruz 273), and GAPDH (FL-335, Santa Cruz 25778). Chemiluminescent signal was detected using the SuperSignal West Dura (Pierce) luminol/peroxide system by the gel DOC detector.

2.8 Lentivirus Packaging and Infection.

Lentiviral PPARγ expression vectors were grown in Stbl3 competent *E.coli* and purified using a plasmid midiprep kit with the addition of 10mM EDTA to the resuspension buffer in order to inhibit the endonuclease in this *end*A1+ strain.

293FT cells were grown in 100mm plates and transfected with 9 µg of lentiviral packaging mix, 3 µg of lentiviral PPARγ expression vector (PPARγ1 to make NPγ1 cells, or PPARγ2 to make NPγ2 cells) and 36 µL of Lipofectamine 2000 in a total volume of 8 mL of antibiotic-free medium. The control plasmid was pLenti6.3/V5-GW/lacZ, supplied with the ViraPower HiPerform Lentiviral Expression Systems kit

(Invitrogen). Medium was replaced on the day after transfection, and virus-containing supernatant was collected two days later, clarified by centrifugation and used directly for infection.

NIH3T3 cells were plated without antibiotics in six-well plates to be ~50% confluent the following day, when the medium was replaced by virus-containing supernatant with 4 μg/mL Polybrene (Sigma). The next day, virus-containing medium was removed and replaced with fresh medium without antibiotics. The following day, 100 units/mL penicillin, 100 μg/mL streptomycin and 2μg/mL blasticidin were included in the medium to select stable infected cells. The selection continued for two weeks, during which time the cells were passaged normally. At the end of selection, frozen stocks of NPγ1, NPγ2 and NLacZ cells were prepared and used for all subsequent experiments to control for transgene expression, which we have observed to decrease over transgenic cell passages.

2.9 Reverse Transcriptase PCR.

Cells were grown in 6-well plates and, when indicated, treated with 20 μM rosiglitazone or DMSO vehicle for 24 hours, then washed with PBS and harvested in 1 mL of TRI Reagent (Sigma). RNA was isolated with 1-bromo-3-chloro-propane and precipitated with isopropanol as instructed by Sigma, washed with 70% Ethanol, resuspended in 50 μL of RNase-free water, and stored at -80°C. RNA quality for reverse transcription and PCR was confirmed by the ratio of UV absorbance at 260/280 nm, quantified by Nanodrop, which ranged between 1.91 and 2.02. cDNA was made from 2 μg (100 ng/μL) of total RNA using the High

Capacity Reverse Transcriptase kit (Applied Biosystems), according to the manufacturer's instructions.

Genes that were upregulated in NIH3T3 cells by lentivirus-infected PPARγ in previously published work [90], either specifically or by more than one PPAR species, were selected for qPCR analysis. PCR primers were designed and verified for specificity in the mouse transcriptome using Primer-BLAST (NCBI) with obligate inclusion of an intron in the PCR product and, when possible, an exon junction within the primer sequence. Primer sequences are listed in Table 1. Gene expression was analysed by end-point PCR using the Amplitech Gold DNA polymerase kit, or by quantitative PCR using ABsolute Blue QPCR CYBR Green Low Rox mix (Thermo Scientific), with 2 µL of the cDNA-containing product as template. End-point PCR products were separated by electrophoresis on a 2% agarose gel and visualized by ethidium bromide UV fluorescence. qPCR products were synthesized and detected using the Stratagene MX3000P thermocycler, and assessed for the presence of nonspecific amplification by multiple absorbance peaks; minimum threshold of detection was determined automatically. Gene expression was normalized to PPIA as the internal control using the $2^{-\Delta\Delta CT}$ method [91].

Table 1. PCR Primers for Measurement of PPARγ Target Gene Expression.
*, Primers do not amplify human PPARG cDNA; PCR product spans two introns

**, Primers amplify both the human and mouse PPARG cDNA; no introns in the PCR product

Gene symbol	Forward primer	Reverse primer	PCR product size, bp	Primer spans exon junction
Fabp4	CCCTCCTGTGCTGCAGCCTT	GTGGCAAAGCCCACTCCCACT	148	yes
Adipoq	AGGGAGAGAAAGGAGATGCAGGTCT	ACAGTGACGCGGGTCTCCAG	181	yes
Cd36	TGTGGAGCAACTGGTGGATGGT	CGTGGCCCGGTTCTACTAATTCATGC	148	yes
Plin4	AGACTGCCACCTCCAGCCCC	TCCGGGCAGAGCTGAAGCCA	133	yes
Pcx	GGTGCTTGGCTGGTACAAGATGC	CGCCGGACATTTGGGGAGGC	111	yes
Pla2g16	AGCAAAGGCATCCACGCTGC	CTGCCCCAGCTCCTGCGATT	198	yes
Cpt2	GAAGCAGCGATGGGCCAGGG	CAGGGGCAAAGCCACCGAGG	181	yes
Acox1	TGCTGCAGACGGCCAGGTTC	GGCCAGACTGCCACCTGCTG	133	yes
Hsl	AGGCCTCAGTGTGACCGCCA	GCAGGCGGCTTACCCTCACA	200	yes
Facl2	TGCCTGAGCTTGCCCGGAGA	ACACACCTCACCCTCGCCCT	126	yes
*mPPARG**	ACGGGGTCTCGGTTGAGGGG	TCCGAAGTTGGTGGGCCAGA	182	no
*PPARG***	CTCCAGCTGAAGCTGAACCAC	AAATGTTGGCAGTGGCTCAG	209	no
Sncg	CAAGGAGCAGGCCAATGCCGT	CCAAGTCCTCCTTGCGCACCAC	125	yes
Mtap2	CAGCCACAGTGGAGGAAGCAGC	GACCTGGTGGTCCGTCGTGC	229	yes

2.10 Chromatin Immunoprecipitation

NIH3T3 cells were grown in 100mm dishes and transfected with expression plasmids for biotinylated PPARγ (pNBio WT, E157D, 5.5 µg, or empty vector, 4.5 µg), RXRα (1 µg), tet-off (1 µg), GFP (1 µg), and the empty pNBio vector (3.5 µg), mixed with 36 µL Lipofectamine 2000. Cells were incubated with 25 uM biotin for 48 hours, then crosslinked in 1% formaldehyde and harvested. Chromatin was sheared using the Branson 450 digital sonicator in repeated 15-second bursts optimized to yield 500-1000 bp-long DNA fragments, then precipitated with streptavidin-coated beads, washed and eluted as previously described [92]. Input and precipitated DNA

samples were analyzed by PCR using primers for the mouse aP2 PPRE region (forward: 5'- GCC ATG CGA CAA AGG CAG AAA -3', reverse: 5'- GTG TTT GGG CTG TGA CAC TTC C -3'), mouse adiponectin promoter spanning the region that is aligned with the human PPRE (forward: 5'-CTT ATG GGA AAG GGA GGT CTC C-3', reverse: 5'-AAT AGC CAA TGA GTG GGC CC-3'), and a control region downstream of the aP2 gene which contains no known PPREs (forward: 5'-CTG TCC CCT GTA CAC CGT CT-3', reverse: 5'-TCT CTT GGA ACT GGT AGC GCA G-3').

2.11 Microarray Analysis of Gene Expression.

NPγ2WT and NPγ2E157D cells were grown in 6-well plates and treated with 20 μM Rosiglitazone or DMSO vehicle for 24 hours. NPγ2 cells were thawed from frozen stocks for three independent experiments. Total RNA for microarray hybridization was isolated as described above, purified on RNeasy columns (Qiagen) and diluted to 50 ng/μL. RNA integrity measured by Agilent Bioanalyzer 2100 ranged between 7.2 and 10. The average RNA integrity number was uniform across treatments (Figure 4). RNA was amplified using cDNA synthesis and purification, followed by in vitro cRNA transcription, then hybridized to Illumina Mouse WG-6 v2.0 cDNA arrays as directed by the manufacturer. The Illumina gene expression image files obtained from the Illumina iScan scanner were uploaded to GenomeStudio (version 2010.3) using the Gene Expression module (v1.8.0). The quality of the samples was assessed using the Control Summary plots; all samples were accepted for analysis based on the number of genes detected (Figure 5 A; acceptable number is 10,000 - 15,000 genes) and the signal-to-noise ratio (Figure 5 B; typically close to 40). No outliers were detected on a dendrogram of all the

samples (Figure 6). Data were normalized using the Rank Invariant method. Differentially expressed probes were identified using the Illumina Custom Error Model with Benjamini and Hochberg False Discovery Rate. The genes considered to be differentially expressed were uploaded to the Genomatix Software Suite to determine over-represented Gene Ontology Biological Processes.

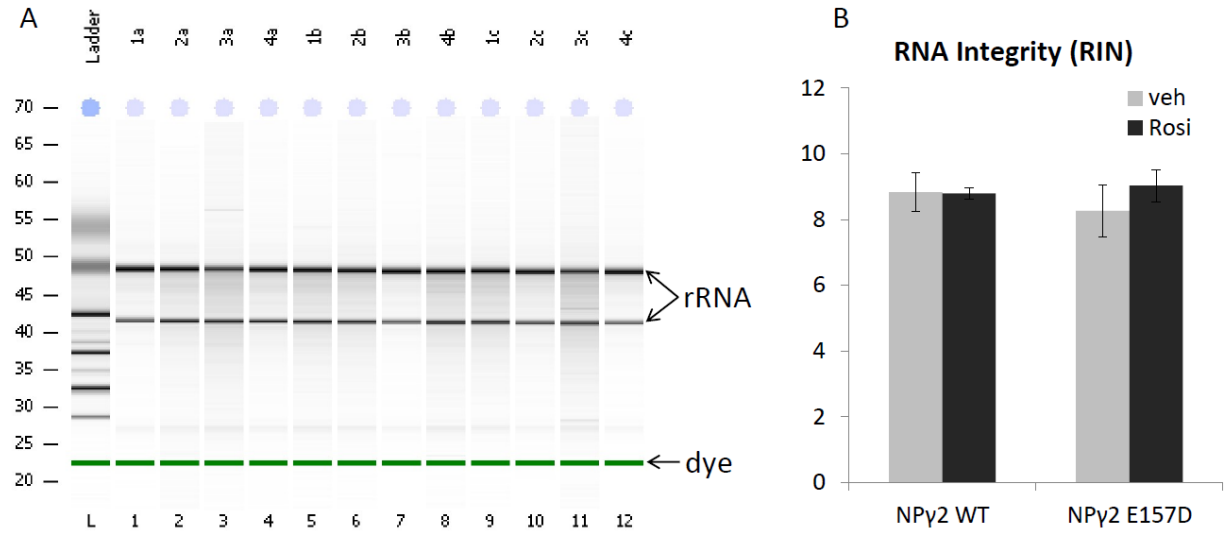

Figure 4. RNA Integrity in Hybridized Microarray Samples, as Assessed By the Bioanalyzer 2100.

A, Total RNA before amplification. Sample identification numbers at the top of the lanes are: 1:WT; 2:MUT; 3:WT+Rosi; 4:MUT+Rosi. a, b and c denote the replicate numbers. B, RNA integrity number (RIN) by sample. No differences between groups were detected by ANOVA.

A

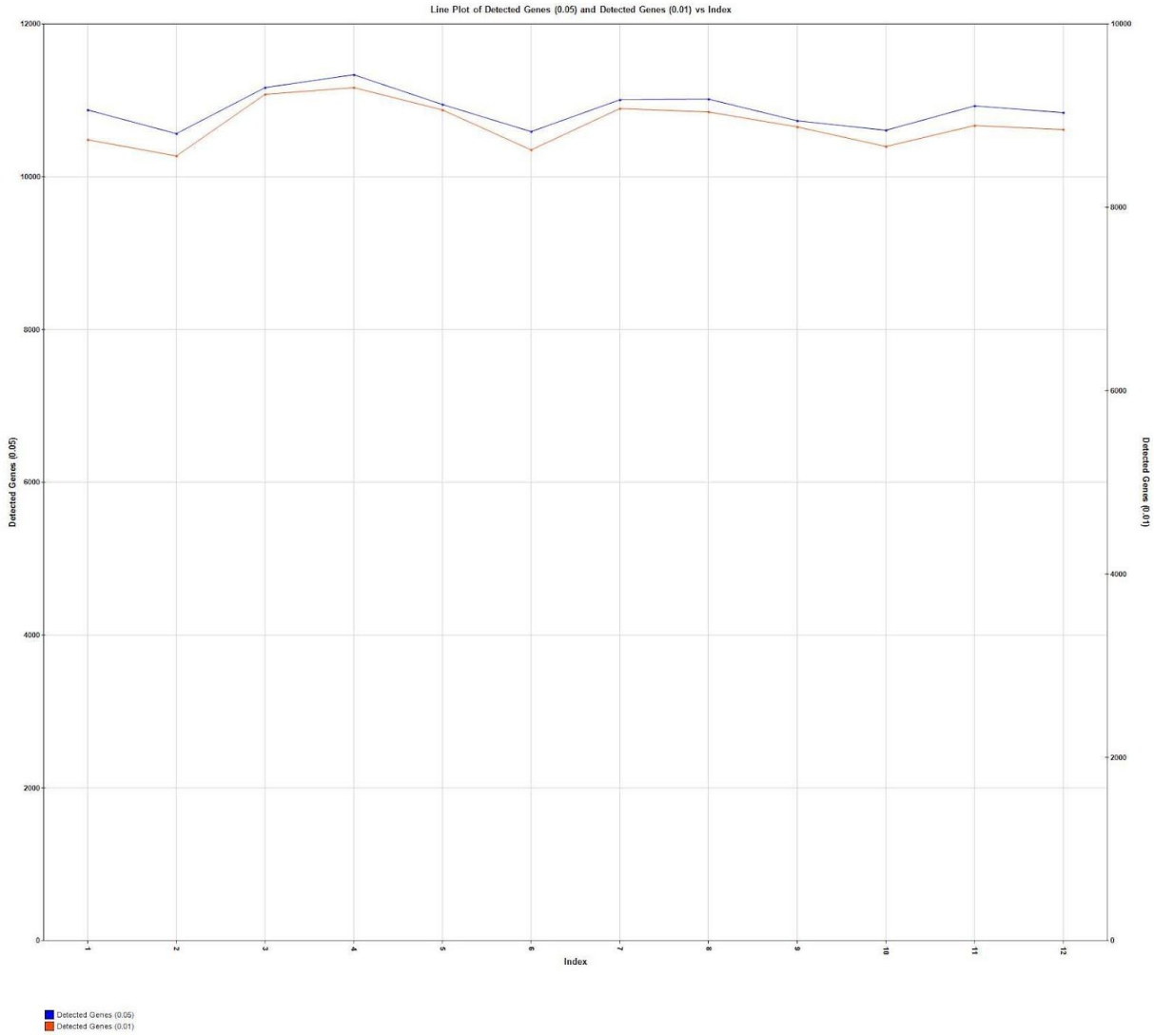

B

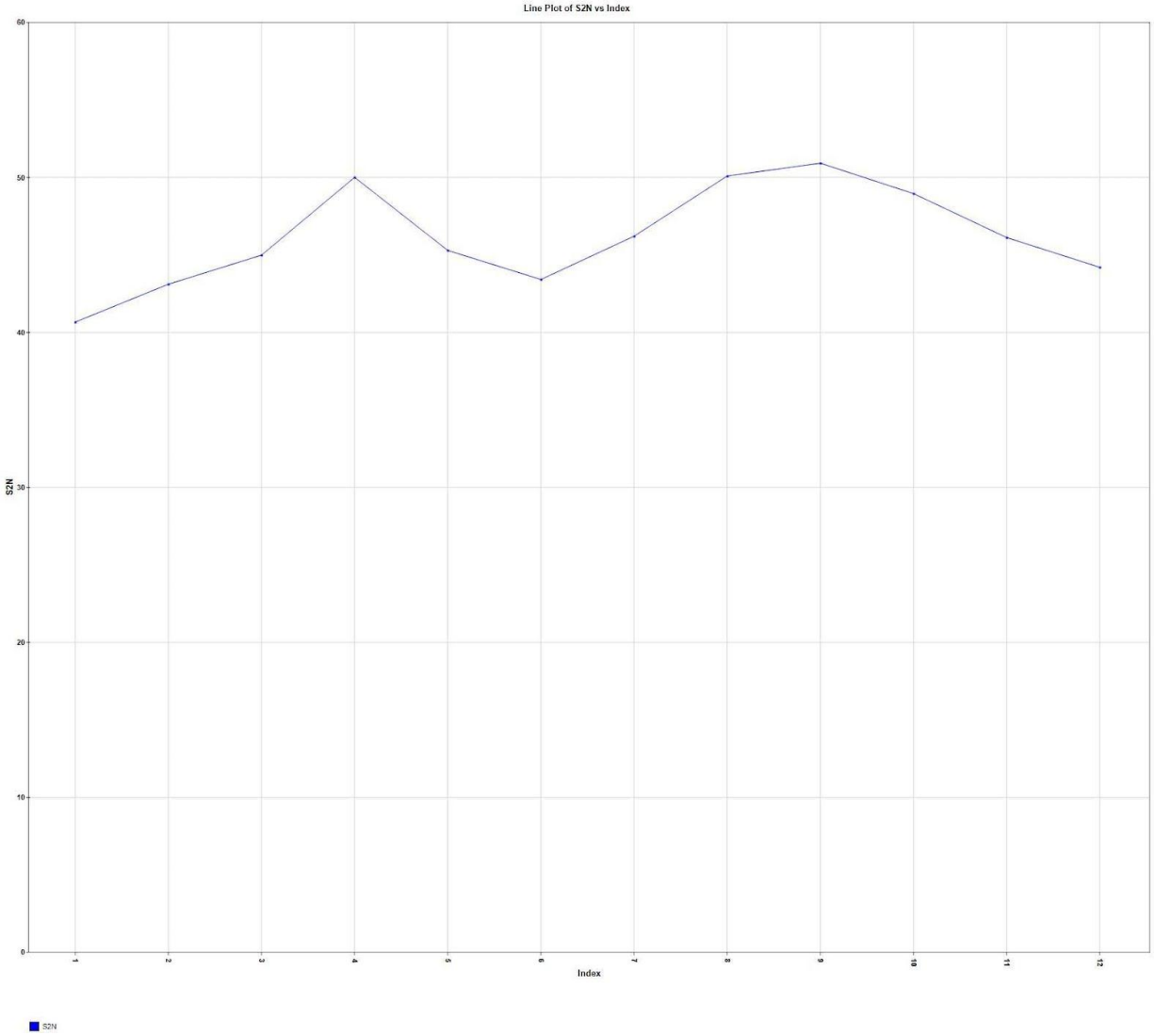

Figure 5. Summary of Quality Control Measurements for Hybridized Microarray Samples.

A, Total number of detected genes detected on hybridized arrays at the 95% (blue line) and 99% (red line) confidence level, in each hybridized sample. The index on the x-axis indicates sample identification: 1-4, replicate a; 5-8, replicate b; 9-12, replicate c; order is WT, WT+Rosi, MUT, MUT+Rosi for each set of replicates. B, Signal-to-noise ratio for each sample presented as in panel C.

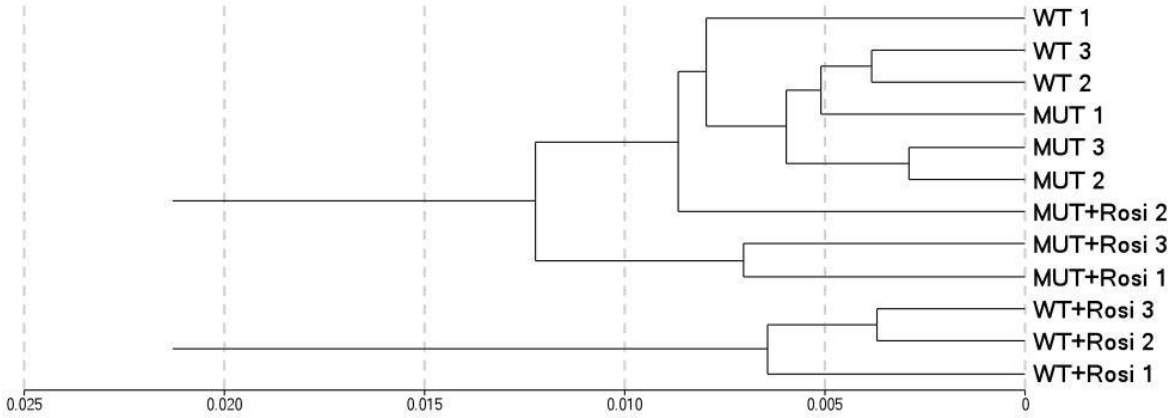

Figure 6. Dendrogram of All Hybridized Microarray Samples.

2.12 Bioinformatic PPRE Prediction.

Gene promoters were defined by the Gene2Promoter function of Genomatix and searched for PPARγ binding sites consistent with the matrices generated by Lefterova et al. (defined in Genomatix MatInspector as V$PPARG.02) and Nielsen et al. (V$PPARG.03). All of the gain-of-function promoters and 1000 randomly selected promoters of the loss-of-function set were scanned for PPREs. The incidences of PPREs in the promoters of gain-of-function and loss-of-function genes were compared using Fisher's exact test. Human-mouse promoter alignments were done in Rvista 2.0 [93], which was also used to confirm the presence of the putative PPREs.

3 *In Silico* ANALYSIS OF E157D PPARγ STRUCTURE

3.1 E157D Is Not a Tolerated Change in Nuclear Receptor Sequence Alignment.

To gain a better perspective on the importance of glutamate 157 for PPARγ function, we analyzed the E157D mutation using SIFT, a program that predicts the functional impact of protein mutations based on the conservation of the mutated site in homologous proteins. Because the phenotypic impact of the E157D mutation in humans is already known in detail, the major goal of this experiment was to examine glutamate 157 as it relates to other members on the nuclear receptor superfamily. SIFT generated an alignment of 86 homologous human protein sequences centered around position 129 of PPARγ1, with a median sequence conservation score of 3.16, indicating that the prediction was not based on sequences that are too closely related. The E to D substitution was assigned a score of 0.00, indicating that this mutation is extremely likely to affect protein function. Given that the biochemical properties of the wild-type and mutant amino acids are taken into account in generating the score, the extremely strong score for the subtle E to D mutation indicates that either the glutamate at position 157 is very highly conserved across different nuclear receptors, or that steric effects play a major role in this part of the protein. The first explanation is unlikely considering our knowledge of the variability of nuclear receptor p-box sequences; in fact, HNF4 is one nuclear receptor which has an aspartate in position 157, although the remainder of its p-box sequence is also very different from PPARγ. The proximity of the p-box to the DNA molecule may require very precise steric structure in order to properly recognize and bind the DNA, and the aspartate in position 157 may not be

viable for interacting with the DNA molecular without also changing the neighboring amino acids in the alignment. Clearly, glutamate 157 is an important part of the p-box, and even such a minor change as deletion of one unit of its carbon chain results in major changes in the protein function.

3.2 E157D Is Not Predicted to Change PPARγ Backbone Structure.

Having ascertained that glutamate 157 is of crucial functional importance for PPARγ, we used in silico modeling to predict the effect of the E157D mutation on PPARγ structure. Figure 7 shows the crystal structure of the PPARγ1-RXRα-PPRE complex in Swiss-Pdb viewer. Glutamate 129 (equivalent to the glutamate 157 in PPARγ2) is located at the base of helix 1 of the DNA binding domain, and the side chain protrudes directly into the major groove of the PPRE 5' half-site. The GROMOS energy minimization algorithm within the Swiss-Model software was applied to both the wild-type PPARγ template, and to its E129D mutated version. The backbone structure of the protein was not detectably altered by the mutation (Figure 7 A and B). Notably, mutating the same site to an alanine, glycine or histidine also did not alter the structure of the backbone, indicating that the functional importance of this site is not likely to be due to its effect on protein folding.

3.3 E157D May Compromise the Hydrogen Bonding Between PPARγ and the PPRE Molecule.

The close relation of glutamate 157 to the PPRE molecule prompted us to examine its hydrogen bonding with the DNA and whether it is affected by the E157D substitution. Figure 7 C shows a magnified view of the helix 1 and the hydrogen bond that glutamate 129 makes with cytosine base of the guanine-cytosine base pair in position three of the 5' PPRE half-site (AG**G**TCA A AGGTCA). In panels D - F of Figure 7, three energy-favorable conformations of the mutated aspartate side chain are shown, of which only one variation comes within hydrogen bonding distance of the cytosine base, and this distance is longer (3.30 Å) than the wild-type hydrogen bond (3.02 Å). The shorter carbon chain of aspartate compared with glutamate moves the carboxyl group further away from the nitrogen atom on the cytosine base, weakening or eliminating the hydrogen bond.

An important limitation of this approach is the fact that the topologies of nucleotides and sugars are not yet supported by the GROMOS algorithm, so the PPRE structure was not taken into account for energy minimization. Our conclusion about the mutant protein-DNA relationship is made on the assumption that the mutated DNA binding helix fits into the major groove in exactly the same spatial relationship as the wild-type, which is not necessarily true. To confirm our findings with another *in silico* approach, we used the Monte Carlo energy minimization algorithm within the ICM-Pre Mol-Soft program, which includes nucleic acids and works on a local environment for a defined residue rather than the whole protein. Using this approach, we detected the hydrogen bond between glutamate 129 and cytosine 4012, which was lost after mutating the glutamate to aspartate (not

shown), with a similar lengthening of the bond distance as we observed using the GROMOS force fields within the Swiss-Model program.

Another important limitation for *in silico* structural analysis, which requires a template with known structure, is that the crystal structure has only been resolved for the consensus PPRE, so any structural changes induced to the protein by various DNA sequences are not taken into account in our experiment. Our in-vitro studies that followed were designed to address the fine differences between various PPRE sequences in their interaction with the wild-type and mutant PPARγ.

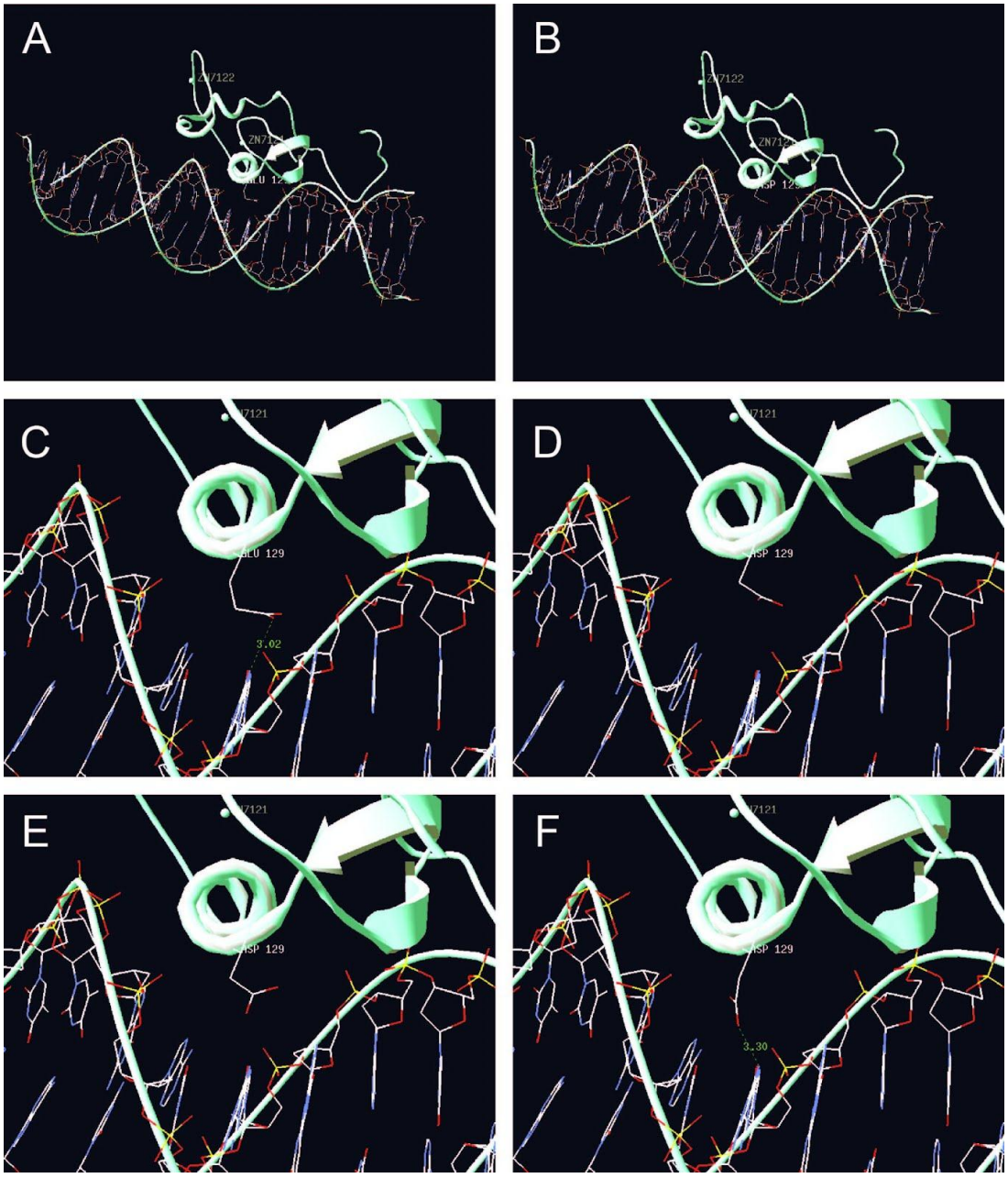

Figure 7. In Silico Modeling of E157D PPARγ.

DNA binding domain of WT (A) and MUT (B) human PPARγ1 with a transverse view of helix 1. The ligand-binding domain of PPARγ and the entire RXRα protein, as well as their respective ligands, were hidden from this view to expose the p-box PPARγ region. E129 of human PPARγ1, shown here, is equivalent to E157 of PPARγ2. C, Hydrogen bond contact between E157 and the PPRE. D-F, Hydrogen bond contacts of various orientations of D157 with the PPRE.

4 E157D PPARγ TRANSCRIPTIONAL ACTIVITY IN REPORTER ASSAYS

4.1 NIH3T3 Cell Line and the Transient Transfection System.

We selected the NIH3T3 cell line for our transient transfection and, later, lentiviral infection experiments. This is a mouse fibroblast cell line that does not express endogenous PPARγ, allowing us to study the activity of the mutant protein overexpressed transiently or by stable infection, without interference by the endogenous wild-type protein. NIH3T3 cells are efficiently (30%-50%) transfected with lipophilic agents, and have been widely used as a host cell line for transient transfection studies of PPARγ activity using the luciferase reporter gene system.

To examine the effect of the E157D mutation on the transcriptional activity of PPARγ, we used a luciferase reporter assay in a transiently transfected cell culture model. The luciferase reporter assay is commonly used to quantify the activity of transcription factors with well-defined DNA binding motifs [94] [95], to characterize regulatory DNA elements [96-98], and has been used to measure the transcriptional activity of PPARγ on various PPREs [99-102], as well as its responsiveness to various ligands [103-106]. Our transcription reporter plasmid contains the firefly luciferase reporter gene under the control of the thymidine kinase promoter, with each of the PPREs listed in Table 2 inserted directly upstream of the promoter. Thus, each reporter plasmid is identical except for the 25-base-pair PPRE sequence, allowing us to directly examine the influence of the DNA binding site on the transcriptional activity of PPARγ. When PPARγ is present in the cell, it binds to the PPRE and enhances the basal level of luciferase transcription, which is quantified by measuring luciferase activity in a luminescence assay of the

cell lysate. Addition of the PPARγ ligand rosiglitazone further increases the transcriptional activity readout.

Table 2. PPREs from Known PPARγ Target Genes.

The DR1 sequence for each PPRE is shown in bold-face. *, PPRE sequence is in the non-coding strand of the gene.

Gene symbol	PPRE symbol	PPRE sequence	Location rel. to TSS	Function	Species	Ref.
Fabp4	ARE7	CTTACT**GGATCAGAGTTCA**CAGATC	-5360	Intracellular lipid metabolism	mouse	[43]
Fabp4	ARE6	CTCTCT**GGGTGAAATGTGC**ATTTCT	-5263	Intracellular lipid metabolism	mouse	[53]
Slc27a1	FATP	AGAAGA**AGGGGAAAGGGCA**GGAAGG	-489	Intracellular lipid metabolism	mouse	[107]
Lpl	LPL*	GGAAGT**GGGGCAAAGGGCA**CAGGAT	-160	Lipolysis of circulating triglycerides	rat	[108]
Adipoq	ADN*	GAAGAT**GGGGCAAAAGTCA**AAACCA	-250	Adipose derived hormone	human	[109]
Sorbs1	CAP	TGACAC**AGGCTAAAGGTCA**TCTGAA	-1090	Intracellular signal transduction protein	mouse	[110]
Aqp7	AQP7*	TTCTCC**AGGGGAGAGGTCA**GTAGGG	-93	Membrane channel; water balance	mouse	[111]
Me1	MEp	CTTTCT**GGGTCAAAGTTGA**TCCCCC	-382	Pyruvate metabolism	mouse	[49]
Acox1	ACO*	GGGACC**AGGACAAAGGTCA**CGTTCG	-572	Fatty acid beta-oxidation	rat	[112]
Pck1	PCK2	ACAACT**GGGATAAAGGTCT**CGCTGC	-998	Gluconeogenesis	rat	[113]

4.2 E157D PPARγ Transcriptional Activity on Various PPREs.

Transient transfection of NIH3T3 cells with PPARγ1 expression plasmids resulted in equal protein levels of the wild-type and E157D PPARγ1 (Figure 8 B), indicating that the mRNA stability, translation dynamics and protein turnover are not likely to be affected by the mutation. The codon frequency change corresponding to the E157D mutation is insignificant (0.03 to 0.026 [114]), so it is unlikely that tRNA availability would affect the rate of the mutant protein synthesis.

PPARγ1 significantly induced luciferase transcription from several well-characterized PPREs compared to the empty vector control (Figure 8 A), and addition of a receptor-saturating concentration of rosiglitazone further enhanced the transcription activation approximately two-fold, validating our assay system. The E157D mutant PPARγ1 was also transcriptionally active on many of these PPREs, and was responsive to ligand activation similarly as the wild-type receptor. However, the transcriptional activity of E157D PPARγ1 was quantitatively lower on almost all PPREs we tested. In fact, there was only one construct - the full extended promoter from the aP2 gene - that was more transcriptionally active in the presence of the mutant PPARγ than the wild-type. Furthermore, we observed that the extent of the transcriptional defect conferred by the mutation was not uniform across all PPRE sequences, but displayed a wide range of behaviors when normalized to the wild-type level of transcription (Figure 9 A). The E157D mutant PPARγ1 had wild-type level of transcriptional activity on the ACO PPRE, was mildly to moderately transcriptionally defective on the ARE6, FATP, ADN and MEp PPREs, and it was transcriptionally dead (no difference compared with the empty vector control) on the full promoter from the FATP gene, the LPL, AQP7 and PCK2 PPREs.

We repeated the experiment with several of the PPREs using PPARγ2 and found that the E157D mutant PPARγ2 behaves similarly as the mutant PPARγ1 when compared to the respective wild-type protein (Figure 8 C and 9 B). The mutant γ2 isoform activates gene transcription from the four PPREs we examined, and is further induced by rosiglitazone. However, the mutation reduces its transcriptional activity compared with the wild-type PPARγ2, and this reduction is not the same on all PPREs. As with the γ1 isoform, the effect of the E157D mutation is greater on the FATP and MEp PPREs than it is on the ACO and ARE6 PPREs. There appears to be no isoform-specific effect of this mutation. This is not surprising given our knowledge that the two PPARγ isoforms behave similarly in *in vitro* studies of transcriptional activity, and we have not explored any differences between the isoforms further in this project.

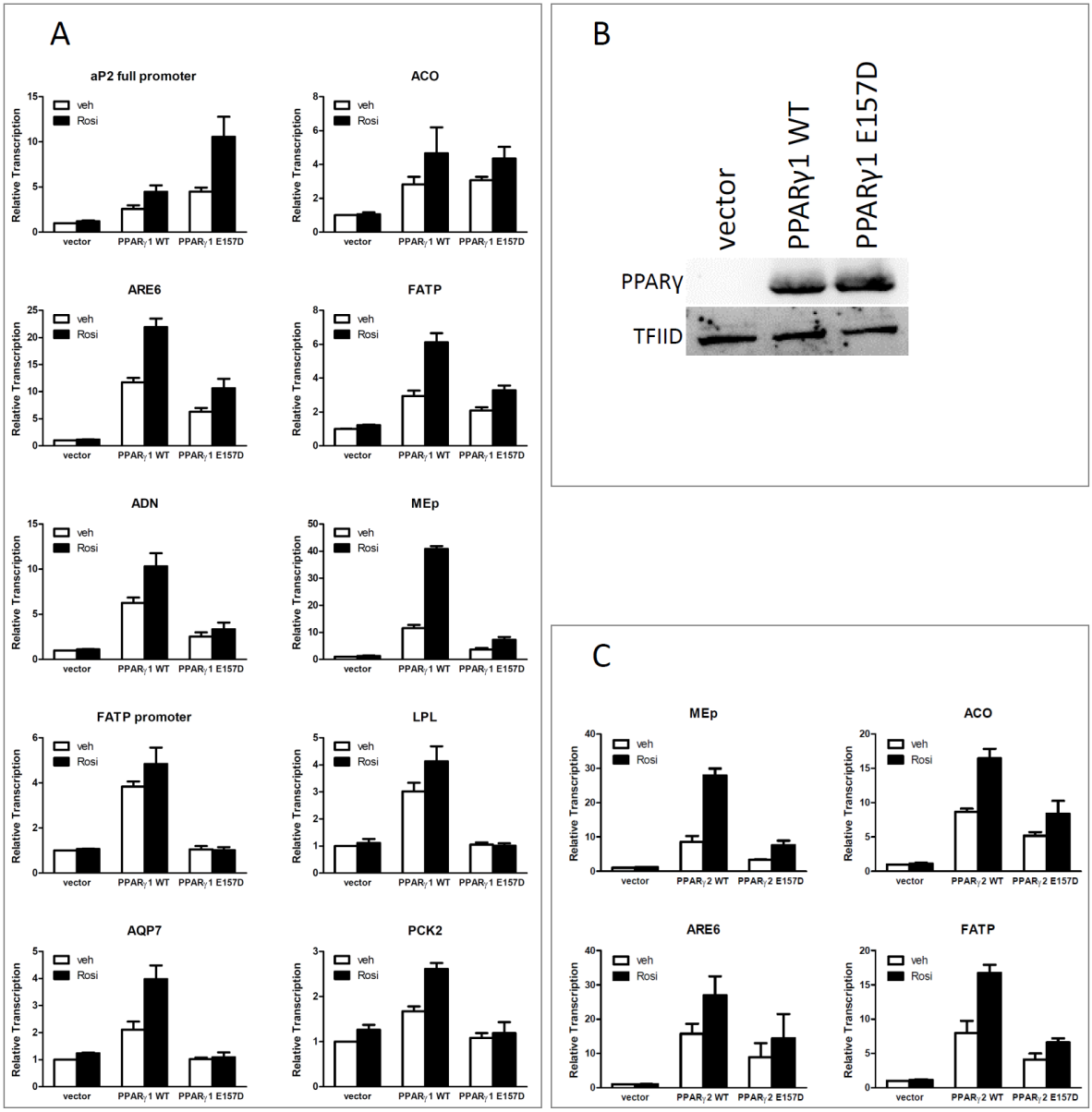

Figure 8. E157D PPARγ Transcriptional Activity in Luciferase Reporter Assays.

A, PPARγ1 wild-type, E157D or empty vector was transiently transfected into NIH3T3 cells with indicated reporter plasmids, and cells were treated for 24 with rosiglitazone (Rosi) or DMSO vehicle (veh). B, Western blot of PPARγ1 expression in transfected cells. C, PPARγ2 transcriptional activity was measured the same way as in A. Data are means and standard errors of at least two independent experiments.

A

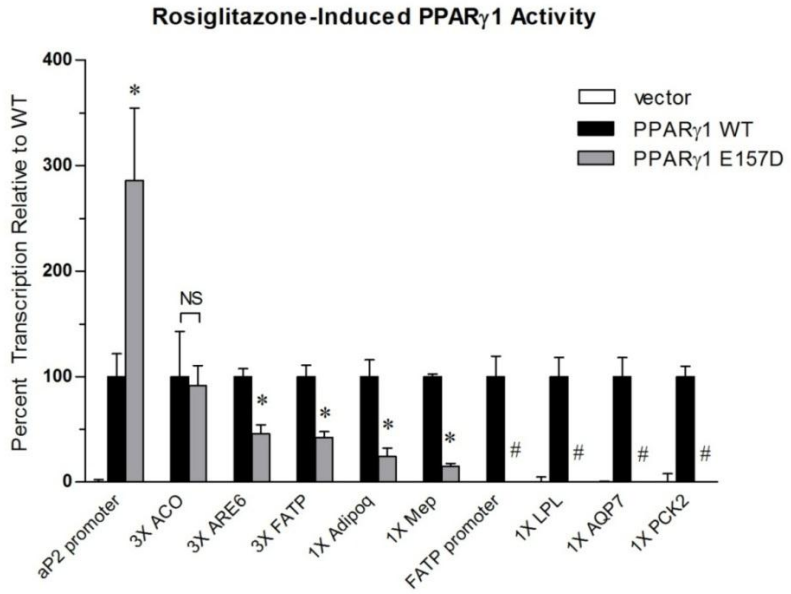

B

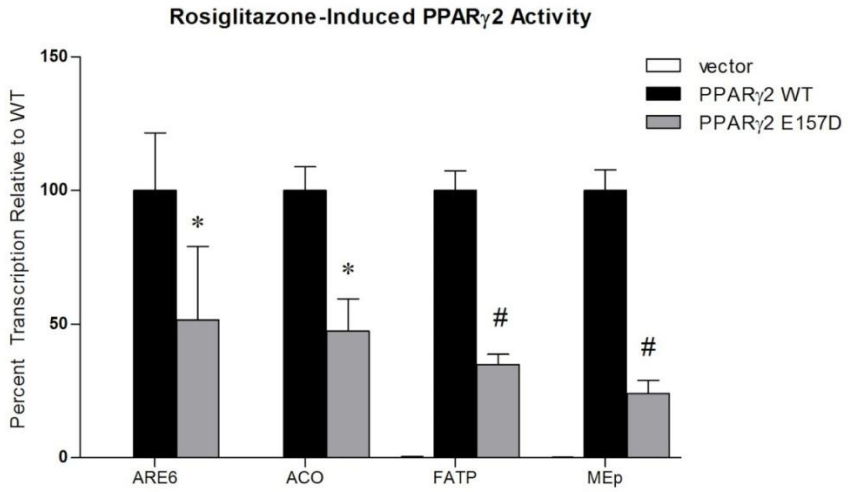

Figure 9. Normalized Transcriptional Activity of PPARγ in Luciferase Reporter Assays.

A, E157D PPARγ1 or B, E157D PPARγ2 transcriptional activity relative to wild-type. Data are means and standard errors of at least three independent experiments. *, $p<0.05$ compared to WT on the same PPRE. #, no difference compared with vector.

4.3 E157D PPARγ Responds to Ligand Activation and Lacks Dominant Negative Activity.

We examined two commonly-occurring mechanisms through which the E157D mutation could potentially decreased the transcriptional activity of PPARγ: decreased ligand responsiveness and dominant negative activity. We considered it unlikely that this DNA-binding domain mutation could reduce the ligand responsiveness of PPARγ, as no such cases have been reported and it is generally believed that the ligand-binding domains of nuclear receptors act independently of their DNA-binding domains. Furthermore, it was evident from our data that the mutant receptor is at least partially activated by saturating concentrations of the synthetic ligand rosiglitazone. However, a mild decrease in endogenous and synthetic ligand affinity could account for the overall reduction of transcriptional activity by the mutant PPARγ. To assess the effect of the E157D mutation on PPARγ ligand affinity quantitatively, we constructed a rosiglitazone dose response curve of luciferase transcription by the wild-type and E157D PPARγ1. When the maximum transcription level is set to 100% for each receptor, the ligand response curves are sigmoid-shaped as expected and are identical for the wild-type and the mutant on the FATP PPRE (Figure 10), indicating that the ligand affinity of PPARγ is not affected by the E157D mutation.

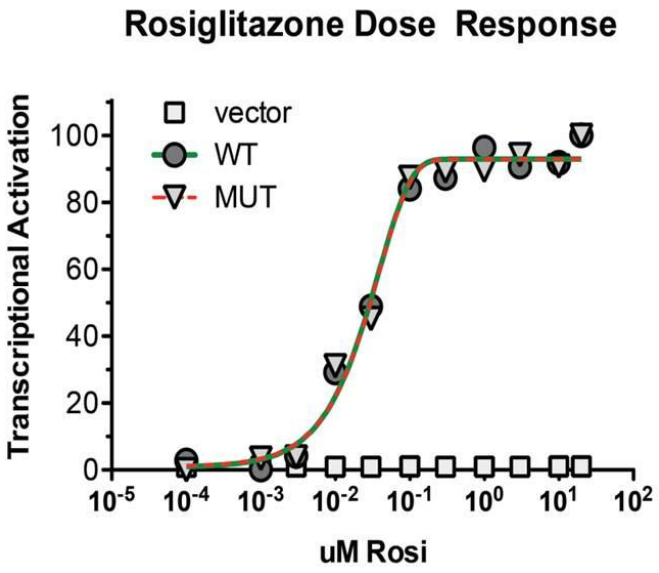

Figure 10. Rosiglitazone Dose Response Curve.

Wild-type (WT) or E157D (MUT) PPARγ1 was transfected into NIH3T3 cells with the FATP PPRE-luciferase reporter plasmid and treated for 24 hours with increasing concentrations of rosiglitazone (Rosi). Data are means of three experiments, normalized to the maximum transcriptional activity for each receptor. Best-fit dose response curves were constructed in GraphPad using the single binding site Michaelis-Menten model.

The potential for any dominant negative activity of the E157D PPARγ was important to assess. The nuclear receptor transcription activation cycle includes DNA binding, interaction with coregulators, chromatin remodeling, initiation of transcription, and release from the promoter with subsequent degradation by the ubiquitin-proteasome system [10, 115-117]. Such cycling of the receptor on and off the target gene promoters is needed for fine-tuned regulation of gene transcription in responses to changes in ligand stimulation. In the condition of continuous presence of ligand, the release of ubiquitinated PPARγ from the PPRE and binding by the next PPARγ molecule is required for continued gene transcription [118-120].

Dominant-negative DNA-binding domain PPARγ mutants have been described [56], and the direct interaction between glutamate 157 and the DNA binding site raises the possibility that this mutation may disrupt the release of PPARγ from the PPRE. In this case, the mutant receptor would bind the PPRE and activate one round of transcription, but fail to free the binding site for further transcriptional activation, making the PPRE inactive for prolonged periods of time. Our observations in the NIH3T3 cell model with ectopic D157D PPARγ overexpression had thus far supported this possibility. In the heterozygous condition, which is the naturally occurring state of this mutation, the dominant-negative E157D PPARγ would prevent the transcriptional activity of the wild-type, leading to the severe metabolic phenotype. On the other hand, previous in vitro studies involving p-box PPARγ mutations have not found a significant effect on DNA binding, and the subtlety of this glutamate-aspartate substitution suggests that a severe disruption in DNA binding and release may be less likely.

To assess the E157D PPARγ for dominant negative activity, we conducted a competition experiment in which both the wild-type PPARγ and increasing amount of the mutant receptor were co-transfected into the same cell in the context of our established transcription reporter assay. As shown in Figure 11, increasing the amount of wild-type receptor produced the expected rise in transcription, indicating that the amounts of transfected plasmid are within the linear portion of the PPARγ transcription curve. Adding increasing amounts of a known dominant-negative PPARγ mutant, P467L, produced the expected inhibition of transcription. This mutant binds DNA, but fails to bind ligands, initiate transcription, and release from PPRE, effectively blocking the wild-type PPARγ from transcribing on that PPRE.

When we added increasing amounts of the E157D PPARγ plasmid, however, no such inhibition of transcription was observed. On the contrary, there was a rise in transcription that did not reach the levels of the wild-type, consistent with decreased transcriptional activity of the mutant receptor. So, even though the mutation is inherited in an autosomal dominant pattern, there is clearly no dominant negative activity in the biochemical sense.

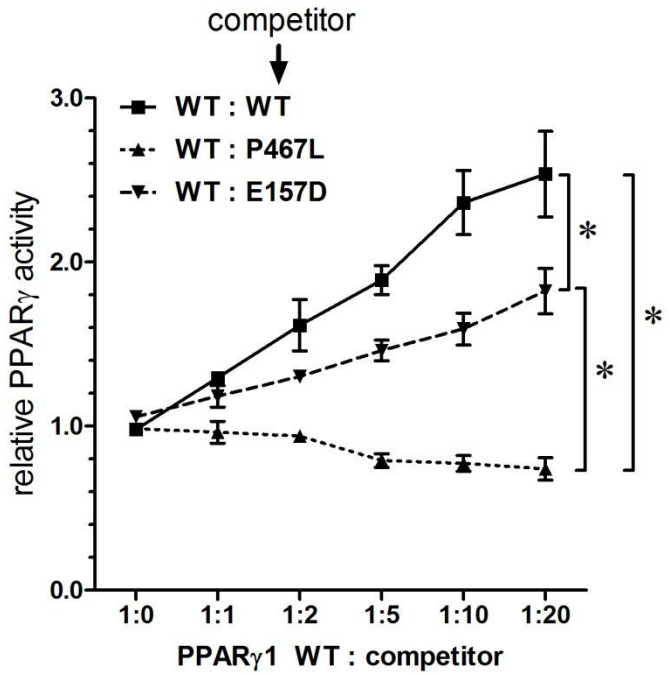

Figure 11. Competition Assay of PPARγ Transcrpitional Activity.

Wild-type and increasing amounts of indicated competing PPARγ1 receptor were co-transfected into NIH3T3 cells with no exogenous ligand. Data are means and standard errors of three independent experiments. *, $p<0.05$ determined by two-way ANOVA.

Our transcription reporter assays on heterologous promoters containing various PPREs have revealed that the E157D mutation generally reduces the

transcriptional activity of PPARγ through a mechanism that does not involve decreased ligand affinity or dominant negative activity. Furthermore, this reduction in transcriptional activity is dependent on the PPRE sequence and varies widely in its effect size compared with the wild-type receptor. These observations were consistent with our hypothesis that the mutation alters the DNA binding site selectivity of PPARγ and prompted us to examine the PPRE sequences tested here for patterns that may predict the behavior of the mutant. The receptor directly contacts the third nucleotide of the 5' half-site of the PPRE, one of the most highly conserved bases in the PPRE, and not surprisingly, all of the PPREs tested here contained a guanine in that position. We next examined the neighboring bases at positions two and four. The second base of the PPRE is a very highly conserved guanine; the fourth is variable and all four bases are represented in our set of assays, but we found no obvious correlation with the severity of the transcriptional defect. Clearly, the sequence of the PPRE is important in regulating the transcriptional activity of the mutant receptor, but we were unable to predict the identity of the base-pairs within the PPRE that would most strongly influence the receptor. The three-dimensional shape of the DNA molecule is a complex structure that is determined by more than just the immediate base-pair sequence [121-123], so a more rigorous analysis of how the mutant PPARγ interacts with various PPRE sequences was necessary.

5 E157D PPARγ BINDS DNA *In Vitro*

We examined the ability of E157D PPARγ to bind PPREs *in vitro* using the electrophoretic mobility shift assay (EMSA). In this assay, synthetic double-stranded biotinylated PPRE molecules (probes) are mixed with nuclear extracts from cells transfected with PPARγ in a binding reaction, then separated on a native polyacrylamide gel and blotted onto a positively-charged nylon membrane. The biotin-labeled probe is then detected using streptavidin, and a slow-traveling (shifted) band represents a protein-DNA complex, compared with the free probe which travels faster. Analysis of the relative intensity of the shifted bands also provides a semi-quantitative assessment of protein affinity for various binding sites. The EMSA has been used successfully to characterize novel PPREs ([99, 100, 124-127] and many more) and to determine the relative PPRE affinity of site-directed p-box PPARγ mutants [22].

We first established the validity of the EMSA using the consensus PPRE as probe. The binding reaction with nuclear extract containing either wild-type or E157D PPARγ produced a shifted band compared to the control nuclear extract, which was transfected with the empty vector (Figure 12). The shifted bands were of similar intensity, and the specificity of PPARγ binding to the probe was confirmed with a 200-fold molar excess of unlabeled PPRE, which eliminated the shifted band, and with a super-shifted band produced by adding the M2 Flag antibody, but not the IgG control. The ADN PPRE also bound the mutant receptor as strongly as the wild-type, a surprising finding considering that the mutant PPARγ was much weaker than the wild-type at transcribing from this same PPRE in our luciferase reporter assay (Figures 8 and 9).

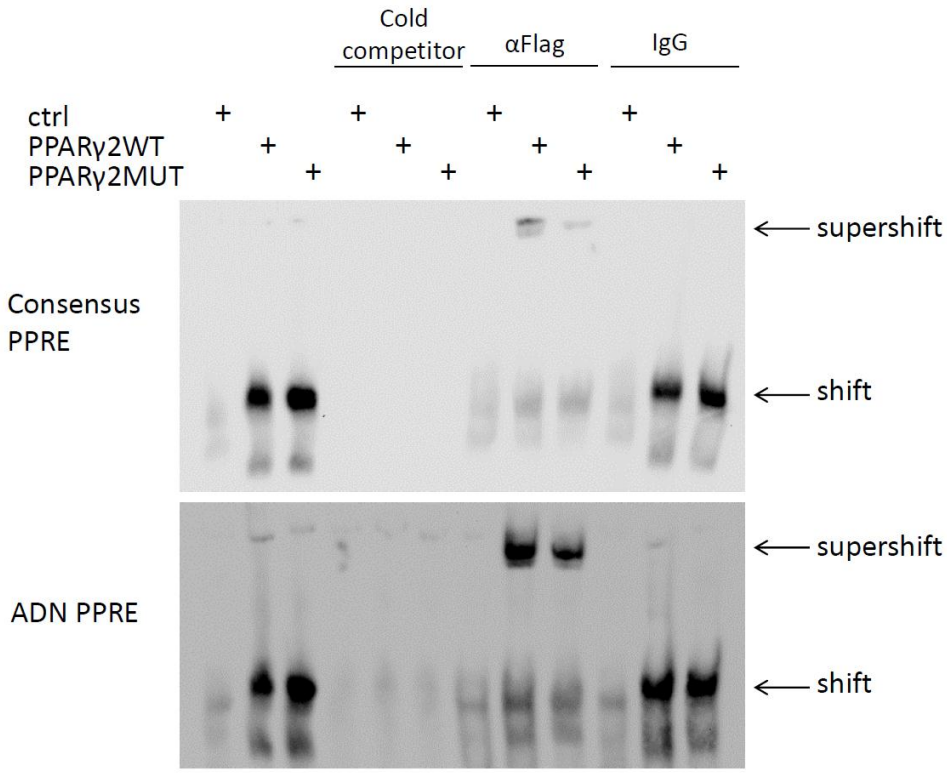

Figure 12. Validation of the Gel-Shift Assay.

Nuclear lysates from CHO cells transfected with the indicated plasmids were incubated in a binding reaction with the consensus (top panel) or ADN (bottom panel) PPRE, plus competitor or antibody, as indicated. Shifted and supershifted bands represent the PPARγ1-RXRα-PPRE complex.

It was possible that permissive EMSA binding conditions or saturating amounts of PPARγ in the binding reaction prevented us from detecting a difference in the binding affinity induced by the E157D mutation. We characterized the DNA binding activity of the mutant in more detail by testing increasing amounts on the nuclear extract and generated a binding curve using the relative intensities of the shifted bands (Figures 13 and 14). To our surprise, the E157D PPARγ bound all of

the PPREs that we tested with equal or slightly stronger affinity as the wild-type receptor.

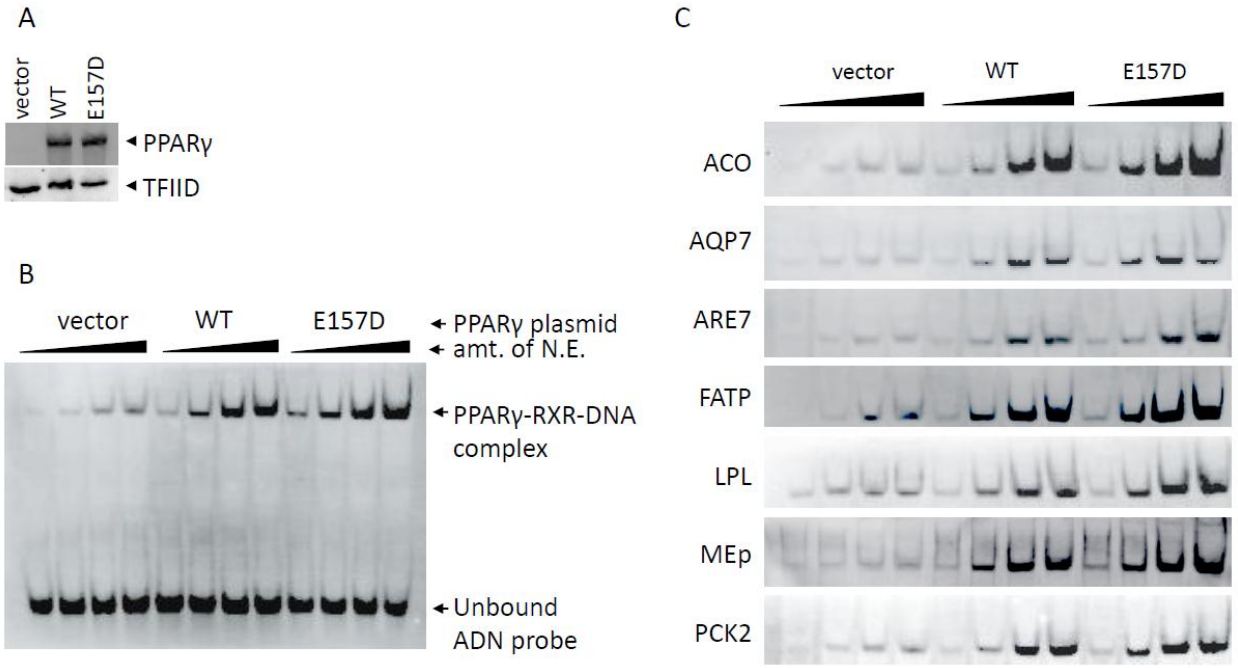

Figure 13. Gel-Shift Assay Blots.

A, Western blot of PPARγ expression in NIH3T3 nuclear extracts used for gel-shift assays. B, Representative gel-shift blot with the ADN PPRE probe and increasing amounts of indicated nuclear extracts. C, Shifted bands from gel-shift blots with the indicated PPRE as probe.

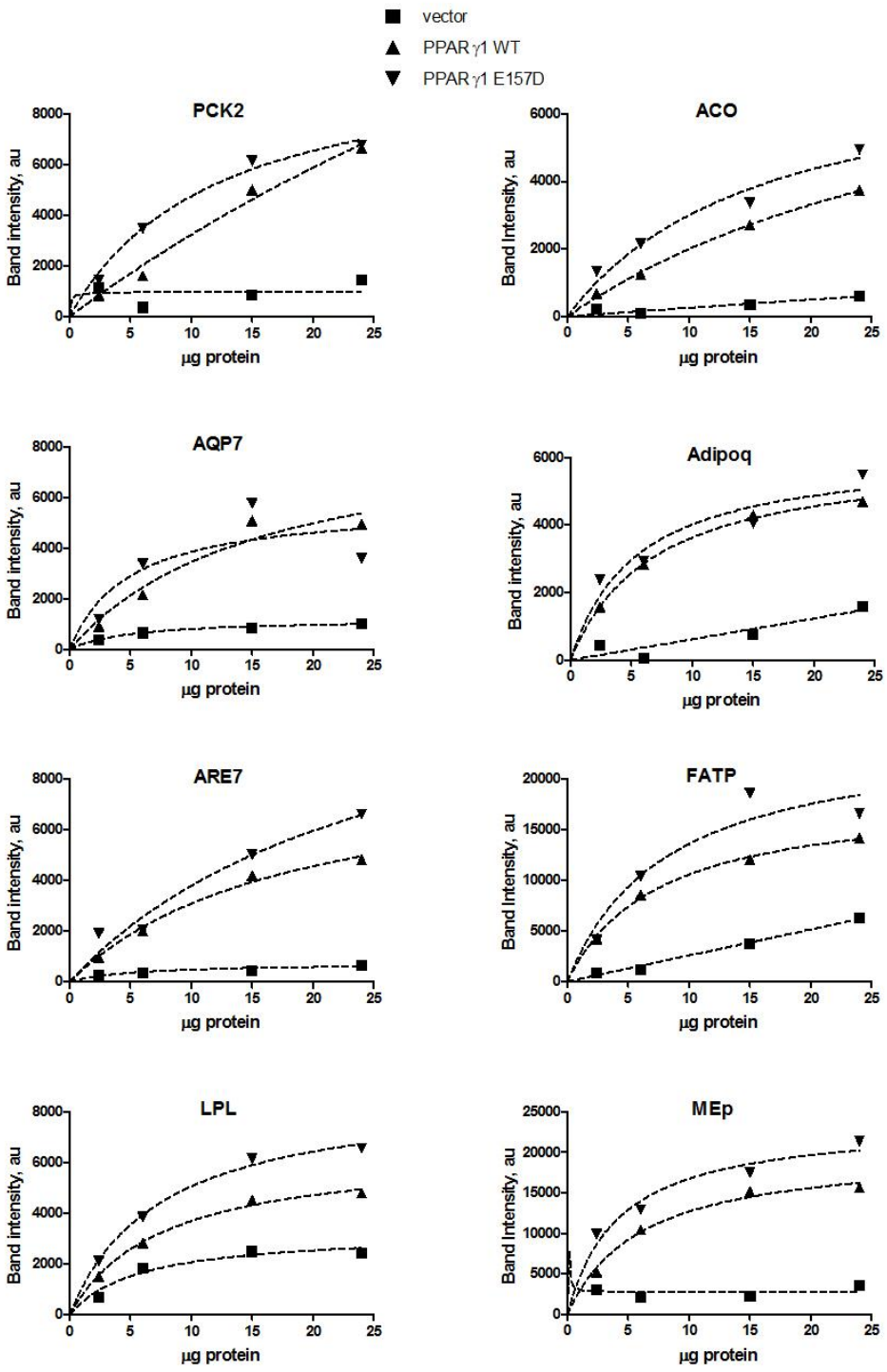

Figure 14. Gel-Shift Binding Curves.

Shifted band densitometry was performed with ImageJ, and best-fit lines constructed in GraphPad using either linear or exponential models.

These results contradict our original hypothesis that the E157D mutation disrupts the binding site selectivity of PPARγ: at least in the in-vitro binding conditions, the PPRE selectivity of PPARγ is unaffected by the mutation. However, our transcriptional activity assays showed that the mutant receptor is transcriptionally defective on most of these same PPREs. The E157D mutation appears to act by a more complex mechanism than a change in the DNA binding affinity of the receptor. A post-DNA binding event in the transcriptional activation cascade is disrupted, leading to decreased transcriptional activity with no dominant-negative of loss-of-function effect on its ability to bind DNA. Furthermore, the sequence of the PPRE is important in determining the extent of transcriptional defect of the mutant receptor, as discussed above. Considering the position of glutamate 157 in the major groove on the PPRE, it becomes clear that the PPRE-PPARγ interaction plays an important role in regulating PPARγ transcriptional activity, beyond just anchoring the receptor on the DNA.

6 E157D PPARγ HAS REDUCED TRANSCRIPTIONAL ACTIVITY ON ENDOGENOUS PROMOTERS

6.1 Generation of Stable PPARγ-Expressing Fibroblasts.

Our experiments thus far have shown that E157D PPARγ binds PPREs in vitro, but fails to induce transcription from most PPREs in the context of a heterologous promoter. Transcriptional activity on native chromatin may be regulated by additional factors including chromatin folding, methylation marks, and *cis*-acting regulatory proteins bound to nearby sites. In addition, overexpressed protein activity in our transient transfection system may be altered compared to normal levels of expression. To investigate the transcriptional activity of E157D PPARγ in a more natural setting, we used the lentiviral gene delivery system to generate NIH3T3 fibroblasts expressing equal, physiologically-relevant levels of the wild-type or E157D PPARγ.

The lentiviral expression plasmid recombines with endogenous DNA at random locations within the chromatin, with on average two insertions of the gene in each infected cell [128]. NIH3T3 cells are readily transduced with lentivirus [128], and have been used to establish PPARγ-expressing cell lines to study the transcriptional activity differences between the different PPAR isoforms [90]. The PPARγ protein expressed from a lentiviral insert in this system induces the expression of many known PPARγ target genes. The pLenti6.3 vector used in our experiments contains the CMV promoter driving the expression of the transgene and, in the same transcript, the blasticidin resistance selection marker, translated from in internal ribosome binding site. In a kill-curve experiment, 2 μg/mL - 10 μg/mL blasticidin concentrations were sufficient to kill non-infected NIH3T3 cells, so

we used the lowest effective 2 μg/mL concentration of blasticidin for all subsequent selection and maintenance of virus-infected cells. Cell death was not significantly induced in the lentivirus-infected wells, while all non-infected control cells were dead after seven days of selection, indicating that infection efficiency was high in our experiments. The infected cells were maintained for an additional week for a total of two weeks selection period before we started the gene expression experiments. We termed the established transgenic cell lines NPγ1WT (NIH3T3-derived PPARγ1 Wild-Type expressing cells), NPγ1E157D (expressing the γ1 isoform of the mutant receptor), NPγ2WT, NPγ2E157D (expressing the corresponding γ2 forms of PPARγ, and NLacZ (infected with the control Lac-Z coding vector).

Lentivirus-delivered PPARγ was expressed at the mRNA and protein level (Figure 15). Compared with the mouse differentiated 3T3-L1 adipocyte cell line, which expresses high levels of PPARγ, our lentivirus-infected cells expressed similar levels of PPARγ mRNA, but slightly reduced levels of the protein. Any regulatory elements of the native PPARγ transcript are absent from the lentiviral PPARγ expression vector, which contains only the cDNA and the Kozak sequence, so translation from this minimal transcript is likely less efficient than the native mRNA species, resulting in reduced protein levels. Nevertheless, PPARγ protein expression in our stable cell lines is likely comparable to the levels of its expression in non-adipose tissues. The control cell line was infected with the lentiviral vector for LacZ, and showed no detectable expression of the endogenous PPARγ gene in these cells. Lastly, we discovered that PPARγ protein expression decreased slowly over time with passaging the transduced cells. Loss of transgene expression in virus-infected "stable" cell lines is not uncommon after several passages, due to either expression

from non-integrated viral particles, silencing of the transgene, or selection for low-expressing cells if the transgene causes slower growth [129]. Therefore, all experiments were carried out using cell lines of equal age and passage number.

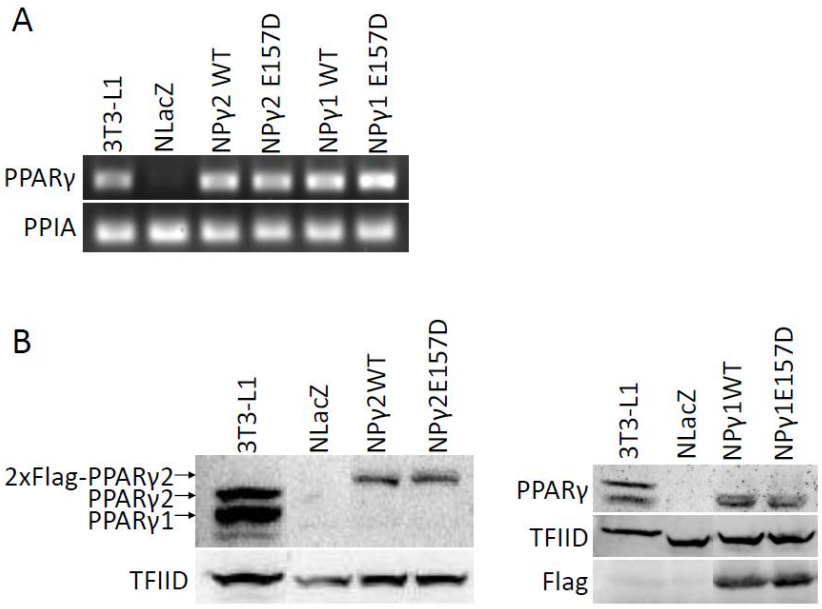

Figure 15. Transgene Expression in Stable Lentivirus-Infected Cell Lines.

A, mRNA and B, protein expression of PPARγ in the indicated lentivirus-infected cell lines or in differentiated 3T3-L1 adipocytes were measured in by rtPCR and western blot.

6.2 E157D PPARγ is Activated by Rosiglitazone on Endogenous Promoters.

To assess the transcriptional activity of E157D PPARγ on native gene promoters, we first confirmed that endogenous PPARγ target genes are induced by PPARγ in the lentivirus-infected expression system. We measured the expression of several genes reported to be induced by PPARγ in similar experimental conditions [90] using end-point reverse transcriptase-PCR after treating the cells for 24 hours

with 20 μM rosiglitazone. Four of the transcripts (fatty acid binding protein aP2, adiponectin, perilipin 4 and fatty acid transporter CD36) were upregulated in wild-type PPARγ2-expressing cells (Figure 16 A) and further induced by rosiglitazone. The adiponectin mRNA was upregulated after 3 hours of rosiglitazone treatment and reached maximal induction at 24 hours (Figure 16 B), indicating that the transcriptional dynamics of the lentivirus-expressed PPARγ are normal. Gene transcription induced by the E157D PPARγ2 failed to reach the levels of wild-type PPARγ2-induced transcription (Figure 16 A), suggesting that the mutant receptor is transcriptionally defective on endogenous promoters, as is the case on heterologous promoters.

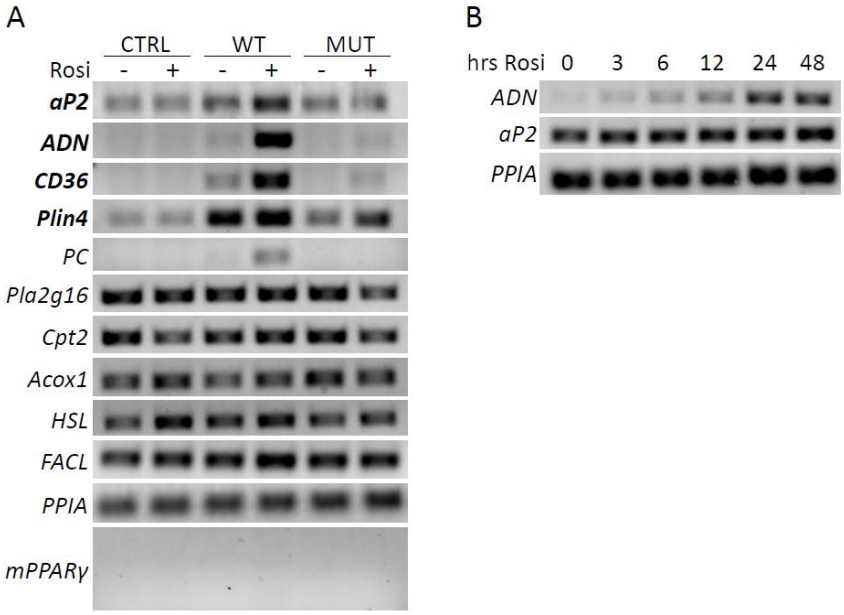

Figure 16. Rosiglitazone Induces Transcription of Endogenous PPARγ Target Genes In Wild-Type and E157D NPγ2 Cells.

A, Expression of endogenous genes was measured by rtPCR in the indicated cells treated for 24 hours with 20 μM rosiglitazone (+ Rosi) or vehicle (- Rosi). B, Gene expression in NPγ2WT cells after exposure to 20 μM rosiglitazone for the indicated durations.

Importantly, no adipogenic changes or evidence of lipid storage were observed in the transgenic cell lines after 24 hours of rosiglitazone treatment. NIH3T3 cells are relatively resistant to adipogenic differentiation, requiring additional stimulation with hormones, and longer than 24 hrs of rosiglitazone. Endogenous ligands alone did not induce adipogenesis in either wild-type or E157D PPARγ-expressing cells.

6.3 E157D PPARγ Activates Transcription of Native PPARγ Target Genes but Fails to Reach Maximal Induction.

End-point PCR can lack the sensitivity needed to detect differences in mRNA abundance, so to better characterize the effect of the E157D mutation on PPARγ transcriptional activity on various endogenous PPREs, we measured the mRNA levels of PPARγ target genes using quantitative PCR. We found that on five PPARγ-responsive promoters, rosiglitazone-activated E157D PPARγ induced transcription but failed to reach the level induced by the wild-type PPARγ. This was true of both the PPARγ1 and PPARγ2 isoforms of the receptor (Figure 17). Furthermore, similarly as on the heterologous promoter constructs, the extent of transcriptional defect conferred by the mutation was not uniform on all endogenous promoters. For instance, induction of the CD36 gene transcription was severely reduced by the E157D mutation (hundreds of fold), while activity on the perilipin and aP2 genes was only mildly reduced (less than ten-fold), and the adiponectin gene was induced about thirty-fold weaker by the mutant than the wild-type PPARγ. These data support our working model in which the DNA binding site sequence regulates the

transcriptional activity of PPARγ, and plays a role in determining how strongly the transcriptional activity of the receptor is affected by this PPRE-interacting mutation.

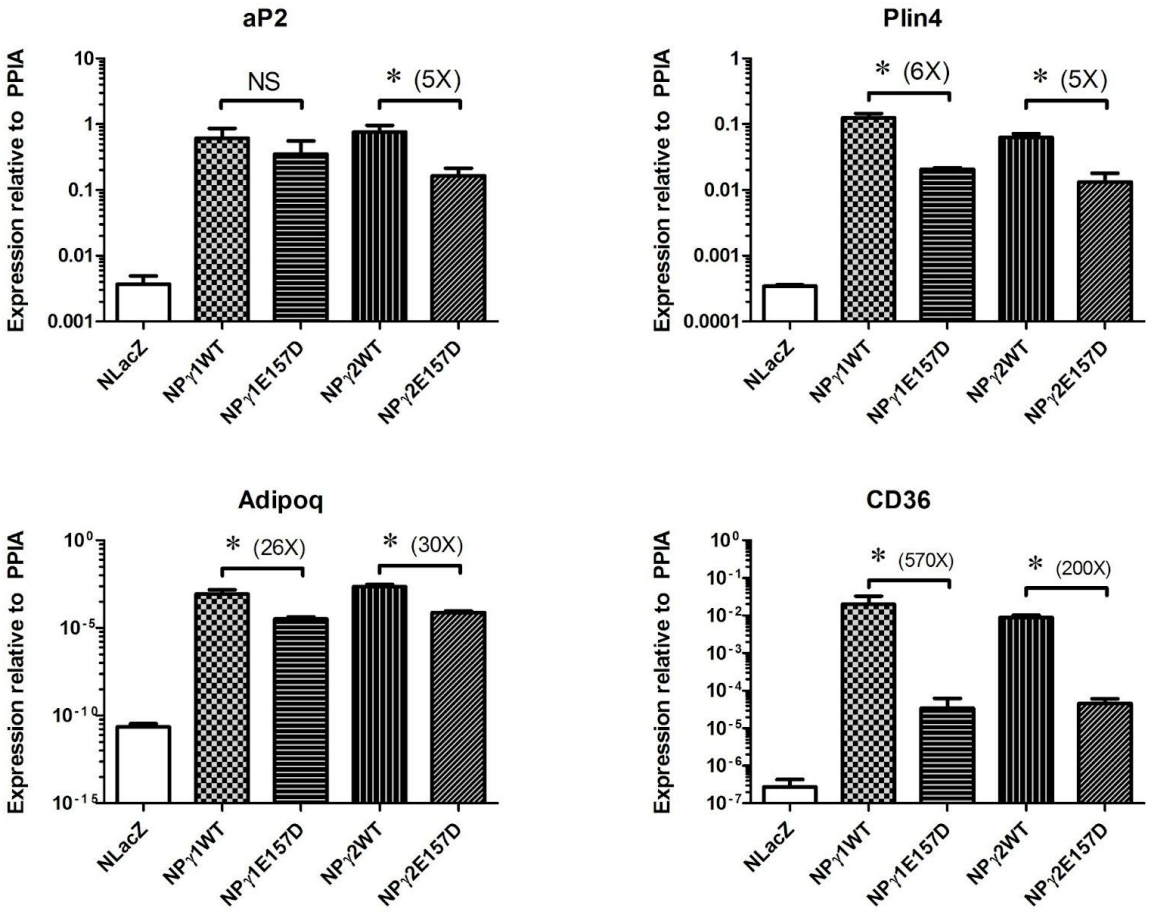

Figure 17. E157D PPARγ Transcriptional Activity on Endogenous PPARγ Target Promoters.

Expression of indicated genes was measured by qPCR and normalized to PPIA. Means and standard errors of three or four independent experiments are shown. *, $p<0.05$ determined by ANOVA with post-hoc Bonferroni tests.

6.4 E157D PPARγ binds endogenous PPREs.

We have shown that cells with stable E157D PPARγ expression have reduced levels of several known PPARγ target transcripts after rosiglitazone induction compared with cells expressing the wild-type receptor, and that this general pattern is not the same for each transcript. These findings very closely mimic our data from the transiently transfected transcription reporter system. To confirm that altered DNA binding affinity does not mediate the changes in induction of endogenous PPARγ genes by the mutant receptor, we measured the E157D PPARγ occupancy on the promoters of two of the genes for which the location of the PPREs in known.

In fibroblasts transfected with either wild-type or E157D biotinylated PPARγ1, streptavidin precipitation resulted in similar enrichment of the PPRE-containing regions compared with the empty vector-transfected contol, indicating that the mutation does not affect the binding affinity of PPARγ on native promoters. This was true on both aP2 and adiponectin gene promoters (Figure 18 B), while a control genomic region containing no known PPREs was not enriched with either protein, confirming specific pull-down. By contrast, the expression profiles of these two genes were dramatically different upon treatment of NPγ1 cells with rosiglitazone (Figure 18 A, same data as in Figure 17). While the E157D mutation did not change the aP2 gene induction by PPARγ, it reduced adiponectin gene induction by almost thirty-fold compared with the wild-type receptor.

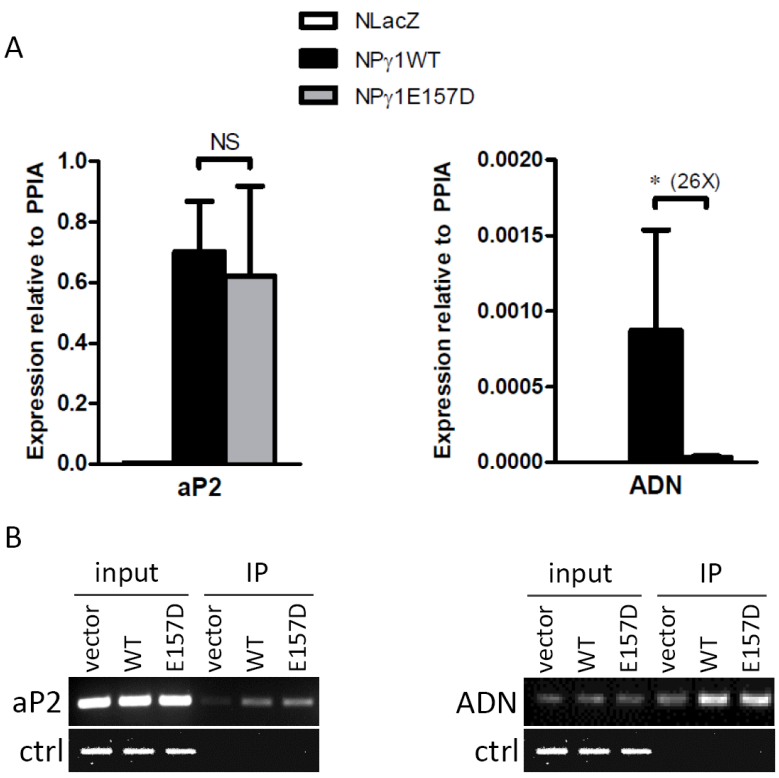

Figure 18. E157D PPARγ occupancy on endogenous PPARγ target promoters.

A, Gene expression in NPγ1 cells was measured by qPCR, data from Figure 17. B, Chromatin immunoprecipitation (IP) assays of transfected biotinylated PPARγ (empty vector control, wild-type or E157D) on the promoter regions of genes shown in panel A.

These findings are fully consistent with our initial in-vitro studies and confirm an unusual mechanistic aspect of the E157D PPARγ mutation, which disrupts the transcriptional activity of the receptor in a PPRE sequence-specific manner, but has no effect on DNA binding affinity. This intrinsic mechanism is evident both on endogenous promoters and in a transiently-transfected system.

7 GLOBAL CHANGES IN E157D PPARγ TRANSCRIPTIONAL ACTIVITY

Our data thus far have demonstrated that E157D PPARγ binds PPREs in vitro equally well as the wild-type, despite the DNA-binding surface mutation, and activates transcription from PPREs in the context of heterologous plasmid and native-chromatin promoters. Transcription induction from most of the classic, well-defined PPREs that we studied was reduced by the E157D mutation, with some PPREs more strongly defective than others in directing E157D PPARγ transcriptional activity. This apparent spectrum of defectiveness, from no effect of the mutation to mildly defective, to strongly defective and transcriptionally dead, led us to investigate whether there are genes that are induced by E157D PPARγ above the levels of the wild-type PPARγ-mediated transcription. In the context of the severe diabetic phenotype of E157D PPARγ carriers, we were interested in any such genes as potential candidate genes in the pathogenesis of insulin resistance - something that is not currently well understood. From the molecular viewpoint, we were interested in the mechanistic aspects of transcriptional activation by E157D PPARγ as directed by the PPRE sequence.

7.1 E157D PPARγ Regulates a Smaller Set of Genes than the Wild-Type Receptor.

To characterize the global extent of E157D PPARγ transcriptional activity, we determined the total set of genes regulated by E157D PPARγ in the stable PPARγ expressing fibroblasts using mRNA profiling. Total RNA was isolated from NPγ2 wild-type or E157D cells expressing equal amounts of PPARγ (Figure 18) in three

independent experiments after 24 hours of activation with rosiglitazone or DMSO vehicle. Amplified cRNA representing the total transcriptome of the cells was hybridized to mouse cDNA arrays for detection of differentially expressed genes from DMSO- versus rosiglitazone-treated cells. We defined the set of genes that were significantly upregulated by rosiglitazone treatment as PPARγ target genes for each of the two cell lines. Wild-type PPARγ induced the expression of 1631 genes, 597 of them by 1.5-fold or greater (Table 3), consistent with previously described transgenic cell culture models [90]; by contrast, the E157D mutant induced 287 genes, only 95 of them over 1.5-fold.

In addition to induction of gene transcription, activation of PPARγ leads to inhibition of certain genes through incompletely understood mechanisms involving either direct activity of PPARγ on the gene promoters or upregulation of genes encoding transcriptional inhibitors. In the currently accepted model of direct inhibition of transcription, ligand binding induces sumoylation of the ligand-binding domain of PPARγ, which targets it to corepressors on the promoters of inflammatory genes and prevent the disassembly of the repression complex upon inflammatory stimulation [130-135]. In our transgenic cell model, activation of PPARγ with rosiglitazone resulted in decreased transcription of 1053 probes (66 of those by more than 50%). The E157D mutant downregulated a significantly smaller set of genes (297; only 8 of those by more than 50%). Whether these genes are regulated through direct or indirect mechanisms, the mutant receptor has decreased inhibitory activity as well as decreased stimulation of gene transcription. These data confirm that, similarly as we observed on a small set of well-known PPARγ target genes, the E157D PPARγ is largely transcriptionally defective on a

global scale: it regulates the transcription of a much smaller set of genes than the wild-type receptor.

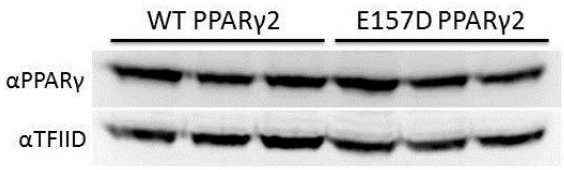

Figure 19. Lentiviral PPARγ Expression in Hybridized Samples.

Protein expression was measured by western blot in NPγ2 WT and E157D cells.

Table 3. Summary of Microarray Analysis of Gene Expression.

The numbers of genes with positive signal from one or more array probe are listed

	NPγ2 WT	NPγ2 E157D
Rosi-induced genes	1631	287
Rosi-induced genes, FC>1.5	597	95
Rosi-downregulated genes	1053	297
Rosi-donregulated genes, FC<0.5	66	8

7.2 E157D PPARγ Exhibits Novel Transcriptional Properties.

In order to better understand the global effect of the E157D mutation on the transcriptional activity of PPARγ, we analyzed the target genes of wild-type and E157D PPARγ as defined by rosiglitazone induction in our NPγ2 cells. The mutant receptor failed to activate transcription of 90% of the wild-type PPARγ target genes (Figure 19). The majority of the E157D PPARγ target genes are also wild-type

targets, and the mutant receptor has reduced transcriptional activity on most (73%) of these genes. We refer to these as the "loss-of-function" genes, indicating the effect of the E157D mutation. The remainder (27%, or 15 genes) of shared wild-type and E157D PPARγ target genes are induced similarly by both receptors. In addition, a significant portion (38%), of E157D PPARγ target genes are not wild-type PPARγ targets, although this is a small number relative to the total number of wild-type PPARγ target genes (34 versus 528 genes). We refer to these 34 genes as the "gain-of-function" genes. Genes repressed by PPARγ followed a very similar pattern, but amounted to roughly a tenth of the total number of genes induced by PPARγ. Here also the mutant receptor was inactive on the vast majority of the genes down-regulated by the wild-type PPARγ, while one gene was repressed by mutant receptor only.

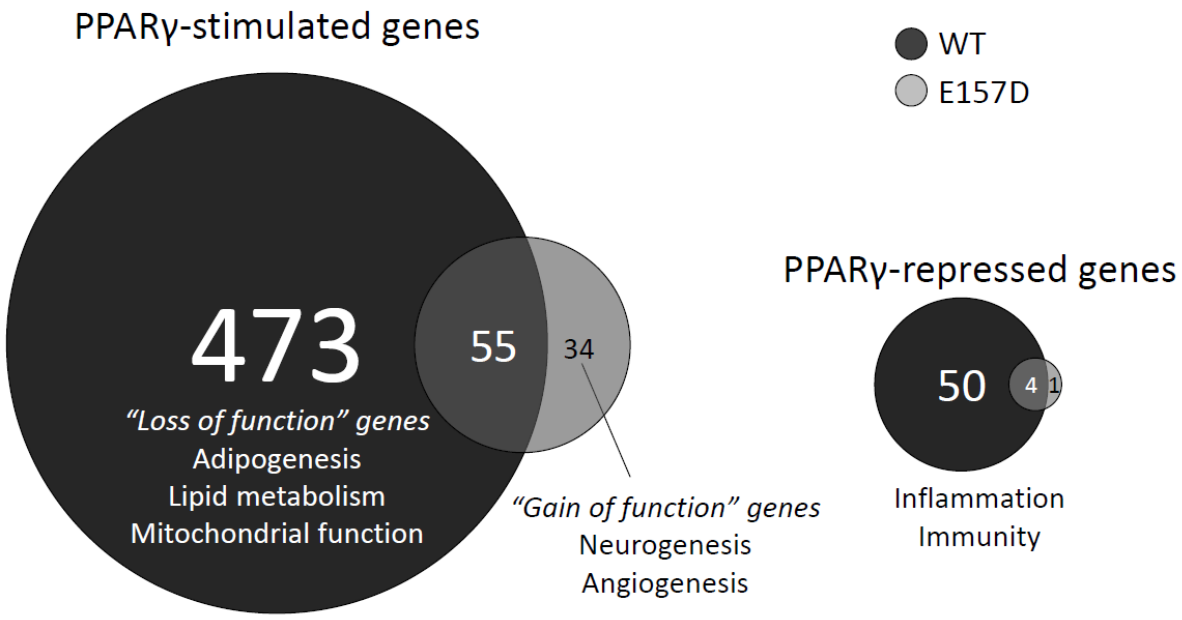

Figure 20. Summary of Wild-Type and E157D PPARγ Target Genes.

Each segment of the Venn diagram represents the number of genes in that category after the fold-change cut-off. Representative enriched biological processes for each segment of the diagram are listed. Note, the numbers of genes in each section is slightly lower than the numbers listed in Table 3 because only the annotated genes were entered into the analysis of biological processes.

To investigate the functional implications of the changes in transcriptional activity of the E157D PPARγ, we used the Genomatix software to identify biological processes that are enriched in the various gene categories with respect to the effect of the mutation. Surprisingly, the gain-of-function genes comprise an entirely functionally distinct set of genes than the wild-type PPARγ targets. Consistent with previous reports and known PPARγ physiology [19, 136-139], the wild-type PPARγ target genes fell into the expected categories of adipogenesis, lipid storage,

mitochondrial function and other categories (Table 4). On the other hand, the loss-of-function genes were enriched for embryonic development, and specifically neurogenic and angiogenic developmental factors (Table 5). Importantly, the enrichment terms of the gain-of-function and the loss-of-function gene sets were completely non-overlapping. Such a striking segregation of gene ontology categories with respect to E157D PPARγ transcriptional activity implies that there is a significant functional meaning in the gain of function conferred by the mutation.

Table 4. Enriched Biological Processes in the E157D PPARγ Loss-of-Function Gene Set.

Metabolic categories are highlighted in blue.

GO-Term	GO-Term id	P-value	# Genes (observed)	# Genes (expected)	# Genes (total)	List of observed genes
cellular process	GO:0009987	5.15E-13	76	40.098	11371	Hspd1, Rreb1, Cat, Ddit3, Egln3, Itgad, Col18a1, Adipoq, Nus1, Trib3, Gpcpd1, Aco2, Mfsd7a, Taldo1, S100a13, Atpaf2, Cebpg, etc.
metabolic process	GO:0008152	3.92E-14	61	25.055	7105	Hspd1, Rreb1, Pnpla8, Cat, Ddit3, Egln3, Cyb5r1, Adipoq, Trib3, Gpcpd1, Aco2, Taldo1, Cebpg, Dgat2, Tpsab1, Pdhb, Cycs, Tob1, etc.
cellular metabolic process	GO:0044237	1.23E-12	54	21.437	6079	Hspd1, Rreb1, Cat, Ddit3, Adipoq, Trib3, Gpcpd1, Aco2, Taldo1, Cebpg, Dgat2, Pdhb, Cycs, Tob1, Aldh1a7, Esrra, Agpat2, Cs, Ahcyl2, etc.
primary metabolic process	GO:0044238	2.08E-10	51	21.966	6229	Hspd1, Rreb1, Pnpla8, Cat, Ddit3, Cyb5r1, Adipoq, Trib3, Gpcpd1, Taldo1, Cebpg, Dgat2, Tpsab1, Pdhb, Tob1, Aldh1a7, Esrra, etc.
small molecule metabolic process	GO:0044281	1.54E-18	34	5.455	1547	Cat, Cyb5r1, Adipoq, Trib3, Gpcpd1, Aco2, Taldo1, Dgat2, Pdhb, Aldh1a7, Cs, Ahcyl2, Aldoa, Fads3, Pcx, Prkar2b, Fitm2, Acadvl, etc.
biosynthetic process	GO:0009058	1.35E-04	26	12.236	3470	Rreb1, Cat, Ddit3, Cyb5r1, Adipoq, Trib3, Cebpg, Dgat2, Pdhb, Tob1, Esrra, Agpat2, Fads3, Pcx, Fitm2, S100a1, Acadvl, Mrpl12, etc.
cellular biosynthetic process	GO:0044249	2.22E-04	25	11.891	3372	Rreb1, Cat, Ddit3, Adipoq, Trib3, Cebpg, Dgat2, Pdhb, Tob1, Esrra, Agpat2, Fads3, Pcx, Fitm2, S100a1, Acadvl,

						Mrpl12, Agpat9, etc.
lipid metabolic process	GO:0006629	1.25E-16	24	2.648	751	Pnpla8, Cat, Cyb5r1, Adipoq, Trib3, Gpcpd1, Dgat2, Aldh1a7, Agpat2, Fads3, Pcx, Prkar2b, Fitm2, Acadvl, Acot2, Crat, Pnpla2, etc.
response to stimulus	GO:0050896	3.40E-05	23	9.250	2623	Hspd1, Cat, Ddit3, Egln3, Adipoq, Trib3, Cebpg, Cycs, Chac1, Mpp1, Cfd, Prkar2b, Acot2, Gadd45g, Aplp2, Itpr1, Acsl1, Vegfa, Acadm, etc.
localization	GO:0051179	5.53E-04	22	10.431	2958	Col18a1, Adipoq, Trib3, Mfsd7a, S100a13, Slc5a6, Tob1, Mpp1, Slc25a10, Fads3, Tfrc, Fitm2, Slc25a1, Crat, Pnpla2, Itpr1, Dgat1, etc.
catabolic process	GO:0009056	2.13E-11	21	3.417	969	Pnpla8, Cat, Adipoq, Trib3, Aco2, Taldo1, Pdhb, Cs, Aldoa, Rnf11, Acadvl, Acot2, Arl4a, Pnpla2, Por, Acsl1, Bckdhb, Cbr3, Lpl, Acadm, etc.
cellular lipid metabolic process	GO:0044255	2.19E-14	19	1.820	516	Cat, Adipoq, Trib3, Dgat2, Aldh1a7, Agpat2, Fads3, Prkar2b, Fitm2, Acadvl, Acot2, Crat, Pnpla2, Agpat9, Dgat1, Acsl1, Lpl, Acadm, etc.
regulation of metabolic process	GO:0019222	6.18E-03	19	10.290	2918	Rreb1, Cat, Ddit3, Adipoq, Trib3, Cebpg, Tob1, Esrra, Prkar2b, Fitm2, S100a1, Acadvl, Gadd45g, Aplp2, Pnpla2, Por, Vegfa, Acadm, etc.
developmental process	GO:0032502	7.90E-03	19	10.533	2987	Col18a1, Adipoq, Nus1, Trib3, S100a13, Cebpg, Tob1, Esrra, Fgfrl1, Prkar2b, Gadd45g, Aplp2, Arl4a, Itpr1, Dmkn, Pex11a, Vegfa, Lpl, etc.
regulation of cellular metabolic process	GO:0031323	7.19E-03	18	9.676	2744	Rreb1, Cat, Ddit3, Adipoq, Trib3, Cebpg, Tob1, Esrra, Prkar2b, Fitm2, S100a1, Acadvl, Gadd45g, Aplp2, Pnpla2, Vegfa, Acadm, Mknk2
transport	GO:0006810	7.87E-03	17	9.010	2555	Adipoq, Trib3, Mfsd7a, S100a13, Slc5a6, Tob1, Slc25a10, Fads3, Tfrc, Slc25a1, Crat, Itpr1, Dgat1, Acsl1, Pex16, Cyc1, Etfdh
establishment of localization	GO:0051234	8.45E-03	17	9.077	2574	Adipoq, Trib3, Mfsd7a, S100a13, Slc5a6, Tob1, Slc25a10, Fads3, Tfrc, Slc25a1, Crat, Itpr1, Dgat1, Acsl1, Pex16, Cyc1, Etfdh
regulation of primary metabolic process	GO:0080090	9.82E-03	17	9.221	2615	Rreb1, Cat, Ddit3, Adipoq, Trib3, Cebpg, Tob1, Esrra, Prkar2b, Fitm2, S100a1, Acadvl, Pnpla2, Por, Vegfa, Acadm, Mknk2
cellular ketone metabolic process	GO:0042180	1.32E-10	16	1.978	561	Adipoq, Trib3, Aco2, Pdhb, Aldh1a7, Cs, Fads3, Pcx, Prkar2b, Acadvl, Acot2, Crat, Acsl1, Bckdhb, Cbr3, Acadm
cellular catabolic process	GO:0044248	9.50E-09	16	2.666	756	Cat, Adipoq, Trib3, Aco2, Cs, Rnf11, Acadvl, Acot2, Arl4a, Pnpla2, Por, Acsl1, Bckdhb, Cbr3, Lpl, Acadm
response to chemical stimulus	GO:0042221	1.60E-06	16	3.897	1105	Hspd1, Cat, Ddit3, Egln3, Adipoq, Trib3, Cycs, Chac1, Mpp1, Acot2, Itpr1, Acsl1, Vegfa, Cyc1, Etfdh, Mgst1
oxoacid metabolic	GO:0043436	9.00E-10	15	1.929	547	Adipoq, Trib3, Aco2, Pdhb, Aldh1a7, Cs, Fads3, Pcx,

process						Prkar2b, Acadvl, Acot2, Crat, Acsl1, Bckdhb, Acadm
carboxylic acid metabolic process	GO:0019752	9.00E-10	15	1.929	547	Adipoq, Trib3, Aco2, Pdhb, Aldh1a7, Cs, Fads3, Pcx, Prkar2b, Acadvl, Acot2, Crat, Acsl1, Bckdhb, Acadm
organic acid metabolic process	GO:0006082	9.23E-10	15	1.932	548	Adipoq, Trib3, Aco2, Pdhb, Aldh1a7, Cs, Fads3, Pcx, Prkar2b, Acadvl, Acot2, Crat, Acsl1, Bckdhb, Acadm
positive regulation of biological process	GO:0048518	2.06E-03	15	6.517	1848	Hspd1, Cat, Ddit3, Col18a1, Adipoq, Trib3, S100a13, Cebpg, Cycs, Esrra, Cfd, Fitm2, Pnpla2, Vegfa, Lpl
cellular developmental process	GO:0048869	2.50E-03	15	6.651	1886	Col18a1, Adipoq, Nus1, Trib3, S100a13, Cebpg, Tob1, Esrra, Gadd45g, Arl4a, Dmkn, Pex11a, Vegfa, Lpl, Acadm
cellular component organization	GO:0016043	8.67E-03	15	7.617	2160	Col18a1, Adipoq, S100a13, Atpaf2, Cebpg, Aldh1a7, Tfrc, Fitm2, Pex19, Aplp2, Hist1h2bh, Pex11a, Hist1h2bk, Pex16, Acadm
alcohol metabolic process	GO:0006066	2.10E-10	14	1.449	411	Cat, Cyb5r1, Adipoq, Gpcpd1, Taldo1, Dgat2, Pdhb, Aldoa, Pcx, Acadvl, Pgm2, Por, Pmm1, Acadm
oxidation reduction	GO:0055114	4.88E-08	14	2.225	631	Cat, Egln3, Cyb5r1, Pdhb, Cycs, Aldh1a7, Fads3, Acadvl, Por, Bckdhb, Cbr3, Acadm, Cyc1, Etfdh
response to stress	GO:0006950	2.63E-04	14	4.736	1343	Hspd1, Cat, Ddit3, Egln3, Cebpg, Cycs, Chac1, Cfd, Acot2, Itpr1, Vegfa, Acadm, Etfdh, Mknk2
cell differentiation	GO:0030154	4.38E-03	14	6.365	1805	Col18a1, Adipoq, Nus1, Trib3, Cebpg, Tob1, Esrra, Gadd45g, Arl4a, Dmkn, Pex11a, Vegfa, Lpl, Acadm
regulation of biological quality	GO:0065008	1.91E-03	13	5.163	1464	Ddit3, Adipoq, S100a13, Cebpg, Aldh1a7, Tfrc, Fitm2, Acadvl, Aplp2, Pnpla2, Itpr1, Dgat1, Vegfa
positive regulation of cellular process	GO:0048522	5.25E-03	13	5.811	1648	Hspd1, Cat, Ddit3, Col18a1, Adipoq, Trib3, S100a13, Cebpg, Cycs, Esrra, Pnpla2, Vegfa, Lpl
monocarboxylic acid metabolic process	GO:0032787	1.81E-09	12	1.146	325	Adipoq, Trib3, Pdhb, Aldh1a7, Fads3, Pcx, Prkar2b, Acadvl, Acot2, Crat, Acsl1, Acadm
lipid biosynthetic process	GO:0008610	2.18E-08	11	1.146	325	Cyb5r1, Trib3, Dgat2, Agpat2, Fads3, Pcx, Fitm2, Acadvl, Agpat9, Dgat1, Lpl
cellular carbohydrate metabolic process	GO:0044262	4.52E-08	11	1.231	349	Adipoq, Gpcpd1, Taldo1, Dgat2, Pdhb, Cs, Aldoa, Pcx, Pgm2, Pmm1, Acadm
carbohydrate metabolic process	GO:0005975	6.80E-07	11	1.615	458	Adipoq, Gpcpd1, Taldo1, Dgat2, Pdhb, Cs, Aldoa, Pcx, Pgm2, Pmm1, Acadm
generation of precursor metabolites and energy	GO:0006091	4.11E-08	10	0.949	269	Cat, Aco2, Pdhb, Cycs, Cs, Aldoa, Fads3, Acadm, Cyc1, Etfdh
small molecule catabolic process	GO:0044282	5.22E-06	10	1.615	458	Adipoq, Taldo1, Pdhb, Aldoa, Acadvl, Acot2, Arl4a, Bckdhb, Cbr3, Acadm
apoptosis	GO:0006915	1.91E-03	10	3.343	948	Hspd1, Ddit3, Egln3, Col18a1, Trib3, Cebpg, Cycs, Chac1, Gadd45g, Vegfa
programmed cell death	GO:0012501	2.10E-03	10	3.385	960	Hspd1, Ddit3, Egln3, Col18a1, Trib3, Cebpg, Cycs, Chac1, Gadd45g, Vegfa

cell death	GO:0008219	2.92E-03	10	3.544	1005	Hspd1, Ddit3, Egln3, Col18a1, Trib3, Cebpg, Cycs, Chac1, Gadd45g, Vegfa
death	GO:0016265	3.09E-03	10	3.572	1013	Hspd1, Ddit3, Egln3, Col18a1, Trib3, Cebpg, Cycs, Chac1, Gadd45g, Vegfa

Table 5. Enriched Biological Processes in the E157D PPARγ Gain-of-Function Gene Set.

Developmental categories are highlighted in green; vasculogenesis in red.

GO-Term	GO-Term ID	P-value	# Genes (observed)	# Genes (expected)	# Genes (total)	List of observed genes
cellular process	GO:0009987	1.01E-04	14	6.3	11371	Cck, Irx5, Kank3, Vav3, Acsbg1, Hvcn1, Sema5a, Mtap2, Sncg, Klf5, Ramp2, Sepp1, Dpt, Net1
regulation of cellular process	GO:0050794	9.10E-06	12	3.5	6345	Cck, Irx5, Kank3, Vav3, Hvcn1, Sema5a, Mtap2, Sncg, Klf5, Ramp2, Dpt, Net1
regulation of biological process	GO:0050789	1.53E-05	12	3.7	6654	Cck, Irx5, Kank3, Vav3, Hvcn1, Sema5a, Mtap2, Sncg, Klf5, Ramp2, Dpt, Net1
biological regulation	GO:0065007	3.05E-05	12	3.9	7087	Cck, Irx5, Kank3, Vav3, Hvcn1, Sema5a, Mtap2, Sncg, Klf5, Ramp2, Dpt, Net1
multicellular organismal process	GO:0032501	2.01E-03	8	2.6	4775	Cck, Irx5, Vav3, Sema5a, Mtap2, Sncg, Klf5, Sepp1
cellular component organization	GO:0016043	8.03E-05	7	1.2	2160	Cck, Kank3, Vav3, Sema5a, Mtap2, Klf5, Dpt
system development	GO:0048731	1.09E-04	7	1.3	2267	Cck, Irx5, Vav3, Sema5a, Mtap2, Klf5, Sepp1
anatomical structure development	GO:0048856	1.68E-04	7	1.3	2426	Cck, Irx5, Vav3, Sema5a, Mtap2, Klf5, Sepp1
multicellular organismal development	GO:0007275	3.66E-04	7	1.5	2749	Cck, Irx5, Vav3, Sema5a, Mtap2, Klf5, Sepp1
developmental process	GO:0032502	6.11E-04	7	1.7	2987	Cck, Irx5, Vav3, Sema5a, Mtap2, Klf5, Sepp1
response to stimulus	GO:0050896	1.99E-03	6	1.5	2623	Cck, Irx5, Acsbg1, Hvcn1, Sncg, Sepp1
cell projection organization	GO:0030030	4.87E-06	5	0.3	485	Cck, Vav3, Sema5a, Mtap2, Klf5
nervous system development	GO:0007399	1.65E-04	5	0.6	1013	Cck, Irx5, Sema5a, Mtap2, Sepp1

anatomical structure morphogenesis	GO:0009653	4.99E-04	5	0.7	1286	Cck, Irx5, Vav3, Sema5a, Klf5
organ development	GO:0048513	2.19E-03	5	1.0	1786	Irx5, Vav3, Sema5a, Klf5, Sepp1
neuron development	GO:0048666	8.54E-05	4	0.2	443	Cck, Irx5, Sema5a, Mtap2
neuron differentiation	GO:0030182	2.34E-04	4	0.3	576	Cck, Irx5, Sema5a, Mtap2
generation of neurons	GO:0048699	3.41E-04	4	0.4	636	Cck, Irx5, Sema5a, Mtap2
cellular component assembly	GO:0022607	3.56E-04	4	0.4	643	Cck, Kank3, Vav3, Klf5
neurogenesis	GO:0022008	4.33E-04	4	0.4	677	Cck, Irx5, Sema5a, Mtap2
cellular component biogenesis	GO:0044085	6.11E-04	4	0.4	742	Cck, Kank3, Vav3, Klf5
cell development	GO:0048468	1.10E-03	4	0.5	868	Cck, Irx5, Sema5a, Mtap2
organelle organization	GO:0006996	2.73E-03	4	0.6	1112	Cck, Kank3, Vav3, Mtap2
negative regulation of biological process	GO:0048519	9.91E-03	4	0.9	1599	Cck, Kank3, Mtap2, Dpt
angiogenesis	GO:0001525	1.58E-04	3	0.1	195	Vav3, Sema5a, Klf5
blood vessel morphogenesis	GO:0048514	3.77E-04	3	0.1	262	Vav3, Sema5a, Klf5
blood vessel development	GO:0001568	5.98E-04	3	0.2	307	Vav3, Sema5a, Klf5
vasculature development	GO:0001944	6.39E-04	3	0.2	314	Vav3, Sema5a, Klf5
regulation of system process	GO:0044057	7.00E-04	3	0.2	324	Cck, Irx5, Sncg
neuron projection development	GO:0031175	1.00E-03	3	0.2	367	Cck, Sema5a, Mtap2
regulation of cellular component organization	GO:0051128	1.61E-03	3	0.2	433	Cck, Kank3, Mtap2
anatomical structure formation involved in morphogenesis	GO:0048646	1.81E-03	3	0.2	451	Vav3, Sema5a, Klf5
behavior	GO:0007610	2.22E-03	3	0.3	484	Cck, Sncg, Sepp1
cellular component movement	GO:0006928	2.69E-03	3	0.3	518	Cck, Vav3, Sema5a

Our gene expression profiling experiments revealed that PPARγ is highly transcriptionally active in the lentiviral expression system in NIH3T3 fibroblasts, and that it regulates genes that have previously been identified as its transcriptional targets. These genes are functionally involved in known PPARγ-regulated pathways including adipogenesis, lipid and carbohydrate metabolism, mitochondrial function and cell proliferation/cell death. The number of genes induced by rosiglitazone was also consistent with previous studies done in the

NIH3T3 and the adipocyte 3T3-L1 cell lines. In addition, no unexpected biological processes were enriched among the genes upregulated by PPARγ in these cells, confirming that the lentivirus-transduced NIH3T3 cell line is a robust cell culture model for studying PPARγ transcriptional activity.

By contrast, the E157D PPARγ regulated a much smaller number of genes than the wild-type, even though the protein was equally abundant in the nucleus. This loss of transcriptional function on PPARγ target genes that are required for adipogenesis and metabolic homeostasis is the most likely cause of lipodystrophy and diabetes in the E157D cohort. These findings contradict our original hypothesis that the E157D mutation disrupts PPARγ transcriptional activity on a small subset of its target genes, on which we would then focus as potential new candidate genes of interest in diabetes pathogenesis. Instead, the mutation has a broad deleterious effect on the vast majority of PPARγ target genes, presumably resulting in reduced expression of genes regulating energy homeostasis and leading to metabolic disease.

From the clinical perspective of diabetes, this result is not new or surprising - the metabolic endpoints in the case of lipodystrophy caused by the E157D PPARγ mutant are pathophysiologically similar to previously reported cases. The major value of our findings is the discovery that a DNA-binding domain mutation can severely reduce the transcriptional function of a nuclear receptor independently of its ability to bind DNA. A similar mechanism of action of a nuclear receptor mutant has never been described before, and these findings challenge the currently accepted model of nuclear receptor domains as structurally and functionally independent entities. In addition, the induction of non-PPARγ target genes by the

E157D mutant raises the intriguing possibility that this gain-of-function activity is causing the atypical clinical presentation in this mutant PPARγ cohort compared with previously reported type III lipodystrophy cases.

8 CHARACTERIZATION OF NOVEL PPRES NEAR E157D PPARγ GAIN-OF-FUNCTION GENES

8.1 Loss-Of-Function And Gain-Of-Function Promoters Contain Similar Numbers And Types Of PPREs.

In order to better understand the mechanisms underlying target gene misregulation by E157D PPARγ, we sought to determine whether the mutant receptor activates the "gain-of-function" genes from typical PPREs. We have already established that the mutation does not affect the affinity of PPARγ for typical PPREs in our gel shift assays. But it is possible that this DNA-binding domain mutation could allow PPARγ to regulate the "gain-of-function" genes from non-DR1 DNA sites. If so, the "gain-of-function" set of genes would be expected to contain fewer DR1 PPREs than the "loss-of-function" set.

To answer this question, we identified putative PPREs in the promoter of genes from the gain-of-function and the loss-of-function sets using MatInspector. 74% of the gain-of-function promoters and 68% of the loss-of-function promoters contained DNA sequences matching the PPRE matrices defined by previous ChIP-on-chip and ChIP-seq studies (Figure 20 A, [19, 20]). Fisher's exact test generated a p value of 0.2 for the comparison, indicating that the two sets of promoters are not different with regard to putative PPRE content.

To compare the PPREs from the gain-of-function promoters to the PPREs from the loss-of-function promoters, we loaded the putative PPRE sequences identified by MatInspector into the MatDefine function of Genomatix. Position-weight matrices for the two sets of PPREs were similar, indicating that there is no readily apparent inherent difference between the sequences of the PPREs in these

two sets of genes (Figure 20 B). These findings are consistent with our previous observations that the E157D PPARγ mutation does not alter the binding site sequence selectivity of the receptor. Rather, it binds the same types of PPREs as the wild-type, but has vastly different transcriptional activity, possibly through a disruption in the way the protein interacts with the DNA once it is bound to the promoter.

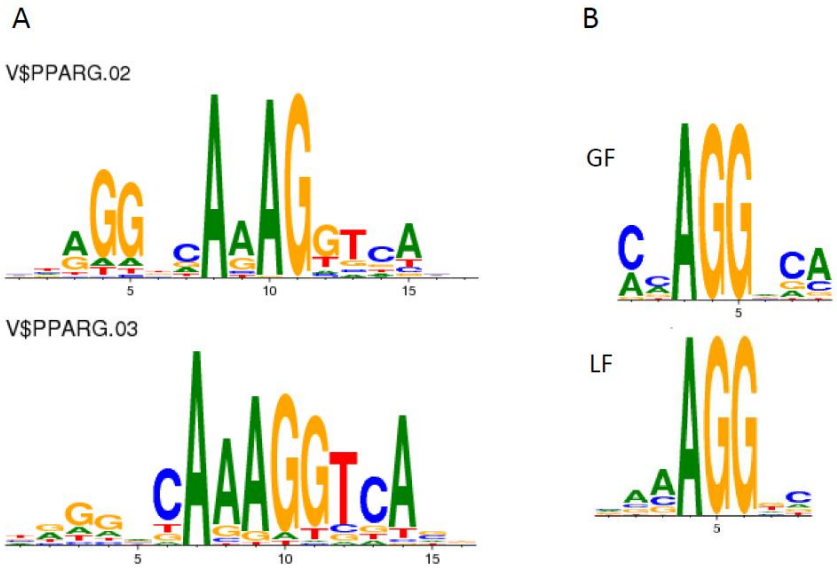

Figure 21. Putative PPREs Identified in the Promoters of Gain-of-Function and Loss-of-Function Genes.

A, MatInspector position-weight matrices identified in 3T3-L1 adipocytes by ChIP-on-chip and ChIP-seq studies were used to identify PPREs in the promoters of genes. B, MatDefine position-weight matrices of the PPREs identified in the gain-of-function (GF) and loss-of-function (LF) gene promoters.

8.2 E157D PPARγ Has Increased Affinity for Weak PPREs in Gain-Of-Function Gene Regulatory Regions.

In order to characterize the dynamics of the wild-type and E157D PPARγ on gain-of-function gene promoters, we selected two of the putative PPREs identified in this set of promoter for in-vitro studies of DNA binding and transcription induction. Recent ChIP-seq studies have shown that PPARγ binding sites occur at many points along its target genes, as well as at extended distances from their promoters and 3' UTRs [21]. We therefore scanned genomic sequences from -10000 of the transcription start site to 10000 downstream of the transcription termination of each gene for putative PPREs using RVista 2.0. This highly permissive scan identifies any sequence that resembles the V$PPARG.02 and V$PPARG.03 matrices, defined above, and resulted in as many as a hundred putative PPREs per gene entry. Reasoning that functionally important PPREs are likely to be conserved across species, we eliminated the majority of the putative PPRE sequences from the mouse genome because they were not conserved and aligned in the human. Finally, we selected the PPREs from two genes whose products are involved in neuron development, one of the gene ontology categories that were enriched in the gain-of-function set of genes: synuclein gamma (*Sncg*) and microtubule associated protein 2 (*Mtap2*).

As shown in Figure 21 A, the SNCG PPRE is located approximately five thousand base pairs upstream of the transcription start site of the gene, in the intron of a neighboring gene, and is highly conserved between the human and mouse. Notably, previous ChIP-seq studies have demonstrated PPARγ binding to the chromatin region containing the SNCG PPRE in mouse adipocytes [20, 140].

The MTAP2 PPRE is located within the first translated exon of the gene. This PPRE was identified by MatInspector and matched both the V$PPARG.02 and V$PPARG.03 matrices (core sequences indicated in Figure 21 B), and also is highly conserved. Upregulation of *Sncg* and *Mtap2* by rosiglitazone in NPγ2 E157D cells was confirmed by qPCR (Figure 21 A and B). Basal expression of *Sncg* was increased nearly three-fold in NPγ2 E157D cells compared with WT, and further induced approximately six-fold by rosiglitazone treatment. *Mtap2* was expressed at similar levels in the wild-type and E157D NPγ2 cells, but was upregulated to almost three times higher level by rosiglitazone in the mutant cell line. Both genes were not regulated by rosiglitazone in the wild-type cell line, confirming their status as gain-of-function genes for the E157D PPARγ.

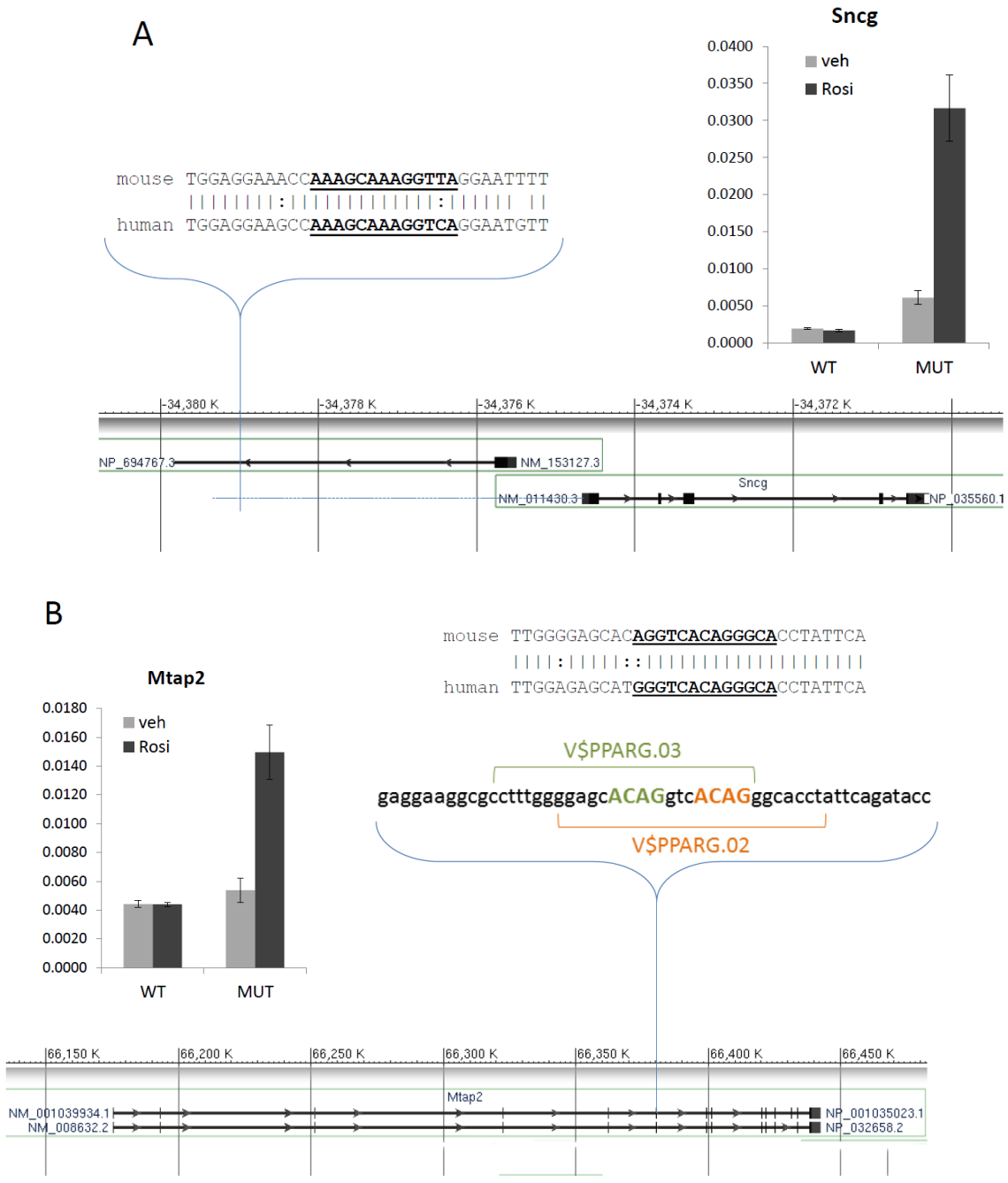

Figure 22. Putative PPREs in Gain-of-Function Promoters.

Genomic locations of putative PPREs near (A) Sncg and (B) Mtap2 genes are shown. Gene expression in NPγ2WT and E157D (MUT) cell lines was confirmed by qPCR. The core DR1 PPRE sequence is shown in bold-face in the mouse-human alignments.

To assess the novel putative PPREs for PPARγ binding, we used biotinylated oligonucleotides containing each PPRE and flanking nucleotides (SNCG: TGGAGGAAACC **AAAGCAAAGGTTA** GGAATTTT; MTAP2: TTGGGGAGCAC **AGGTCACAGGGCA** CCTATTCA) in a gel shift assay with nuclear extracts from NIH3T3 cells transfected with either wild-type or E157D PPARγ2. Equal expression of the wild-type and mutant PPARγ used in these assays was confirmed on a Western blot (Figure 22 C). Shown in Figure 22 A, both the wild-type and mutant proteins shifted the SNCG probe band, indicating PPRE binding, but the E157D PPARγ bound more probe than the wild-type PPARγ. The specificity of binding was confirmed by competition with a 200-fold excess of unfolded probe, which abrogated the shifted band, and with a flag antibody, which resulted in a super-shifted band. The MTAP2 PPRE was also shifted by both wild-type and E157D PPARγ, with a higher intensity shifted band produced by the mutant than the wild-type, and with a high specificity demonstrated by cold probe competitor and supershift (Figure 22 B). These data suggest that both the SNCG and the MTAP2 PPREs discovered by our bioinformatic approach are bona-fide PPARγ binding elements that may have a higher affinity for the E157D PPARγ than the wild-type.

To rule out the possibility that stronger PPRE binding by the mutant receptor is due to an artifact of nuclear extract collection, we compared the shifted bands produced by the SNCG and MTAP2 PPREs to the consensus PPRE (AATGGTGGGC **AAAACT AGGTCA A AGGTCA** TGAGGTGGA) and the ADN PPRE (CAGCAACA **GAAGAT GGGGCA A AAGTCA** AAACCACAGCAGGA) as controls. Shows in Figure 22 d, E157D PPARγ bound the consensus and ADN probes equally well as the wild-type receptor, consistent with our previous experiments. By contrast, the mutant

produced a much stronger intensity shifted band with the SNCG and MTAP2 probes than the wild-type, confirming that these may be naturally weak PPREs and that the E157D mutation allows PPARγ to binds them with increased affinity.

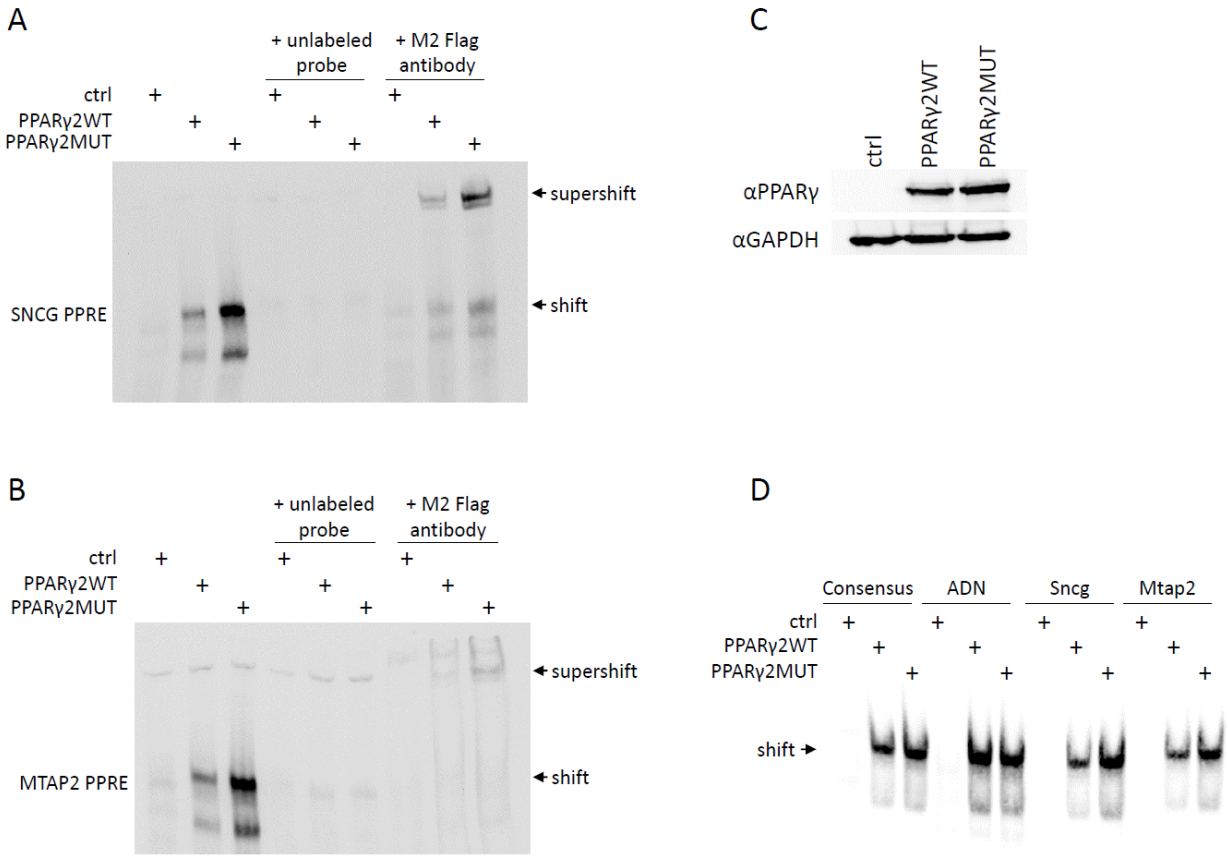

Figure 23. Gel-Shift Assays of PPARγ Binding to Novel PPREs.

Nuclear extracts from CHO cells transfected with the indicated plasmids were incubated in binding reactions with (A) SNCG or (B) MTAP2 PPREs. C, Equal expression of wild-type and E157D PPARγ was confirmed on a western blot. D, Gel-shift was done as in A and B with the indicated PPREs as probes.

We assessed the ability of the SNCG and MTAP2 PPREs to drive transcription of a luciferase reporter gene in a reporter plasmid construct similar to the ones we

used previously to study well characterized PPREs. Shown in Figure 23, the ARE6 PPRE was transcriptionally active in the presence of the wild-type and less so with the mutant PPARγ, confirming the validity of the assay. However, neither of the newly identified PPREs alone was able to induce transcription in the context of the heterologous promoter, either through the wild-type or E157D PPARγ. There was a slight suppression of reporter transcription by both the wild-type and mutant receptors from the SNCG PPRE, and the mutant, but not the wild-type PPARγ suppressed transcription from the MTAP2 PPRE. These minor reductions in transcription could be due to a nonspecific effect of PPARγ presence in the nucleus, such as driving coregulators of transcription away from the reporter gene, rather than a PPRE-dependent suppression of transcription. The results of these transcription reporter studies indicate that the SNCG and MTAP2 PPREs are transcriptionally inactive in the context of a heterologous promoter. However, this does not rule out the possibility that E157D PPARγ is transcriptionally active on these PPREs *in vivo*, as endogenous promoters may contain additional transcription factor binding sites and other regulatory elements that enhance PPARγ transcriptional activity.

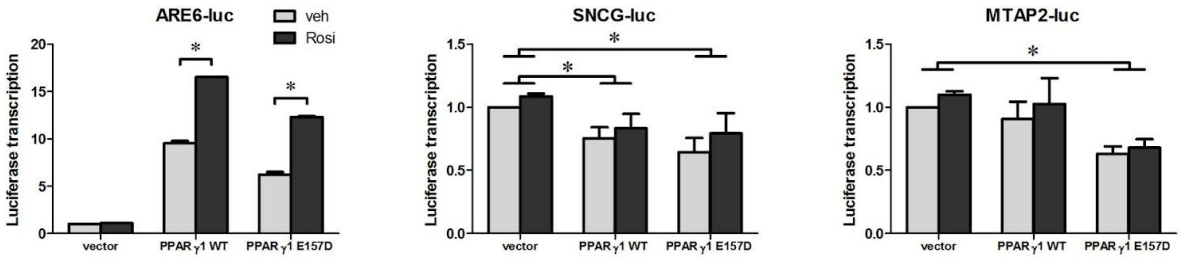

Figure 24. SNCG and MTAP2 PPREs Are Not Transcriptionally Active in Heterologous Promoters.

NIH3T3 cells were transfected with luciferase reporter plasmids containing the indicated PPRE, and the wild-type or E157D PPARγ expression plasmid, or the empty vector. Means and standard errors of three independent experiments are shown. *, $p<0.05$ determined by two-way ANOVA with post-hoc Bonferroni tests.

9 E157D ENHANCES PPARγ INTERACTION WITH TRANSCRIPTION COREPRESSORS

9.1 Existing Evidence of DNA as an Allosteric Regulator of Nuclear Receptors.

Our findings so far have outlined a novel mechanism by which the E157D PPARγ mutation causes lipodystrophy and metabolic syndrome. We have shown that this conservative DNA-binding domain mutation, which directly contacts the PPRE, does not affect the affinity of PPARγ for typical PPRE sites, but reduces its ability to activate transcription of the majority of its target genes in a non-dominant negative manner. The disruption must involve a step in the transcriptional activation process that occurs after DNA binding. The major role of PPARγ in this process, once it is bound to the PPRE, is to recruit transcription coregulators to the DNA, which results in chromatin remodeling and regulation of transcription initiation complex assembly. We therefore proposed a new working hypothesis that the E157D mutation alters the interaction of PPARγ with transcription coactivators and/or corepressors, leading to reduced transcription of its target genes.

The novelty of such a mechanism lies in its implication of a functional interaction between the DNA binding and ligand binding/activation domains of the nuclear receptor. These two domains, located on opposite ends of the receptor molecule, have previously been thought to be completely independent of each other by way of the flexible hinge domain separating them. However, recent x-ray crystallography and nuclear magnetic resonance studies of nuclear receptor structure have challenged this view, showing that the glucocorticoid receptor and the retinoid X receptor assume a slightly different conformation when bound to

their respective DNA site than when free in solution [141, 142]. This new structural evidence suggests that the DNA molecule can be considered an allosteric regulator of nuclear receptor structure, affecting not just the DNA binding domain but inducing structural shifts in the entire protein. Moreover, the x-ray studies of the glucocorticoid receptor demonstrate that the DNA-bound receptor structural shifts are specific to the DNA sequence to which the receptor is bound, indicating that the interaction between the DNA and the receptor is informed by the specific sequence of the binding site. In turn, we have shown that different PPRE sequences influence the behavior of E157D PPARγ in different ways, ranging from extremely to mildly defective, to overactive. Given the position of glutamate 157, we predict that this variability can be explained by the specificity of its spatial position within each PPRE sequence and the effect of that interaction on the structure of the entire receptor. Finally, the glucocorticoid receptor studies also showed that the subtle structural changes in the receptor on different DNA binding sequences were functionally significant, manifested in recruitment of unique transcription coregulator complexes. This supports our working hypothesis of distinct transcription coregulator complexes recruited by the E157D PPARγ, influenced both by the receptor mutation and by the PPRE sequence to which it is bound, and resulting in changes in its transcriptional activity.

9.2 Nuclear Receptor Corepressors Suppress E157D PPARγ Activity More Than Wild-Type.

In order to assess the interaction of E157D PPARγ with transcription coregulators, we measured the transcriptional activity of the wild-type and mutant

receptors using the luciferase reporter assay in the presence of increasing amounts of various coregulators. Shown in Figure 24 (left panel), the transcriptional activity of the wild-type PPARγ on the aP2 promoter was suppressed in the presence of increasing amounts of SMRT until it reached a plateau of approximately 70% of its basal activity level. E157D PPARγ was also suppressed by SMRT, and its plateau level was significantly lower than that of the wild-type, at approximately 40% of maximal transcription. As expected, SMRT did not suppress the activity of wild-type or mutant PPARγ in the presence of saturating levels of rosiglitazone (data not shown). Similarly, increased amounts of NCoR1 reduced the basal but not the rosiglitazone-stimulated transcriptional activity of PPARγ (Figure 24, right panel). As with SMRT, there was a significant difference between the maximal suppression level of the wild-type and E157D PPARγ transcriptional activity on the aP2 promoter, with the mutant receptor activity being suppressed more effectively by the corepressor. Increased variability in this experiment resulted in loss of statistical significance at the maximal suppression level, but the difference between the suppression curves for the wild-type and mutant PPARγ is significant.

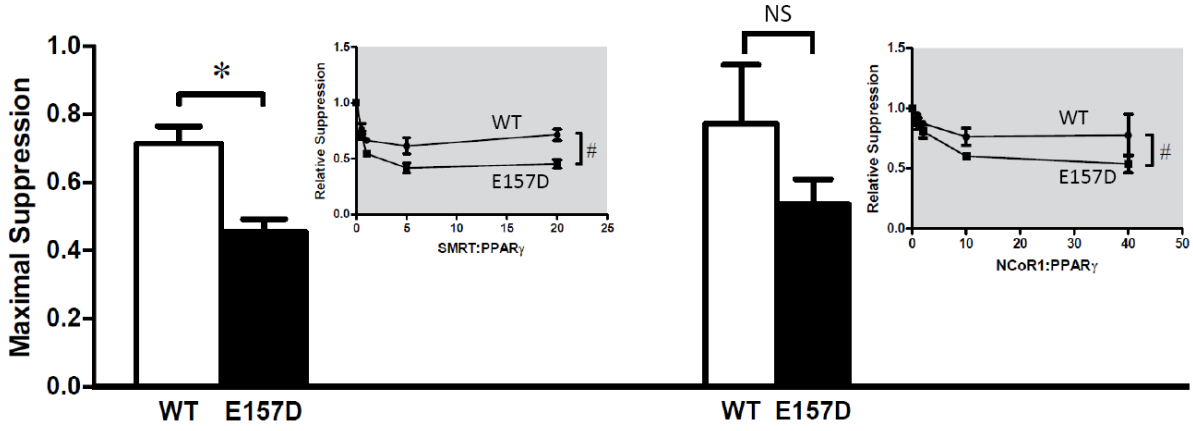

Figure 25. Suppression of Wild-Type and E157D PPARγ Transcriptional Activity by nuclear receptor corepressors.

NIH3T3 cells were transfected with the wild-type (circles) or E157D (squares) PPARγ, increasing amounts of the indicated corepressor protein, and the aP2 luciferase reporter plasmid. Insets show suppression curves for, and bar graphs represent maximal suppression by each corepressor. Data are means and standard errors of three independent experiments. *, $p<0.05$ determined by two-way ANOVA.

These data suggest that the E157D mutation generally renders PPARγ more vulnerable to suppression by transcription corepressors. In the context of our alternative model of nuclear receptor activity, the mutant receptor interaction with certain PPRE sequences may result in structural rearrangements which make the corepressor binding surfaces of the mutant more exposed than the wild-type receptor. Interestingly, in the presence of saturating concentration of rosiglitazone and large amounts of NCoR1, E157D PPARγ failed to increase transcription to the same extent as the wild-type (data not shown). The increase in PPARγ transcriptional activity in this environment is most likely due to increased availability of transcription coactivators as a result of wide-spread suppression of gene transcription in the cell. Reduced activity of the mutant in these experiments indirectly implies that the mutant PPARγ interacts less effectively with the transcription coactivators that become increasingly available when transcription in the cell is non-specifically suppressed by NCoR1. Thus, even though we have not identified a coactivator that directly enhances PPARγ transcriptional activity in our transfected system, there is indirect evidence that the E157D mutation reduces the

ability of PPARγ to effectively interact with transcription coactivators when bound to certain PPRE sequences. Overall, these results support our proposed model in which the DNA binding site allosterically and specifically regulates PPARγ transcriptional activity by altering its coregulator interaction surface structure, and this effect is disrupted by the E157D mutation.

10 DISCUSSION

10.1 Molecular Characterization of E157D PPARγ.

We have characterized the molecular mechanisms of action of a novel PPARγ mutant, E157D, which causes lipodystrophy and severe insulin-resistant diabetes in a human cohort. This mutation, located at the interface of PPARγ and the DNA molecule, works through a previously unreported mechanism in which DNA binding is mostly unaffected, yet activation of target gene transcription is severely impeded on the majority of PPARγ-regulated promoters.

The mutant PPARγ demonstrated a small, but consistent increase in DNA binding affinity in our gel-shift dose-response assays (Figure 14). Because the mutated residue is shorter than the wild-type, and protrudes directly into the major groove, it is possible that helix 1 of the mutant receptor inserts itself deeper into the major groove of the PPRE. Such a change may be proposed to result in a more favorable binding state due to replacement of more water molecules, a major driving force in protein-DNA interactions [143]. But we have clearly shown a lack of any dominant negative effect in transcription assays (Figure 11), so it is unlikely that this slightly increased DNA binding affinity results in blocking the PPRE through reduced promoter recycling. This difference is more likely to be negligible or very small.

Not all PPARγ target transcripts are equally affected by this mutation, and the changes in transcriptional activity include a gain of function on some genes that are not regulated by the wild-type PPARγ, while a small number of PPARγ-regulated transcripts remain unaffected by the E157D mutation. There are multiple factors besides the PPRE sequence that determine PPARγ transcriptional activity on a given

DNA site. Cell type, endogenous versus overexpressed promoters, native versus heterologous constructs are all important variables that affect transcriptional readouts. By reducing the varied DNA binding site to just the PPRE sequence, we demonstrated that the E157D mutation affects PPARγ transcriptional activity by disrupting a regulatory function that is intrinsic to the sequence of the PPRE. Expanding the region to include whole promoters and endogenous chromatin, we showed that other DNA-associated factors play a role in the effect the mutation has on the receptor function. Finally, taking the whole-genome approach allowed us to identify networks of genes that are misregulated by the mutant.

The results of our transcription reporter assays should not be generalized to other tissues and molecular contexts: the exact set of genes that is misregulated by E157D PPARγ in NIH3T3 cells is not expected be also similarly affected in human tissues. In fact, even in our transiently-transfected model system, the effect of the mutation was completely reversed on a full-promoter aP2 reporter construct compared with the isolated PPRE from the aP2 gene (Figure 9). Rather than directly translating our findings into the clinical scenario, they should be considered a general proof of concept that the E157D PPARγ mutation alters the way it interacts with DNA binding sites and results in various transcriptional changes. The "gain of function" genes in our transgenic cells likely share a common feature that allows the mutant receptor to bind and induce transcription more effectively than the wild-type, and the same is likely to be true in the human tissues, but the precise set of these transcripts may be different. Overall, our findings underscore the importance of glutamate 157, and likely the p-box in general, in the interaction with the DNA binding site, beyond simply acting as an anchor for PPARγ.

10.2 Comparisons with Other Known P-Box Mutants.

Overall, it is clear that not all amino acids in the p-box of nuclear receptors play an equal role in the receptor function. The two cysteines participate in coordinating the zinc atom and required for the correct folding of the zinc finger structure, and are therefore necessary for DNA binding. This is evidenced by numerous reports of naturally-occurring or site-directed cysteine mutations which abolish DNA binding, resulting in complete loss of function of the receptor [62, 144-147]. However, the other four amino acids in the p-box have a more subtle role and are known to be important for DNA binding site discrimination. For instance, replacing just two amino acids in the p-box of the thyroid hormone receptor to make it identical to the glucocorticoid receptor p-box sequence completely redirects the DNA binding site preference of the receptor, abolishing thyroid hormone response element binding and rendering the mutant receptor able to bind and activate glucocorticoid response elements [148].

E157D is the first reported naturally-occurring p-box mutation in PPARγ, but other nuclear receptors in which similar mutations have been reported include steroidogenic factor 1 (SF-1) and photoreceptor-specific orphan nuclear receptor NR2E3 (Table 6). The latter involves an in-frame deletion of three p-box amino acids including a zinc coordinating cysteine, resulting in disruption of the zinc finger structure. DNA binding is abolished by this p.N65_C67del NR2E3 mutation, causing a rare retinal disorder in humans called autosomal-recessive enhanced S-cone syndrome. Two SF-1 p-box mutants have been reported in the human population: C33S and G35E. The former one disrupts the zinc coordination lattice, similarly to p.N65_C67del in NR2E3 and C190S in PPARγ [62, 149], resulting in complete loss

of DNA binding and transcriptional activity. This mutation causes 46, XY partial gonadal dysgenesis and underandrogenization [150].

The G35E mutation, however, preserves the zinc-finger folding of the DNA binding domain, and disrupts its binding to most SF-1 response elements, while still maintaining the ability to bind a certain subset of the DNA sequences [151, 152]. Glycine 35 of SF-1 is equivalent to glycine 161 of PPARγ, located on the same aspect of the a-helix as glutamate 157, and facing the major groove of the DNA molecule. The variability in SF-1 binding to target DNA sites when this glycine is mutated to a glutamate reflects the importance of various DNA sequences in the way the receptors interacts with the DNA. Binding to non-SF-1 response elements was not investigated, but is an intriguing possibility given that this mutant is transcriptionally active on a subset of its target sites. Furthermore, 46XY humans heterozygous for G35E SF-1 have the added clinical feature of adrenal failure, in addition to the sex-reversal caused by the complete loss-of-function SF-1 C33S mutant. If the G35E mutation causes SF-1 to recognize and non-SF-1 target sites and regulate transcription of a different gene network, the adrenal failure could be a result of this added activity. This hypothesis parallels our own model in which E157D, a non-cysteine p-box mutation interfacing with the DNA major groove, gains transcriptional activity on weak PPREs and leads to non-classical lipodystrophy features in the human cohort.

A chance discovery lead to the identification of the D69A mutation in the HNF4 gene in multiple sources of the human hepatoma HepG2 cell line [153]. Although not found in a human population, this mutant is of particular interest to us as it involves the amino acid that is the equivalent of glutamate 157 in PPARγ. Even

though aspartate 69 is a highly conserved residue in the HNF4 gene, replacing it with an alanine has only a mild effect on its transcriptional activity on known HNF4-regulated promoters. Specifically, the D69A HNF4 mutant retains full transcriptional activity in reporter assays from a classic HNF4 target promoter, and showed an increased activity on several other promoters. DNA binding site discrimination by this mutant was not investigated in more detail.

Table 6. Naturally-Occurring Nuclear Receptor P-Box Mutations Reported to Date.

Nuclear receptor mutation	P-box change	Clinical presentation	Molecular mechanism	Ref.
SF-1 G35E	wt: CESCK**G** mut: CESCK**E**	Adrenal failure and complete 46XY sex-reversal	Impaired DNA binding	[151, 152]
SF-1 C33S	wt: CES**C**KG mut: CES**S**KG	46XY partial gonadal dysgenesis and underandrogenization	No DNA binding	[150]
NR2E3 p.N65_C67del	wt: C**NGC**SG mut: C___SG	Autosomal-recessive enhanced S-cone syndrome	No DNA binding	[149]
HNF4 D69A	wt: C**D**GCKG mut: C**A**GCKG	HepG2 cell line mutant	Increased activity on select promoters	[153]

These studies, together with the ones discussed in the background section, have shaped our understanding of the way nuclear receptors discriminate between DNA sequences and the specific roles of p-box amino acids in this process. Although limited in number and mechanistic scope, studies of nuclear receptor p-box mutants are testaments to the complexity and subtlety of receptor-DNA interaction. Our

studies of the E157D PPARγ mutant reveal a deeper importance of the p-box in mediating fine-tuned transcriptional activity changes on various PPRE sequences.

10.3 DNA Binding Site as an Allosteric Regulator of Nuclear Receptor Activity.

Since the domain structure of nuclear receptors has been described, the DNA binding domain has been traditionally understood as an independent moiety from the ligand-binding and transactivation functions that are separated from it by a flexible hinge. This classic model treats the DNA binding domain as little more than an anchor, able to recognize and specifically bind various versions of a consensus DNA sequence, while the transcriptional regulation activity was carried out by the ligand-binding domain. While the major functional roles of each domain are accurately explained by this model, it fails to address the significance of subtle variations in DNA binding site sequences that have evolved to regulate gene expression. Tissue-specific nuclear receptor activity has been attributed largely to coregulator make-up, and with the regard to PPARγ, much work has been done to characterize the activity of various natural and synthetic ligands. Crystallizing whole nuclear receptor molecules for x-ray imaging has proved to be technically challenging, leading to a shift in the research of nuclear receptor structure and function to the isolated ligand-binding domains. As a result, relatively little advancement has been made in the past several decades in our understanding of the nuclear receptor-DNA interactions on a structural level.

Contrary to the conventional nuclear receptor domain model described here, our understanding of the general interactions between proteins and DNA implies

that there are reciprocal changes in structure imposed by binding. DNA bending by proteins that specifically bind to major grooves has been characterized in detail and shown to be categorically different and more severe than the slight changes caused by non-specific binding of proteins to minor grooves [154]. The major groove DNA distortion occurs in a sequence-specific manner and implies that the structure of the DNA-bound protein may also be altered to adjust to the binding state. In the case of nuclear receptors, this may result in DNA sequence-dependent regulation of coregulator complex recruitment mediated by structural changes in the DNA-binding domain and propagated to the ligand-binding and activation domains.

Several recent studies have revealed that the DNA binding domain and the DNA binding site may play a more important role in regulating the transcriptional activity of nuclear receptors than previously recognized. The x-ray crystal structure of the full-length PPARγ-RXRα heterodimer bound to the consensus PPRE molecule has shown that the DNA-binding domain of PPARγ makes extensive energy-favorable contacts with various regions of RXRα, suggesting that it contributes to heterodimer formation and transactivation of the complex [84]. Discrete structural rearrangements in the holoprotein RAR when free in solution versus bound to its DNA response element have been shown by NMR spectroscopy [142]. Crystallizing the glucocorticoid receptor homodimer on several known glucocorticoid response elements, Dr. Yamamoto and colleagues have shown that the receptor holoprotein assumes slightly different conformations on different DNA sequences [141]. These structural changes result in variations in the coregulator interaction surfaces that are exposed when the receptor is bound to different DNA sequence, and lead to recruitment of different compositions of coregulator complexes onto the DNA.

All of these recent observations suggest that the significance of the DNA binding site to nuclear receptor function is beyond merely that of an anchoring site. The interaction between a nuclear receptor and the DNA molecule is a complex process involving reciprocal structural changes in both partners and is ultimately reflected in the transcription coregulator recruitment process. In this emerging new model of nuclear receptors, the DNA molecule is thought of as an allosteric regulator of nuclear receptor transcriptional activity via the DNA binding domain, much like the specific ligands that regulate its activity at the ligand binding domain. In this way, fine-tuned transcriptional regulation of gene networks in achieved by a combination of many factors including the specific ligand, the DNA binding site sequence, and the transcriptional co-regulator abundance in the cell [155]. Our detailed analysis of the E157D PPARγ mutant supports the role of DNA as an allosteric regulator of PPARγ function. The PPRE sequence-dependent transcriptional activity of the mutant, compared with the wild-type, suggests that the p-box substitution plays a greater role on some PPREs than others. These findings indicate that not all PPRE sequences behave the same when bound to PPARγ, and the differences in transcriptional activity of the mutant on various PPREs are most likely explained by structural changes induced by these binding sites.

10.4 Implications for Nuclear Receptor Gene Evolution.

The discovery of differential nuclear receptor structure and behavior on different DNA binding sequences indicates that the diversity in nuclear receptor binding sites is non-trivial and may have regulatory significance for nuclear receptor transcriptional activity. The nuclear receptor superfamily has evolved from an

ancient common nuclear hormone receptor ancestor that is present in all bilateria [156]. One of the earliest indications that p-box and PPREs co-evolved came from the mutational analysis study which identified the p-box amino acids as determinants of nuclear receptor binding site selectivity [14]. By showing that replacing the p-box of the glucocorticoid receptor with that of the thyroid hormone receptor causes the chimeric receptor to bind and activate transcription from thyroid hormone DNA response elements, the authors provided a simple explanation for the co-evolution of nuclear receptors and hormone-responsive gene networks. Conversely, mutating the p-box of thyroid hormone receptor to mimic that of the glucocorticoid receptor (the GS125 mutation) enables the thyroid hormone receptor to recognize, bind and regulate transcription from GREs while abolishing TRE binding [148].

Recent advances in gene sequencing have enabled sequence conservation analyses across a wide array of species. The Mutual Information method was recently used to analyse co-evolving pairs of amino acids in PPARγ and RXRα with the goal of highlighting amino acid residues most important for specific DNA binding [157]. This study revealed that the PPARγ:RXRα heterodimerization interface, as well as the C-terminal extension of the DNA binding domain which binds the minor groove of the DNA in the 5’ PPRE flanking region, are both highly co-evolved and may be important for binding site recognition. The minor groove contact had previously been shown to play a role in DNA binding, both by PPRE sequence analysis [49] and crystal structure [84]. One proposed mechanism driving the co-evolution of DNA response elements and DNA binding interfaces of nuclear receptors involved conservation of the response element sequence and the cDNA

sequence of the nuclear receptor region that binds there [158]. Although this has only been demonstrated for the glucocorticoid receptor, one possibility is that nuclear receptor DNA recognition surfaces may preferentially bind DNA sequences that are identical to their cognate codons.

Our genome-wide study of E157D PPARγ transcriptional activity has identified a set of genes, some of which are functionally related, that are activated by the mutant receptor but not by the wild-type. Previous studies of PPARγ binding sites suggest that the wild-type PPARγ binds to PPREs in the vicinity of some of those genes. In the context of PPARγ and PPRE evolution, our findings indicate that these "gain-of-function" genes represent a gene network that co-evolved to have PPREs that weakly bind PPARγ. The E157D substitution disrupts this evolutionary process and makes PPARγ more active on these weak PPREs, and conversely makes it less active on stronger PPREs, changing the gene network regulated by this receptor and leading to atypical type III lipodystrophy.

11 FUTURE DIRECTIONS

11.1 Elucidate the Structural Features of PPARγ Interaction With Various PPREs.

At the heart of the allosteric DNA regulation model is the concept of subtle structural changes in the nuclear receptor upon binding to various DNA sequences. X-ray crystallography and, more recently, nuclear magnetic resonance have been used to study nuclear receptors bound to their respective DNA recognition sites, and specifically to demonstrate structural changes in the glucocorticoid receptor and RXR [141, 142] when bound to various DNA sequences. Both of these methods have the necessary sensitivity to detect slightly different positioning of the coregulator interacting surfaces, the functionally important outcome of allosteric regulation by DNA. But positional changes in the PPARγ protein when bound to PPREs have not been investigated to date.

The E157D mutation provides an opportunity to determine the role of the p-box in structural interactions between the protein and DNA. Our plans for the near future include resolving the structures of the wild-type and E157D PPARγ bound to several known PPREs. We predict that PPARγ, similarly to other nuclear receptors, will assume a slightly different conformation when bound to DNA than when free in solution. Furthermore, the positioning of coactivator interaction surfaces is predicted to be specific for each PPRE sequence, as has been shown for the glucocorticoid receptor [141]. The E157D mutation is predicted to have a variable effect on these structural relationships, resulting in variable disruptions in coregulator surface arrangement.

11.2 Characterize the Composition of Transcription Coregulator Complexes on Various PPREs.

To confirm that the PPRE sequence guides the recruitment of transcription coregulators to the promoter, we plan to carry out co-precipitation experiments to compare the amounts of known nuclear receptor corepressors and coactivators that bind PPARγ on different PPREs. This interaction will be tested in vitro using biotin-labeled PPREs and nuclear extracts containing transfected PPARγ, NCoR1 and SMRT proteins. The binding reaction will be carried out similarly as in the gel-shift experiment, with the addition of nuclear receptor corepressors after the PPARγ-PPRE complex has formed. The entire bound complex will then be precipitated by streptavidin-linked magnetic beads, washed and eluted. The amounts of coregulator molecules co-precipitated with the wild-type and E157D PPARγ on different PPREs will be compared on a Western blot. The results from this in vitro study will reveal whether there is indeed an intrinsic regulatory interaction between the PPRE and PPARγ that instructs the recruitment of coregulator molecules to the DNA binding site in a sequence-specific manner.

To test the validity of this model in the context of native chromatin, and any effect of DNA structure and chromatin-associated proteins, the promoter occupancy of various endogenous nuclear receptor coregulators at known PPARγ binding sites will be determined using chromatin immunoprecipitation. In addition, this method will be used to measure histone modifications at these sites as the functional outcome of differential coregulator recruitment. Commonly measured histone marks, such as H3K4 and H3K27, may emerge as the mechanistic step mediating the transcriptional effects of PPRE-directed recruitment of transcription

coregulators. Finally, by comparing these measurements in cells expressing wild-type and E157D PPARγ, the role of the p-box in the PPRE-PPARγ interaction proposed here will be confirmed in both the in-vitro and in-vivo models.

11.3 Analyze the Regulatory Regions of PPARγ-Inhibited Genes For Putative Negative PPREs.

Our genome-wide transcriptional activity studies revealed a set of genes involved in inflammation and the immune response that were downregulated by PPARγ in a ligand-dependent manner (Figure 19). Inhibition of inflammatory genes by PPARγ has been widely recognized, but this activity is poorly understood on the molecular level, and it is possible that downregulation of these genes is mediated by indirect factors upon PPARγ activation. However, direct ligand-dependent gene inhibition by the glucocorticoid receptor has been demonstrated on "negative GREs" [159]. These response elements have unique sequence features that differentiate them from previously defined GREs with positive transcription regulation activity. Negative PPREs have not been reported to date. Our results provide an opportunity for bioinformatic identification of putative negative PPREs which may mediate the downregulation of inflammatory genes by PPARγ.

REFERENCES

1. *OBESITY: Halting the epidemic by making health easier*, in *AT A GLANCE*2011, National Center for Chronic Disease Prevention and Health Promotion: Atlanta, GA: U.S.
2. Shah, N.R. and E.R. Braverman, *Measuring adiposity in patients: the utility of body mass index (BMI), percent body fat, and leptin.* PLoS One, 2012. **7**(4): p. e33308.
3. Pasco, J.A., et al., *Prevalence of obesity and the relationship between the body mass index and body fat: cross-sectional, population-based data.* PLoS One, 2012. **7**(1): p. e29580.
4. *National diabetes fact sheet: national estimates and general information on diabetes and prediabetes in the United States, 2011.*, 2011, Centers for Disease Control and Prevention: Atlanta, GA: U.S.
5. Linja, M.J., et al., *Expression of androgen receptor coregulators in prostate cancer.* Clin Cancer Res, 2004. **10**(3): p. 1032-40.
6. Klinge, C.M., et al., *Binding of type II nuclear receptors and estrogen receptor to full and half-site estrogen response elements in vitro.* Nucleic Acids Res, 1997. **25**(10): p. 1903-12.
7. Chen, J., H.K. Kinyamu, and T.K. Archer, *Changes in attitude, changes in latitude: nuclear receptors remodeling chromatin to regulate transcription.* Mol Endocrinol, 2006. **20**(1): p. 1-13.
8. Hebbar, P.B. and T.K. Archer, *Chromatin remodeling by nuclear receptors.* Chromosoma, 2003. **111**(8): p. 495-504.

9. Collingwood, T.N., F.D. Urnov, and A.P. Wolffe, *Nuclear receptors: coactivators, corepressors and chromatin remodeling in the control of transcription.* J Mol Endocrinol, 1999. **23**(3): p. 255-75.

10. Perissi, V., et al., *A corepressor/coactivator exchange complex required for transcriptional activation by nuclear receptors and other regulated transcription factors.* Cell, 2004. **116**(4): p. 511-26.

11. Rosenfeld, M.G., V.V. Lunyak, and C.K. Glass, *Sensors and signals: a coactivator/corepressor/epigenetic code for integrating signal-dependent programs of transcriptional response.* Genes Dev, 2006. **20**(11): p. 1405-28.

12. Jacobs, M.N., M. Dickins, and D.F. Lewis, *Homology modelling of the nuclear receptors: human oestrogen receptorbeta (hERbeta), the human pregnane-X-receptor (PXR), the Ah receptor (AhR) and the constitutive androstane receptor (CAR) ligand binding domains from the human oestrogen receptor alpha (hERalpha) crystal structure, and the human peroxisome proliferator activated receptor alpha (PPARalpha) ligand binding domain from the human PPARgamma crystal structure.* J Steroid Biochem Mol Biol, 2003. **84**(2-3): p. 117-32.

13. Robinson-Rechavi, M., H. Escriva Garcia, and V. Laudet, *The nuclear receptor superfamily.* J Cell Sci, 2003. **116**(Pt 4): p. 585-6.

14. Umesono, K. and R.M. Evans, *Determinants of target gene specificity for steroid/thyroid hormone receptors.* Cell, 1989. **57**(7): p. 1139-46.

15. Mader, S., et al., *Three amino acids of the oestrogen receptor are essential to its ability to distinguish an oestrogen from a glucocorticoid-responsive element.* Nature, 1989. **338**(6212): p. 271-4.

16. Glass, C.K., *Differential recognition of target genes by nuclear receptor monomers, dimers, and heterodimers.* Endocr Rev, 1994. **15**(3): p. 391-407.

17. Danielsen, M., L. Hinck, and G.M. Ringold, *Two amino acids within the knuckle of the first zinc finger specify DNA response element activation by the glucocorticoid receptor.* Cell, 1989. **57**(7): p. 1131-8.

18. Desvergne, B. and W. Wahli, *Peroxisome proliferator-activated receptors: nuclear control of metabolism.* Endocr Rev, 1999. **20**(5): p. 649-88.

19. Lefterova, M.I., et al., *PPARgamma and C/EBP factors orchestrate adipocyte biology via adjacent binding on a genome-wide scale.* Genes Dev, 2008. **22**(21): p. 2941-52.

20. Nielsen, R., et al., *Genome-wide profiling of PPARgamma:RXR and RNA polymerase II occupancy reveals temporal activation of distinct metabolic pathways and changes in RXR dimer composition during adipogenesis.* Genes Dev, 2008. **22**(21): p. 2953-67.

21. Heinaniemi, M., et al., *Meta-analysis of primary target genes of peroxisome proliferator-activated receptors.* Genome Biol, 2007. **8**(7): p. R147.

22. Temple, K.A., et al., *An intact DNA-binding domain is not required for peroxisome proliferator-activated receptor gamma (PPARgamma) binding and activation on some PPAR response elements.* J Biol Chem, 2005. **280**(5): p. 3529-40.

23. Oliver, W.R., Jr., et al., *A selective peroxisome proliferator-activated receptor delta agonist promotes reverse cholesterol transport.* Proc Natl Acad Sci U S A, 2001. **98**(9): p. 5306-11.

24. Lehmann, J.M., et al., *An antidiabetic thiazolidinedione is a high affinity ligand for peroxisome proliferator-activated receptor gamma (PPAR gamma).* J Biol Chem, 1995. **270**(22): p. 12953-6.

25. Tontonoz, P. and B.M. Spiegelman, *Fat and beyond: the diverse biology of PPARgamma.* Annu Rev Biochem, 2008. **77**: p. 289-312.

26. Forman, B.M., et al., *15-Deoxy-delta 12, 14-prostaglandin J2 is a ligand for the adipocyte determination factor PPAR gamma.* Cell, 1995. **83**(5): p. 803-12.

27. Forman, B.M., et al., *Identification of a nuclear receptor that is activated by farnesol metabolites.* Cell, 1995. **81**(5): p. 687-93.

28. Kliewer, S.A., et al., *A prostaglandin J2 metabolite binds peroxisome proliferator-activated receptor gamma and promotes adipocyte differentiation.* Cell, 1995. **83**(5): p. 813-9.

29. Diaz-Delfin, J., M. Morales, and C. Caelles, *Hypoglycemic action of thiazolidinediones/peroxisome proliferator-activated receptor gamma by inhibition of the c-Jun NH2-terminal kinase pathway.* Diabetes, 2007. **56**(7): p. 1865-71.

30. Steppan, C.M., et al., *The hormone resistin links obesity to diabetes.* Nature, 2001. **409**(6818): p. 307-12.

31. Hevener, A.L., et al., *Macrophage PPAR gamma is required for normal skeletal muscle and hepatic insulin sensitivity and full antidiabetic effects of thiazolidinediones.* J Clin Invest, 2007. **117**(6): p. 1658-69.

32. Odegaard, J.I., et al., *Macrophage-specific PPARgamma controls alternative activation and improves insulin resistance.* Nature, 2007. **447**(7148): p. 1116-20.

33. Straus, D.S. and C.K. Glass, *Anti-inflammatory actions of PPAR ligands: new insights on cellular and molecular mechanisms.* Trends Immunol, 2007. **28**(12): p. 551-8.

34. Han, S. and J. Roman, *Peroxisome proliferator-activated receptor gamma: a novel target for cancer therapeutics?* Anticancer Drugs, 2007. **18**(3): p. 237-44.

35. Takada, I., et al., *Suppression of PPAR transactivation switches cell fate of bone marrow stem cells from adipocytes into osteoblasts.* Ann N Y Acad Sci, 2007. **1116**: p. 182-95.

36. Grey, A., et al., *The peroxisome proliferator-activated receptor-gamma agonist rosiglitazone decreases bone formation and bone mineral density in healthy postmenopausal women: a randomized, controlled trial.* J Clin Endocrinol Metab, 2007. **92**(4): p. 1305-10.

37. Wan, Y., L.W. Chong, and R.M. Evans, *PPAR-gamma regulates osteoclastogenesis in mice.* Nat Med, 2007. **13**(12): p. 1496-503.

38. Leisewitz, A.V., et al., *A PPARs cross-talk concertedly commits C6 glioma cells to oligodendrocytes and induces enzymes involved in myelin synthesis.* J Cell Physiol, 2008. **217**(2): p. 367-76.

39. Kim, J., et al., *Peroxisome proliferator-activated receptor gamma is a target of progesterone regulation in the preovulatory follicles and controls ovulation in mice.* Mol Cell Biol, 2008. **28**(5): p. 1770-82.

40. Minge, C.E., et al., *Peroxisome proliferator-activated receptor-gamma agonist rosiglitazone reverses the adverse effects of diet-induced obesity on oocyte quality.* Endocrinology, 2008. **149**(5): p. 2646-56.

41. Zhu, Y., et al., *Structural organization of mouse peroxisome proliferator-activated receptor gamma (mPPAR gamma) gene: alternative promoter use and different splicing yield two mPPAR gamma isoforms.* Proc Natl Acad Sci U S A, 1995. **92**(17): p. 7921-5.

42. Fajas, L., et al., *The organization, promoter analysis, and expression of the human PPARgamma gene.* J Biol Chem, 1997. **272**(30): p. 18779-89.

43. Tontonoz, P., et al., *mPPAR gamma 2: tissue-specific regulator of an adipocyte enhancer.* Genes Dev, 1994. **8**(10): p. 1224-34.

44. Ren, D., et al., *PPARgamma knockdown by engineered transcription factors: exogenous PPARgamma2 but not PPARgamma1 reactivates adipogenesis.* Genes Dev, 2002. **16**(1): p. 27-32.

45. Werman, A., et al., *Ligand-independent activation domain in the N terminus of peroxisome proliferator-activated receptor gamma (PPARgamma). Differential activity of PPARgamma1 and -2 isoforms and influence of insulin.* J Biol Chem, 1997. **272**(32): p. 20230-5.

46. Kliewer, S.A., et al., *Retinoid X receptor interacts with nuclear receptors in retinoic acid, thyroid hormone and vitamin D3 signalling.* Nature, 1992. **355**(6359): p. 446-9.

47. Kliewer, S.A., et al., *Convergence of 9-cis retinoic acid and peroxisome proliferator signalling pathways through heterodimer formation of their receptors.* Nature, 1992. **358**(6389): p. 771-4.

48. Hsu, M.H., et al., *A carboxyl-terminal extension of the zinc finger domain contributes to the specificity and polarity of peroxisome proliferator-activated receptor DNA binding.* J Biol Chem, 1998. **273**(43): p. 27988-97.

49. A, I.J., et al., *Polarity and specific sequence requirements of peroxisome proliferator-activated receptor (PPAR)/retinoid X receptor heterodimer binding to DNA. A functional analysis of the malic enzyme gene PPAR response element.* J Biol Chem, 1997. **272**(32): p. 20108-17.

50. Nakachi, Y., et al., *Identification of novel PPARgamma target genes by integrated analysis of ChIP-on-chip and microarray expression data during adipocyte differentiation.* Biochem Biophys Res Commun, 2008. **372**(2): p. 362-6.

51. Sears, D.D., et al., *Selective modulation of promoter recruitment and transcriptional activity of PPARgamma.* Biochem Biophys Res Commun, 2007. **364**(3): p. 515-21.

52. Wakabayashi, K., et al., *The peroxisome proliferator-activated receptor gamma/retinoid X receptor alpha heterodimer targets the histone modification enzyme PR-Set7/Setd8 gene and regulates adipogenesis through a positive feedback loop.* Mol Cell Biol, 2009. **29**(13): p. 3544-55.

53. Juge-Aubry, C., et al., *DNA binding properties of peroxisome proliferator-activated receptor subtypes on various natural peroxisome proliferator response elements. Importance of the 5'-flanking region.* J Biol Chem, 1997. **272**(40): p. 25252-9.

54. Garg, A., R.M. Peshock, and J.L. Fleckenstein, *Adipose tissue distribution pattern in patients with familial partial lipodystrophy (Dunnigan variety).* J Clin Endocrinol Metab, 1999. **84**(1): p. 170-4.

55. Herbst, K.L., et al., *Kobberling type of familial partial lipodystrophy: an underrecognized syndrome.* Diabetes Care, 2003. **26**(6): p. 1819-24.

56. Agostini, M., et al., *Non-DNA binding, dominant-negative, human PPARgamma mutations cause lipodystrophic insulin resistance.* Cell Metab, 2006. **4**(4): p. 303-11.

57. Francis, G.A., et al., *Peroxisomal proliferator activated receptor-gamma deficiency in a Canadian kindred with familial partial lipodystrophy type 3 (FPLD3).* BMC Med Genet, 2006. **7**: p. 3.

58. Hegele, R.A., et al., *PPARG F388L, a transactivation-deficient mutant, in familial partial lipodystrophy.* Diabetes, 2002. **51**(12): p. 3586-90.

59. Jeninga, E.H., et al., *Impaired peroxisome proliferator-activated receptor gamma function through mutation of a conserved salt bridge (R425C) in familial partial lipodystrophy.* Mol Endocrinol, 2007. **21**(5): p. 1049-65.

60. Li, G. and T. Leff, *Altered promoter recycling rates contribute to dominant-negative activity of human peroxisome proliferator-activated receptor-gamma mutations associated with diabetes.* Mol Endocrinol, 2007. **21**(4): p. 857-64.

61. Ludtke, A., et al., *New PPARG mutation leads to lipodystrophy and loss of protein function that is partially restored by a synthetic ligand.* J Med Genet, 2007. **44**(9): p. e88.

62. Ludtke, A., et al., *Peroxisome proliferator-activated receptor-gamma C190S mutation causes partial lipodystrophy.* J Clin Endocrinol Metab, 2007. **92**(6): p. 2248-55.

63. Young, J., et al., *Type A insulin resistance syndrome revealing a novel lamin A mutation.* Diabetes, 2005. **54**(6): p. 1873-8.

64. Hegele, R.A. and R.L. Pollex, *Genetic and physiological insights into the metabolic syndrome.* Am J Physiol Regul Integr Comp Physiol, 2005. **289**(3): p. R663-9.

65. Mori, Y., et al., *Effect of troglitazone on body fat distribution in type 2 diabetic patients.* Diabetes Care, 1999. **22**(6): p. 908-12.

66. Kelly, I.E., et al., *Effects of a thiazolidinedione compound on body fat and fat distribution of patients with type 2 diabetes.* Diabetes Care, 1999. **22**(2): p. 288-93.

67. Joy, T. and R.A. Hegele, *Genetics of metabolic syndrome: is there a role for phenomics?* Curr Atheroscler Rep, 2008. **10**(3): p. 201-8.

68. Guettier, J.M., et al., *Leptin therapy for partial lipodystrophy linked to a PPAR-gamma mutation.* Clin Endocrinol (Oxf), 2008. **68**(4): p. 547-54.

69. Jeninga, E.H., M. Gurnell, and E. Kalkhoven, *Functional implications of genetic variation in human PPARgamma.* Trends Endocrinol Metab, 2009. **20**(8): p. 380-7.

70. Agarwal, A.K. and A. Garg, *A novel heterozygous mutation in peroxisome proliferator-activated receptor-gamma gene in a patient with familial partial lipodystrophy.* J Clin Endocrinol Metab, 2002. **87**(1): p. 408-11.

71. Barroso, I., et al., *Dominant negative mutations in human PPARgamma associated with severe insulin resistance, diabetes mellitus and hypertension.* Nature, 1999. **402**(6764): p. 880-3.

72. Hegele, R.A., et al., *A frameshift mutation in peroxisome-proliferator-activated receptor-gamma in familial partial lipodystrophy subtype 3 (FPLD3; MIM 604367).* Clin Genet, 2006. **70**(4): p. 360-2.

73. Monajemi, H., et al., *Familial partial lipodystrophy phenotype resulting from a single-base mutation in deoxyribonucleic acid-binding domain of peroxisome proliferator-activated receptor-gamma.* J Clin Endocrinol Metab, 2007. **92**(5): p. 1606-12.

74. Florez, J.C., et al., *Effects of the type 2 diabetes-associated PPARG P12A polymorphism on progression to diabetes and response to troglitazone.* J Clin Endocrinol Metab, 2007. **92**(4): p. 1502-9.

75. Yong, E.L., J. Li, and M.H. Liu, *Single gene contributions: genetic variants of peroxisome proliferator-activated receptor (isoforms alpha, beta/delta and gamma) and mechanisms of dyslipidemias.* Curr Opin Lipidol, 2008. **19**(2): p. 106-12.

76. Deeb, S.S., et al., *A Pro12Ala substitution in PPARgamma2 associated with decreased receptor activity, lower body mass index and improved insulin sensitivity.* Nat Genet, 1998. **20**(3): p. 284-7.

77. Ristow, M., et al., *Obesity associated with a mutation in a genetic regulator of adipocyte differentiation.* N Engl J Med, 1998. **339**(14): p. 953-9.

78. Yen, C.J., et al., *Molecular scanning of the human peroxisome proliferator activated receptor gamma (hPPAR gamma) gene in diabetic Caucasians:*

identification of a Pro12Ala PPAR gamma 2 missense mutation. Biochem Biophys Res Commun, 1997. **241**(2): p. 270-4.

79. Nelson, C.C., S.C. Hendy, and P.J. Romaniuk, *Relationship between P-box amino acid sequence and DNA binding specificity of the thyroid hormone receptor. The effects of half-site sequence in everted repeats.* J Biol Chem, 1995. **270**(28): p. 16981-7.
80. Zilliacus, J., et al., *Evolution of distinct DNA-binding specificities within the nuclear receptor family of transcription factors.* Proc Natl Acad Sci U S A, 1994. **91**(10): p. 4175-9.
81. Ng, P.C. and S. Henikoff, *Predicting deleterious amino acid substitutions.* Genome Res, 2001. **11**(5): p. 863-74.
82. Kumar, P., S. Henikoff, and P.C. Ng, *Predicting the effects of coding non-synonymous variants on protein function using the SIFT algorithm.* Nat Protoc, 2009. **4**(7): p. 1073-81.
83. Guex, N., M.C. Peitsch, and T. Schwede, *Automated comparative protein structure modeling with SWISS-MODEL and Swiss-PdbViewer: a historical perspective.* Electrophoresis, 2009. **30 Suppl 1**: p. S162-73.
84. Chandra, V., et al., *Structure of the intact PPAR-gamma-RXR- nuclear receptor complex on DNA.* Nature, 2008. **456**(7220): p. 350-6.
85. Kaplan, W. and T.G. Littlejohn, *Swiss-PDB Viewer (Deep View).* Brief Bioinform, 2001. **2**(2): p. 195-7.
86. Gunsteren, W.F.v., *Biomolecular simulation: the GROMOS96 manual and user guide.*1996: Vdf Hochschulverlag ETHZ.

87. Bordner, A.J. and R.A. Abagyan, *Large-scale prediction of protein geometry and stability changes for arbitrary single point mutations.* Proteins, 2004. **57**(2): p. 400-13.

88. Abagyan, R. and M. Totrov, *Biased probability Monte Carlo conformational searches and electrostatic calculations for peptides and proteins.* J Mol Biol, 1994. **235**(3): p. 983-1002.

89. Tengholm, A., M.N. Teruel, and T. Meyer, *Single cell imaging of PI3K activity and glucose transporter insertion into the plasma membrane by dual color evanescent wave microscopy.* Sci STKE, 2003. **2003**(169): p. PL4.

90. Hummasti, S. and P. Tontonoz, *The peroxisome proliferator-activated receptor N-terminal domain controls isotype-selective gene expression and adipogenesis.* Mol Endocrinol, 2006. **20**(6): p. 1261-75.

91. Livak, K.J. and T.D. Schmittgen, *Analysis of relative gene expression data using real-time quantitative PCR and the 2(-Delta Delta C(T)) Method.* Methods, 2001. **25**(4): p. 402-8.

92. Kulyyassov, A., M. Shoaib, and V. Ogryzko, *Use of in vivo biotinylation for chromatin immunoprecipitation.* Curr Protoc Cell Biol, 2011. **Chapter 17**: p. Unit17 12.

93. Loots, G.G. and I. Ovcharenko, *rVISTA 2.0: evolutionary analysis of transcription factor binding sites.* Nucleic Acids Res, 2004. **32**(Web Server issue): p. W217-21.

94. Fan, F. and K.V. Wood, *Bioluminescent assays for high-throughput screening.* Assay Drug Dev Technol, 2007. **5**(1): p. 127-36.

95. Miraglia, L.J., F.J. King, and R. Damoiseaux, *Seeing the light: luminescent reporter gene assays.* Comb Chem High Throughput Screen, 2011. **14**(8): p. 648-57.

96. Rosenthal, N., *Identification of regulatory elements of cloned genes with functional assays.* Methods Enzymol, 1987. **152**: p. 704-20.

97. Soichot, M., et al., *Identification of a variable number of tandem repeats polymorphism and characterization of LEF-1 response elements in the promoter of the IDO1 gene.* PLoS One, 2011. **6**(9): p. e25470.

98. Pontiller, J., et al., *Identification of CHO endogenous gene regulatory elements.* Mol Biotechnol, 2010. **45**(3): p. 235-40.

99. Okuno, Y., et al., *Human catalase gene is regulated by peroxisome proliferator activated receptor-gamma through a response element distinct from that of mouse.* Endocr J, 2010. **57**(4): p. 303-9.

100. Takazawa, T., et al., *Peroxisome proliferator-activated receptor gamma agonist rosiglitazone increases expression of very low density lipoprotein receptor gene in adipocytes.* J Biol Chem, 2009. **284**(44): p. 30049-57.

101. Nagai, S., et al., *Identification of a functional peroxisome proliferator-activated receptor responsive element within the murine perilipin gene.* Endocrinology, 2004. **145**(5): p. 2346-56.

102. Kim, H.I., et al., *Identification and functional characterization of the peroxisomal proliferator response element in rat GLUT2 promoter.* Diabetes, 2000. **49**(9): p. 1517-24.

103. Goto, T., et al., *Farnesyl pyrophosphate regulates adipocyte functions as an endogenous PPARgamma agonist.* Biochem J, 2011. **438**(1): p. 111-9.

104. Yokoi, H., et al., *Hydroxy monounsaturated fatty acids as agonists for peroxisome proliferator-activated receptors.* Biol Pharm Bull, 2010. **33**(5): p. 854-61.

105. Landrier, J.F., et al., *Adiponectin expression is induced by vitamin E via a peroxisome proliferator-activated receptor gamma-dependent mechanism.* Endocrinology, 2009. **150**(12): p. 5318-25.

106. Schopfer, F.J., et al., *Nitrolinoleic acid: an endogenous peroxisome proliferator-activated receptor gamma ligand.* Proc Natl Acad Sci U S A, 2005. **102**(7): p. 2340-5.

107. Frohnert, B.I., T.Y. Hui, and D.A. Bernlohr, *Identification of a functional peroxisome proliferator-responsive element in the murine fatty acid transport protein gene.* J Biol Chem, 1999. **274**(7): p. 3970-7.

108. Schoonjans, K., et al., *PPARalpha and PPARgamma activators direct a distinct tissue-specific transcriptional response via a PPRE in the lipoprotein lipase gene.* EMBO J, 1996. **15**(19): p. 5336-48.

109. Iwaki, M., et al., *Induction of adiponectin, a fat-derived antidiabetic and antiatherogenic factor, by nuclear receptors.* Diabetes, 2003. **52**(7): p. 1655-63.

110. Baumann, C.A., et al., *Cloning and characterization of a functional peroxisome proliferator activator receptor-gamma-responsive element in the promoter of the CAP gene.* J Biol Chem, 2000. **275**(13): p. 9131-5.

111. Kishida, K., et al., *Enhancement of the aquaporin adipose gene expression by a peroxisome proliferator-activated receptor gamma.* J Biol Chem, 2001. **276**(51): p. 48572-9.

112. Tugwood, J.D., et al., *The mouse peroxisome proliferator activated receptor recognizes a response element in the 5' flanking sequence of the rat acyl CoA oxidase gene.* EMBO J, 1992. **11**(2): p. 433-9.

113. Tontonoz, P., et al., *PPAR gamma 2 regulates adipose expression of the phosphoenolpyruvate carboxykinase gene.* Mol Cell Biol, 1995. **15**(1): p. 351-7.

114. Zeeberg, B., *Shannon information theoretic computation of synonymous codon usage biases in coding regions of human and mouse genomes.* Genome Res, 2002. **12**(6): p. 944-55.

115. Reid, G., et al., *Cyclic, proteasome-mediated turnover of unliganded and liganded ERalpha on responsive promoters is an integral feature of estrogen signaling.* Mol Cell, 2003. **11**(3): p. 695-707.

116. Fowler, A.M. and E.T. Alarid, *Dynamic control of nuclear receptor transcription.* Sci STKE, 2004. **2004**(256): p. pe51.

117. Kinyamu, H.K., J. Chen, and T.K. Archer, *Linking the ubiquitin-proteasome pathway to chromatin remodeling/modification by nuclear receptors.* J Mol Endocrinol, 2005. **34**(2): p. 281-97.

118. Floyd, Z.E. and J.M. Stephens, *Interferon-gamma-mediated activation and ubiquitin-proteasome-dependent degradation of PPARgamma in adipocytes.* J Biol Chem, 2002. **277**(6): p. 4062-8.

119. Hauser, S., et al., *Degradation of the peroxisome proliferator-activated receptor gamma is linked to ligand-dependent activation.* J Biol Chem, 2000. **275**(24): p. 18527-33.

120. Molinari, E., M. Gilman, and S. Natesan, *Proteasome-mediated degradation of transcriptional activators correlates with activation domain potency in vivo.* EMBO J, 1999. **18**(22): p. 6439-47.

121. Rohs, R., et al., *The role of DNA shape in protein-DNA recognition.* Nature, 2009. **461**(7268): p. 1248-53.

122. Wang, D., N.B. Ulyanov, and V.B. Zhurkin, *Sequence-dependent Kink-and-Slide deformations of nucleosomal DNA facilitated by histone arginines bound in the minor groove.* J Biomol Struct Dyn, 2010. **27**(6): p. 843-59.

123. Cui, F. and V.B. Zhurkin, *Structure-based analysis of DNA sequence patterns guiding nucleosome positioning in vitro.* J Biomol Struct Dyn, 2010. **27**(6): p. 821-41.

124. Tao, H. and T. Hajri, *Very low density lipoprotein receptor promotes adipocyte differentiation and mediates the proadipogenic effect of peroxisome proliferator-activated receptor gamma agonists.* Biochem Pharmacol, 2011. **82**(12): p. 1950-62.

125. Rigamonti, E., et al., *Induction of CXCR2 receptor by peroxisome proliferator-activated receptor gamma in human macrophages.* Arterioscler Thromb Vasc Biol, 2008. **28**(5): p. 932-9.

126. Shimada, T., et al., *Peroxisome proliferator-activated receptor gamma (PPARgamma) regulates trefoil factor family 2 (TFF2) expression in gastric epithelial cells.* Int J Biochem Cell Biol, 2007. **39**(3): p. 626-37.

127. Chen, J.G., et al., *Identification of a peroxisome proliferator responsive element (PPRE)-like cis-element in mouse plasminogen activator inhibitor-1 gene promoter.* Biochem Biophys Res Commun, 2006. **347**(3): p. 821-6.

128. Chilton, J.M. and J.M. Le Doux, *Quantitative analysis of retroviral and lentiviral gene transfer to murine embryonic stem cells.* J Biotechnol, 2008. **138**(1-2): p. 42-51.

129. Kita-Matsuo, H., et al., *Lentiviral vectors and protocols for creation of stable hESC lines for fluorescent tracking and drug resistance selection of cardiomyocytes.* PLoS One, 2009. **4**(4): p. e5046.

130. Pascual, G., et al., *A SUMOylation-dependent pathway mediates transrepression of inflammatory response genes by PPAR-gamma.* Nature, 2005. **437**(7059): p. 759-63.

131. Glass, C.K. and S. Ogawa, *Combinatorial roles of nuclear receptors in inflammation and immunity.* Nat Rev Immunol, 2006. **6**(1): p. 44-55.

132. Remels, A.H., et al., *PPARgamma inhibits NF-kappaB-dependent transcriptional activation in skeletal muscle.* Am J Physiol Endocrinol Metab, 2009. **297**(1): p. E174-83.

133. Sharma, A.M. and B. Staels, *Review: Peroxisome proliferator-activated receptor gamma and adipose tissue--understanding obesity-related changes in regulation of lipid and glucose metabolism.* J Clin Endocrinol Metab, 2007. **92**(2): p. 386-95.

134. Glass, C.K. and K. Saijo, *Nuclear receptor transrepression pathways that regulate inflammation in macrophages and T cells.* Nat Rev Immunol, 2010. **10**(5): p. 365-76.

135. Bloch, M., et al., *High-mobility group A1 protein: a new coregulator of peroxisome proliferator-activated receptor-gamma-mediated transrepression in the vasculature.* Circ Res, 2012. **110**(3): p. 394-405.

136. Hamza, M.S., et al., *De-novo identification of PPARgamma/RXR binding sites and direct targets during adipogenesis.* PLoS One, 2009. **4**(3): p. e4907.

137. Kast-Woelbern, H.R., et al., *Rosiglitazone induction of Insig-1 in white adipose tissue reveals a novel interplay of peroxisome proliferator-activated receptor gamma and sterol regulatory element-binding protein in the regulation of adipogenesis.* J Biol Chem, 2004. **279**(23): p. 23908-15.

138. Lecka-Czernik, B., et al., *Activation of peroxisome proliferator-activated receptor gamma (PPARgamma) by rosiglitazone suppresses components of the insulin-like growth factor regulatory system in vitro and in vivo.* Endocrinology, 2007. **148**(2): p. 903-11.

139. Park, U.H., et al., *Additional sex comb-like (ASXL) proteins 1 and 2 play opposite roles in adipogenesis via reciprocal regulation of peroxisome proliferator-activated receptor {gamma}.* J Biol Chem, 2011. **286**(2): p. 1354-63.

140. Lefterova, M.I., et al., *Cell-specific determinants of peroxisome proliferator-activated receptor gamma function in adipocytes and macrophages.* Mol Cell Biol, 2010. **30**(9): p. 2078-89.

141. Meijsing, S.H., et al., *DNA binding site sequence directs glucocorticoid receptor structure and activity.* Science, 2009. **324**(5925): p. 407-10.

142. van Tilborg, P.J., et al., *Millisecond to microsecond time scale dynamics of the retinoid X and retinoic acid receptor DNA-binding domains and dimeric complex formation.* Biochemistry, 1999. **38**(7): p. 1951-6.

143. Jayaram, B. and T. Jain, *The role of water in protein-DNA recognition.* Annu Rev Biophys Biomol Struct, 2004. **33**: p. 343-61.

144. Kawate, H., et al., *Impaired nuclear translocation, nuclear matrix targeting, and intranuclear mobility of mutant androgen receptors carrying amino acid substitutions in the deoxyribonucleic acid-binding domain derived from androgen insensitivity syndrome patients.* J Clin Endocrinol Metab, 2005. **90**(11): p. 6162-9.

145. Ramos, R.A., et al., *Dysfunctional glucocorticoid receptor with a single point mutation ablates the CCAAT/enhancer binding protein-dependent growth suppression response in a steroid-resistant rat hepatoma cell variant.* FASEB J, 1999. **13**(1): p. 169-80.

146. Liu, W., A.G. Hillmann, and J.M. Harmon, *Hormone-independent repression of AP-1-inducible collagenase promoter activity by glucocorticoid receptors.* Mol Cell Biol, 1995. **15**(2): p. 1005-13.

147. Severne, Y., et al., *Metal binding 'finger' structures in the glucocorticoid receptor defined by site-directed mutagenesis.* EMBO J, 1988. **7**(8): p. 2503-8.

148. Shibusawa, N., A.N. Hollenberg, and F.E. Wondisford, *Thyroid hormone receptor DNA binding is required for both positive and negative gene regulation.* J Biol Chem, 2003. **278**(2): p. 732-8.

149. Kanda, A. and A. Swaroop, *A comprehensive analysis of sequence variants and putative disease-causing mutations in photoreceptor-specific nuclear receptor NR2E3.* Mol Vis, 2009. **15**: p. 2174-84.

150. Kohler, B., et al., *Five novel mutations in steroidogenic factor 1 (SF1, NR5A1) in 46,XY patients with severe underandrogenization but without adrenal insufficiency.* Hum Mutat, 2008. **29**(1): p. 59-64.

151. Achermann, J.C., et al., *A mutation in the gene encoding steroidogenic factor-1 causes XY sex reversal and adrenal failure in humans.* Nat Genet, 1999. **22**(2): p. 125-6.

152. Ito, M., J.C. Achermann, and J.L. Jameson, *A naturally occurring steroidogenic factor-1 mutation exhibits differential binding and activation of target genes.* J Biol Chem, 2000. **275**(41): p. 31708-14.

153. Lausen, J., et al., *Naturally occurring mutations in the human HNF4alpha gene impair the function of the transcription factor to a varying degree.* Nucleic Acids Res, 2000. **28**(2): p. 430-7.

154. El Hassan, M.A. and C.R. Calladine, *Two distinct modes of protein-induced bending in DNA.* J Mol Biol, 1998. **282**(2): p. 331-43.

155. Taubert, S., J.D. Ward, and K.R. Yamamoto, *Nuclear hormone receptors in nematodes: evolution and function.* Mol Cell Endocrinol, 2011. **334**(1-2): p. 49-55.

156. Bertrand, S., et al., *Evolutionary genomics of nuclear receptors: from twenty-five ancestral genes to derived endocrine systems.* Mol Biol Evol, 2004. **21**(10): p. 1923-37.

157. Willis, S. and P.R. Griffin, *Mutual information identifies sequence positions conserved within the nuclear receptor superfamily: approach reveals functionally important regions for DNA binding specificity.* Nucl Recept Signal, 2011. **9**: p. e001.

158. Harris, L.F., M.R. Sullivan, and D.F. Hickok, *Conservation of genetic information: a code for site-specific DNA recognition.* Proc Natl Acad Sci U S A, 1993. **90**(12): p. 5534-8.

159. Sakai, D.D., et al., *Hormone-mediated repression: a negative glucocorticoid response element from the bovine prolactin gene.* Genes Dev, 1988. **2**(9): p. 1144-54.

ABSTRACT

MECHANISTIC STUDIES OF A NOVEL PPARγ MUTANT THAT CAUSES LIPODYSTROPHY AND DIABETES

by

OLGA ASTAPOVA

May 2014

Advisor: Dr. Todd Leff

Major: Pathology

Degree: Doctor of Philosophy

PPARγ is a nuclear receptor that plays a central role in metabolic regulation by regulating extensive gene expression networks in adipose, liver, skeletal muscle and many other tissues. Human PPARγ mutations are rare and cause a monogenetic form of severe type II diabetes with metabolic syndrome, known as familiar partial lypodystrophy. The E157D PPARγ mutant causes atypical lipodystrophy in a large Canadian kindred, presenting with multiple musculoskeletal, neurological and hematological abnormalities in addition to the classic lipodystrophy features of insulin-resistant diabetes, hypertension and dyslipidemia. This mutation is localized to the p-box of PPARγ, a small region that interacts directly with the DNA molecule and is required for DNA binding site specificity. Mechanistic analysis revealed that E157D PPARγ binds PPARγ response elements (PPREs), but is mildly, moderately or severely defective at inducing transcription from most promoters, without dominant negative activity. This suppression of transcriptional activity may be mediated by an increased effect of

nuclear receptor corepressors on E157D PPARγ. In addition, the mutant binds atypical PPREs in the regulatory regions of a small set of genes outside of the PPARγ-regulated network, and induces transcription of these genes. The loss of transcriptional activity on PPARγ-regulated promoters leads to the metabolic disease in the E157D PPARγ cohort, while the gain of activity on non- PPARγ target promoters may explain the atypical clinical presentation associated with this mutation. The misregulation of target genes by this DNA-contacting mutant highlights a previously under-appreciated importance of the DNA molecule as an allosteric regulator of the transcriptional activity of nuclear receptors. In summary, this dissertation describes a human PPARγ mutation that works through a novel mechanism to cause atypical lipodystrophy, and provides support for a more integrated view of the nuclear receptor-DNA interaction and transcription activation.

AUTOBIOGRAPHICAL STATEMENT

OLGA ASTAPOVA

Education	2006-2012	Wayne State University, Detroit, MI MD/PhD Candidate
	2002-2006	University of Michigan B.S., Biochemistry

Funding F30 Fellowship 1F30DK083195-01A2
NIH (NIDDK), Issue Date: 09/04/2009

Research Publications

Veiga-Lopez A, **Astapova OI**, Aizenberg EF, Lee JS, Padmanabhan V (2009) Developmental programming: contribution of prenatal androgen and estrogen to estradiol feedback systems and periovulatory hormone dynamics in sheep. *Biology of Reproduction* 80(4):718-25

Savabieasfahani M, Kannan K, **Astapova OI**, Evans NP, and Padmanabhan V (2006) Developmental programming: differential effects of prenatal exposure to bisphenol-A or methoxychlor on reproductive function. *Endocrinology* 147(12):5956-66

Book Chapter

Astapova O and Leff T. (2009) PPARγ: A Key Regulator of Adipose Tissue Formation, Remodeling and Metabolism. in *Adipose Tissue in Health and Disease*. Wiley-VCH, Weinheim, Germany.

National Meetings (Talks)

Astapova OI, Campeau PM, Gagné C, Hegele RA, and Leff T. A Human PPARγ Mutation Causes Inherited Diabetes Through a Unique Mechanism of Action. 2010. Nuclear Receptors & Disease. Cold Spring Harbor, NY.

Astapova O, Herkimer C, Olton PR, Lee JS, Flak J, and Padmanabhan V. Developmental Programming: Defects in Preovulatory Estradiol Rise and Gonadotropin Surge Dynamics in Prenatal Testosterone-Treated Ewes are Not Programmed by Androgenic Action of Testosterone. 2006. 39th Annual Meeting, Society for the Study of Reproduction. Omaha, NE.